



**COMPARISON OF NOVEL CARBONEOUS STRUCTURES TO TREAT  
NITROAROMATIC IMPACTED WATER**

THESIS

Benjamin M. Doane, Contractor, USAF  
AFIT-ENV-MS-15-D-047

**DEPARTMENT OF THE AIR FORCE  
AIR UNIVERSITY**

**AIR FORCE INSTITUTE OF TECHNOLOGY**

---

---

**Wright-Patterson Air Force Base, Ohio**

**DISTRIBUTION STATEMENT A.**  
APPROVED FOR PUBLIC RELEASE; DISTRIBUTION UNLIMITED.

The views expressed in this thesis are those of the author and do not reflect the official policy or position of the United States Air Force, Department of Defense, or the United States Government. This material is declared a work of the U.S. Government and is not subject to copyright protection in the United States.

AFIT-ENV-MS-15-D-047

COMPARISON OF NOVEL CARBONEOUS STRUCTURES TO TREAT  
NITROAROMATIC IMPACTED WATER

THESIS

Presented to the Faculty

Department of Systems Engineering and Management

Graduate School of Engineering and Management

Air Force Institute of Technology

Air University

Air Education and Training Command

In Partial Fulfillment of the Requirements for the  
Degree of Master of Science in Environmental Engineering and Science

Benjamin M. Doane, BS

Contractor, USAF

December 2015

DISTRIBUTION STATEMENT A. APPROVED FOR PUBLIC RELEASE;  
DISTRIBUTION UNLIMITED.

AFIT-ENV-MS-15-D-047

COMPARISON OF NOVEL CARBONEOUS STRUCTURES TO TREAT  
NITROAROMATIC IMPACTED WATER

Benjamin M. Doane, BS

Contractor, USAF

Committee Membership:

Lt Col D. M. Kempisty, PhD  
Chair

Dr. S. R. Kanel  
Member

Dr. D. L. Felker  
Member

### Abstract

Carbonaceous materials such as carbon nanotube (CNT), granular activated carbon (GAC), and biochar are promising materials for the removal of organic contaminants from aqueous phase solutions. CNTs have astonishing mechanical strength, chemical and thermal stability and high surface area. While biochar, similar to GAC, having an extremely porous structure and high surface area, can be produced in more austere conditions with native materials. In this study, novel CNT-Hybrid structures (CNT-HS), hardwood pellet (HWP) Biochar and standard GAC (F-600 GAC) were used as adsorbents to treat water contaminated by a model nitroaromatic compound, 2,4-dinitrotoluene (DNT). The DNT adsorption capacity of pristine CNT-HS and HWP-Biochar was measured in the laboratory and compared with pulverized GAC over a range of dissolved DNT concentrations (0.15 - 40 mg L<sup>-1</sup>). The kinetics of DNT adsorption on CNT-HS, HWP-Biochar and F-600 GAC, were investigated. Scanning electron microscopy (SEM) was used to characterize size, and surface morphology of adsorbents. Adsorption isotherms and adsorption kinetics of DNT were investigated in batch experiments. Adsorption of DNT was fit to Freundlich and Langmuir isotherm models. The Freundlich constants,  $K_F$ , for GAC was found to be 111.69 (mg g<sup>-1</sup>) (L mg<sup>-1</sup>)<sup>1/n</sup> and 1/n to be 0.24 while  $K_F$  for HWP-Biochar was found to be 37.33 (mg g<sup>-1</sup>) (L mg<sup>-1</sup>)<sup>1/n</sup> and 1/n to be 0.51. Low overall surface area of CNT is believed to be responsible for poorly observed adsorption; however, wettability issues may have also complicated obtaining values for CNT-HS. This study demonstrates the capacity of pristine HWP-Biochar and

begins to investigate the ability of CNT-HS to remove DNT from water and is a first step in using these novel materials in environmental applications.

## **Acknowledgments**

First and foremost, I would like to thank my faculty advisor, Lt Col David Kempisty, for his direction and encouragement during this research endeavor. Special thanks to committee member Dr. Sushil Kanel, for both the patience and freedom provided to me throughout the project. Thank you to committee member Dr. Daniel Felker for his guidance in data analysis and GC-MS method development.

I am also very grateful to Wright State University for providing the carbon nanotube material used during the research and to USAFSAM/OEA Industrial Hygiene Laboratory for the support and use of their analytical equipment. Lastly, I would like to thank Mr. Cody Fourman, for assisting me with the literature review and experimental research.

Benjamin M. Doane

## Table of Contents

Abstract .....	iv
Table of Contents .....	vii
List of Figures .....	ix
List of Appendix Figures .....	x
List of Tables .....	xii
List of Equations .....	xiii
I. INTRODUCTION .....	1
1.1 GENERAL ISSUE .....	1
1.2 PROBLEM STATEMENT .....	8
1.3 RESEARCH QUESTION .....	9
1.4 SCOPE AND APPROACH .....	9
1.5 SIGNIFICANCE .....	10
1.6 PREVIEW .....	11
II. SCHOLARLY ARTICLE .....	12
2.1 ABSTRACT .....	12
2.2 INTRODUCION .....	13
2.3 MATERIALS AND METHODS .....	19
2.4 RESULTS AND DISCUSSION .....	28
2.5 CONCLUSIONS .....	42
2.6 REFERENCES .....	43
III. CONCLUSIONS .....	44
3.1 CHAPTER OVERVIEW .....	44
3.2 REVIEW OF FINDINGS .....	44
3.3 LIMITATIONS .....	45



3.4	SIGNIFICANCE OF FINDINGS.....	45
3.5	FUTURE RESEARCH .....	46
APPENDIX A. EXPANDED LITERATURE REVIEW .....		48
A.1	2, 4-DINITROTOLUENE (DNT) .....	48
A.2	DNT REMEDIATION TECHNOLOGIES .....	49
A.3	GRANULAR ACTIVATED CARBON (GAC).....	50
A.4	CARBON NANOTUBES (CNT).....	53
APPENDIX B. EXPANDED METHODOLOGY, RESULTS AND DISCUSSION .....		56
B.1	NORMALIZED ADSORBENT CONCENTRATIONS .....	56
B.2	ADDITIONAL GAC KINETIC EXPERIMENTS.....	58
B.3	EXPERIMENTAL IMAGES.....	62
B.4	UV-VIS CALIBRATION CURVE PROCEDURE AND FIGURE .....	63
B.5	GC-MS CALIBRATION CURVE METHOD AND FIGURES.....	64
B.7	HWP-BIOCHAR SECOND ORDER RATE ANALYSIS.....	69
B.8	F-600 GAC FREUNDLICH ISOTHERM OUTLIER ANALYSIS .....	71
B.9	ISOTHERM ANALYSIS WITH CNT-HS .....	72
B.10	DNT PEAKS OBSERVED USING THE GC-MS SIM METHOD.....	74
B.11	pH ANALYSIS.....	76
B.12	EQUATIONS.....	78
REFERENCES .....		87

## **List of Figures**

Figure 1. DNT nitroaromatic structure. ....	3
Figure 2. SEM images of the grinded GAC granules .....	30
Figure 3. SEM images of HWP-Biochar pellets .....	30
Figure 4. SEM images of the nano-substrates. ....	31
Figure 5. Kinetic solid phase concentrations at time (hrs).....	32
Figure 6. Normalized liquid phase concentrations at time (hrs).....	34
Figure 7. Second order kinetic rate analysis .....	36
Figure 8. Freundlich Isotherm models for GAC and HWP-Biochar .....	39
Figure 9. Langmuir Isotherm models for GAC and HWP-Biochar .....	40

## List of Appendix Figures

Figure B 1. Normalized GAC concentrations with control .....	56
Figure B 2. Normalized HWP-Biochar concentrations with control.....	57
Figure B 3. Normalized CNT-Foam concentrations with control .....	57
Figure B 4. Pulverized versus as-received GAC kinetics .....	59
Figure B 5. GAC pulverized versus as-received second order kinetic rate analysis .....	60
Figure B 6. Pulverized GAC kinetics mass concentration analysis.....	61
Figure B 7. Pulverized second order kinetic rate analysis .....	61
Figure B 8. Experimental reactor bottle configurations.....	62
Figure B 9. CNT-Hybrid structures cut to mass .....	62
Figure B 10. UV-Vis spectrophotometer calibration curves .....	63
Figure B 11. GC-MS calibration curve for GAC kinetic experiment.....	64
Figure B 12. GC-MS calibration curve for CNT-HS kinetic experiment.....	65
Figure B 13. GC-MS calibration curve 0 - 1.5 mg L <sup>-1</sup> DNT for GAC and CNT-HS isotherm study .....	65
Figure B 14. GC-MS calibration curve 5 - 15 mg L <sup>-1</sup> DNT for GAC and CNT-HS isotherm study .....	66
Figure B 15. GC-MS calibration curve for GAC 25 mg L <sup>-1</sup> and 40 mg L <sup>-1</sup> DNT isotherm study .....	66
Figure B 16. GC-MS calibration curve 0 - 1.5 mg L <sup>-1</sup> DNT for Biochar isotherm and kinetic study .....	67
Figure B 17. GC-MS calibration curve 5 - 15 mg L <sup>-1</sup> DNT for Biochar isotherm and kinetic study .....	67

Figure B 18. Zeroth order kinetic rate analysis.....	68
Figure B 19. First order kinetic rate analysis .....	69
Figure B 20. HWP-Biochar second order kinetic rate analysis with outlier.....	70
Figure B 21. HWP-Biochar $T^2$ statistic outlier analysis conducted in JMP® .....	70
Figure B 22. F-600 GAC Freundlich Isotherm analysis with outlier. ....	71
Figure B 23. F-600 GAC $T^2$ statistic outlier analysis conducted in JMP® .....	72
Figure B 24. Freundlich Isotherm models for CNT-HS adsorbents .....	73
Figure B 25. Langmuir Isotherm models for CNT-HS adsorbents.....	73
Figure B 26. DNT peak observed for $C_0$ of $\sim 0.15 \text{ mg L}^{-1}$ control collected during the CNT-Foam isotherm experiment .....	74
Figure B 27. DNT peak observed for $C_0$ of the $\sim 1.5 \text{ mg L}^{-1}$ control collected during the CNT-Foam isotherm experiment .....	75
Figure B 28. DNT peak observed for $C_0 \sim 15 \text{ mg L}^{-1}$ control collected during the CNT- Foam isotherm experiment.....	75
Figure B 29. pH of solutions observed during the kinetic studies .....	77

## List of Tables

Table 1. Estimated values of CNT-Foam (RVC 80 ppi) characteristics.....	29
Table 2. Calgon F-600 GAC Characteristics and Pore Size Distribution.....	29
Table 3. Second order reaction rate constants determined from linear regression analysis. .....	36
Table 4. Freundlich constants $K_F$ and $1/n$ . The $R^2$ value was determined from linear regression analysis using Figure 8 .....	40
Table 5. Averaged solid phase concentrations ( $q_e$ ) observed from the Isotherm study at the initial known concentrations .....	40
Table 6. Freundlich model constants ( $K_F$ and $1/n$ ) of DNT adsorption onto various adsorbents.....	41
Table 7. Q-test with a 90% CI conducted on F-600 GAC kinetic and control GC-MS triplicate data samples .....	79
Table 8. Q-test with a 90% CI conducted on CNT-Foam kinetics and control GC-MS data .....	81
Table 9. Q-test with a 90% CI conducted on HWP-Biochar kinetic, isotherm, and control GC-MS data .....	82
Table 10. Q-test with a 90% CI conducted on CNT-Foam and F-600 GAC isotherm GC- MS data .....	84
Table 11. Q-test with a 90% CI conducted on F-600 GAC isotherm 25 – 40 mg/L GC- MS data .....	86

## **List of Equations**

Equation 1. Mass-balance .....	78
Equation 2. Solid-phase concentration $q_e$ (mg DNT/g adsorbent).....	78
Equation 3. Linear Freundlich Isotherm equation .....	78
Equation 4. Linear Langmuir isotherm equation .....	78

# COMPARISON OF NOVEL CARBONEOUS STRUCTURES TO TREAT NITROAROMATIC IMPACTED WATER

## I. INTRODUCTION

### 1.1 GENERAL ISSUE

In this study, we compared the adsorptive capacity of bituminous-coal based granular activated carbon (GAC) versus pristine novel carbon nanotube hybrid structures (CNT-HS) and hardwood pellet (HWP) Biochar to treat water contaminants of Department of Defense (DOD) concern. We used 2,4-dinitrotoluene (DNT) as a model explosive contaminant for the study.

The study addressed the following investigative questions:

1. To what extent do various carbonaceous materials remove DNT from aqueous sources?
2. Can Hardwood Pellet (HWP) Biochar and carbon nanotubes (CNT) that have been fixed to reticulated vitreous carbon (RVC) foam and fabric substrates be effective adsorbents to remove DNT?

The objective of this study was to compare the DNT adsorptive capacities of various carboneous materials. At environmentally relevant concentration of 0.15 – 40 mg L<sup>-1</sup> DNT, both advanced and primitive adsorbents were investigated and compared to conventional GAC. This was accomplished by quantifying the carbon adsorption of DNT using UV-Vis spectrophotometer, gas chromatography–mass spectrometry (GC-MS), and characterizing the carbon's topography using a scanning electron microscope

(SEM). The rate and extent of DNT adsorption were established and evaluated against literature. The research focused on adsorption isotherms and experimental kinetics of DNT removal from aqueous solution using GAC, HWP-Biochar and CNT-Foam and CNT-Fabric structures as adsorbents at fixed ionic strengths. This study conducted batch experiments to compare the DNT adsorptive capabilities of the adsorbents using similar methods established from previous scientific work. The adsorption of DNT onto the carbon structures is fit to Freundlich and Langmuir isotherm models. The study provides information on the capability of novel biochar and nano-carbonaceous structures to remove DNT from water. We hypothesize that certain carbon structures will adsorb DNT more effectively than others. To the best of our knowledge, this is the first study that carbon nanotubes fixed to a substrate and HWP-Biochar has been used to remove nitroaromatic compounds from an aqueous solution. An evaluation of novel carbonaceous material is helpful in future environmental studies and provides a valuable resource for scientists and researchers concerned with remediation of nitroaromatic compounds and advancements in the field of biochar and environmental application of CNT.

DNT is a nitroaromatic compound often found in groundwater and soil in the U.S. and listed as a priority pollutant under the Clean Water Act (Figure 1). The conjugated double bonds make DNT a probable candidate for  $\pi$ - $\pi$  bonding on activated carbon's interlocking aromatic rings known as basal planes (Ridder, 2012). Carbon atoms have a  $\pi$  electron orbitals that reside perpendicular to its surface. Nitroaromatics are electron acceptors and can form  $\pi$ - $\pi$  bonds with CNT (Pan and Xing, 2008). This DNT characteristic makes it a suitable candidate for adsorption onto various carbonaceous



structures including biochar, CNTs, and GAC. Pore filling may also contribute to the adsorption of DNT onto GAC and biochar. Previous work has shown that in solutions with low concentrations, pore filling is a primary mechanism of organic sorption onto biochar (Kasozi et al., 2010). The surface area of biochar is believed to be comprised primarily with micropores and mesopores where significant pore filling with organic compounds occurs (Pignatello et al., 2006). Additionally, the adsorption of DNT onto biochar could occur by hydrophobic interaction. Pristine biochars that lack oxygen functional groups are hydrophobic and have shown to sorb neutral organic compounds similar to DNT (Inyang and Dickenson, 2015).

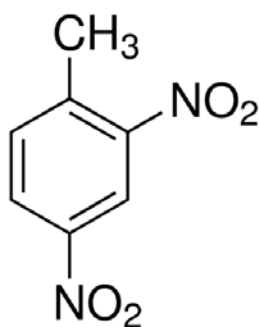


**Figure 1. DNT nitroaromatic structure. The double bonds make the structure a probable candidate for  $\pi$ - $\pi$  bonding and adsorption onto carbeneous materials. The chemical formula of DNT is  $\text{CH}_3\text{C}_6\text{H}_3(\text{NO}_2)_2$  and has a molecular weight of  $182.13 \text{ g mole}^{-1}$**

This effort is of particular interest to the US Air Force. The DoD owns and manages federal land used for military instruction and training that includes firing ranges for munitions and explosives testing. DNT is used in the manufacture of ammunitions and explosives and has been found in military installations' munitions dumps, operational ranges and training sites (Clausen et al., 2011). DNT residue is deposited into the soil when munitions are expended which may leach into water sources. This creates a human

health concern when firing ranges are located near aquifers that are used as sources of drinking water, or when dermal contact with the contaminated soil is possible (EPA, 2014). The EPA has classified DNT as a probable (Class B2) carcinogen and toxic substance (EPA, 1990). For this reason, DNT is a contaminant of DoD concern due to the potential risk it may cause to human health. Furthermore, multiple Base Closure and Realignment Acts identified many military bases and government facilities for closure, realignment or transfer. It is imperative that these sites be remediated before being transferred to the local communities. Ensuring these sites are free of hazards will prevent the local populace from being exposed to probable carcinogens and prevent legal issues that may arise from medical suits. Effectively remediating DNT from soil and water sources is a critical step if these sites are to be used for recreational, industrial or residential lots.

A variety of materials and methods are used in water treatment protocols. Traditionally, powder activated carbon (PAC) has been used to treat contaminated water and soil. Though effective in treatment, a disadvantage to PAC is the difficulty in recovering the adsorbent post-treatment. Along with PAC, granular activated carbon has been used to treat contaminated water. Historically, GAC has been utilized in pump and treat methods. Sizes can vary, but 20,000 lb GAC contactors are not uncommon for use in remediation projects. During pump and treat operations, trucks deliver and remove exhausted GAC and replace with new GAC. However, since highly effective for the removal of organics, other (non-target) organic compounds may reduce the treatment system's capacity for the contaminant of interest and require more frequent replacement of GAC and increased material costs. The cost of disposing used carbon is estimated to

be 50% of the original price (Suthersan, 1999). Conversely, if the carbon is able to be regenerated, the cost will be substantially less.

Ho and Daw (1988) conducted DNT adsorption and desorption studies with Calgon Filtrasorb FS300 and FS400 GAC. Their experiment was conducted at the bench scale with 0.25 - 1.25 g L<sup>-1</sup> of GAC in 25-120 mg L<sup>-1</sup> DNT impacted de-ionized water. Isotherm studies suggest a Freundlich fit to DNT adsorption. Work was also conducted by the US Army and investigated the capacity of GAC to remove explosive contaminants from an Army ammunition plant's effluent wastewater (Hinshaw et al., 1987). The study investigated 5 types of GAC including Calgon Filtrasorb 200, 300 and 400. The results were fit to Freundlich and Langmuir isotherms. The batch experiments obtained equilibrium concentrations of 0.0007 mg L<sup>-1</sup> that met the objective of the study.

Current practices have tailored carbon nanotubes in various commercial applications such as electrical conductive fillers in plastics, flame-retardants additives, transistors, lithium ion batteries, and biosensors (De Volder et al., 2013). More recently, CNTs have been used to treat contaminated water, and commercially, CNT filters are being used to treat drinking water (De Volder et al., 2013). CNTs are excellent adsorbents due to their distinctive properties that include chemical, mechanical and thermal stability, and high surface area. Because of these properties, CNTs have been successfully applied to treat contaminated water and are being used in many applications as sorbents, catalysts, filters, and membranes (Basu-Dutt et al., 2012; Liu et al., 2013; Mubarak et al., 2014; Nepal et al., 2006). Filtration techniques use the powder form of CNT and mix it with contaminants creating a slurry (Yang et al., 2013). Similar to PAC, it is very difficult to recover the CNT powder from the slurry. Loss of nano material to

the environment is a cause of concern due to potential adverse environmental and human health effects resulting from ingestion or inhalation of CNTs. However, CNTs are being produced as solid structures, which claim the same characteristics as CNT powder but allow easier recovery post-treatment.

CNTs possibly could be applied as an adsorbent to clean up hazmat spills, as filters to sorb contaminants in groundwater, or to remediate lakes and rivers impacted with toxins produced from hazardous algal blooms. CNTs in water treatment have been investigated and proven effective in purifying water contaminated with bacteria and viruses (Liu et al., 2013; Tiraferri et al., 2011; Vecitis et al., 2011). More recently, experimental research has studied the ability of CNTs to adsorb nitroaromatic compounds, and current research has investigated the ability of CNTs to adsorb DNT from aqueous solutions (Kanel et al., 2015; Oh et al., 2013; Shen et al., 2009). The ability of hybrid carbon nanotube structures fixed to graphene substrates to remove contaminants from wastewater has also been pursued (Vijwani et al., 2015). Vijwani et al. (2015) investigated the adsorption of methylene blue (MB) dye from an aqueous solution using hybrid carbon nanostructures. The carbon nanostructures were created using a 2-step process by plasma deposition of a silicon dioxide nanolayer followed by CNT growth using chemical vapor deposition (CVD). The experimental design used 250 mL reactor bottle with 100 mL of aqueous solution and dye concentrations ranging from 0.35 -10 mg L<sup>-1</sup>. The samples were analyzed using a UV-Vis Spectrophotometer, and the adsorption data was fit to Langmuir and Freundlich isotherms. The study determined that the adsorption of the dye followed pseudo-second order kinetics and the adsorption

capacity of the hybrid nanostructures were comparable to the sorbent materials reported in the literature (Vijwani et al., 2015).

Biochar, similar to Granular Activated Carbon (GAC), having an extremely porous structure, can be produced in more austere conditions with native materials. Biochar is a carboneous material that is created from thermal decomposition of biomass (Oh et al., 2013). The use of biochar as an adsorbent is being pursued due to its relatively cheap production cost, unique structure, and high surface area. Biochar in water treatment has been investigated, and studies have been undertaken involving organic and inorganic contaminants including heavy metal and microbial contaminants (Inyang and Dickenson, 2015; Mohan et al., 2014). A comparative study investigating equilibrium adsorption capacity of biochar and GAC was recently pursued (Kearns et al., 2014) and biochar and GAC sorption of explosive contaminants have been researched (Oh and Seo, 2014)

Kearns et al. (2014) compared the capacity of biochar to GAC data found in the literature to adsorb 2,4-dichlorophenoxyacetic acid (2,4-D), an herbicide. 2,4-D is a synthetic organic chemical with an aromatic structure comparable to that of DNT. Similar to Ho and Dow (1988), Kearns et al. (2014) utilized 40 mL reactor bottles for their batch sorption study. The reactor bottles were placed on an orbital shaker for 24 hours and samples were analyzed using a liquid chromatograph. The sorption data was fit to the Freundlich isotherm model. The findings suggest that the adsorption capacity of 2,4-D by certain biochars are comparable to that of activated carbon data found in literature (Kearns et al., 2014).

Furthermore, the capacity of biochar to adsorb DNT has been investigated. Oh and Seo (2014) used 40 mL amber vials with 20 mL of the explosive contaminated solution and  $2.5 - 250 \text{ g L}^{-1}$  of sorbent material in their isotherm experiments. The material used to make the biochar included biosolids, coffee grounds, corn stalks, poultry litter, fallen leaves, and rice straw. The nitroaromatic adsorption capacities of the biochars were compared to GAC and graphite. Samples were placed on an orbital shaker and sorption equilibrium was reached at 24 hours. Samples were analyzed using a liquid chromatograph, and the data was fit to the Langmuir model. GAC achieved the highest DNT adsorption capacity of  $15.17 \text{ mg g}^{-1}$  followed closely by graphite with  $10.11 \text{ mg g}^{-1}$ . Poultry litter and corn stalk biochar achieved a comparable DNT adsorption capacity to graphite (Oh and Seo, 2014).

Comparative research investigating the DNT adsorptive capacities and kinetics of F-600 GAC, CNT-HS, and HWP-Biochar under similar conditions are lacking in current literature. This study quantified the DNT adsorption capacities and kinetics of HWP-Biochar, CNT-HS using GC-MS, and compared the data to conventional F-600 GAC and results found in the literature.

## **1.2 PROBLEM STATEMENT**

Numerous U.S. military installations and facilities listed as Formerly Used Defense Sites (FUDS) have identified explosive contamination associated with former munition range operations (EPA, 2015). The identified government and military installations need to remediate DNT from firing and explosive ranges before transfer to

the public or state and local agencies. What technology and best practices will be employed to effectively remediate DNT from these locations prior to transfer?

### **1.3 RESEARCH QUESTION**

At an environmentally relevant concentrations of 0.15 - 40 mg L<sup>-1</sup> DNT, with an ionic strength of 10 mM KCl, DNT adsorptive characteristics of three different adsorbents were evaluated. Capacity and kinetics of Hardwood Pellet Biochar and hybrid carbon nanotubes that have been fixed to reticulated vitreous carbon foam and fabric substrates were evaluated to compare alternative adsorbents to conventional CalgonCarbon FILTRASORB® F-600 granular activated carbon.

### **1.4 SCOPE AND APPROACH**

We hypothesize that certain carboneous materials will adsorb DNT more effectively than others. Bench scale kinetic and isotherm studies were conducted at the Air Force Institute of Technology laboratory to test our hypothesis. Samples were drawn at designated times to determine DNT concentrations during the kinetic and isotherm studies. Findings from the study were compared to previous work found in the literature.

It was assumed that there was no loss of mass after the adsorbent was weighed and transferred to the reactor bottles. It is also assumed that equal volumes of solution and adsorbent material are removed from each reactor bottle during sampling throughout the kinetic experiments.

## **1.5 SIGNIFICANCE**

This research explores the novel use of biochar and carbon nanotubes fixed on two unique substrates to remove a nitroaromatic compound (DNT) from an aqueous solution. CNT-HS are at the forefront of innovative technology that is in the process of being optimized. Ideally, the hybrid structure will allow superior adsorption due to the mechanical strength, chemical and thermal stability and high surface area of CNTs. At the same time, the substrate will retain the nanomaterial and prevent loss to the environment. There also exists the potential for regeneration from the hybrid structures that may reduce overall cost compared to conventional GAC if these structures can be routinely re-used. On the contrary, biochar can be created from a diverse range of biomass at extremely low costs in underdeveloped regions, and retain similar characteristics to GAC. The study may give insight into innovative biochar and CNT applications to remediate nitroaromatic compounds from contaminated water sources that are the responsibility of the DoD.

This effort is important to the DoD because of the financial and social commitment that the government has to restore areas contaminated by expended munitions. The Defense Environmental Programs (DERP) annual report to Congress for FY 2013 allocated \$1.8 billion for environmental programs. More specifically for fiscal year 2015, approximately \$1.1 billion was requested for Active Installations, and Formerly Used Defense Sites (FUDS) and approximately \$264 million was requested for BRAC Locations (U.S. Department of Defense, 2014). The Installation Restoration Program inventory in the FY 2013 DERP identified 4,861 contaminated sites that are in the process of being restored and an additional 1,859 sites that require remediation that



has not been initiated. The DoD has estimated that 15 million acres of land have been contaminated by military munitions and are largely properties of FUDS (EPA, 2015).

## **1.6 PREVIEW**

This thesis follows the scholarly article format with the objective for submission to the Journal of Environmental Engineering. Chapter II of this document presents the journal article, formatted to preserve uniformity within the thesis. The journal article covers the detection and quantification of DNT in kinetic and isotherm studies using GC-MS and solid and liquid phase adsorption capacity onto GAC, CNTs, and biochar. The conclusion of the thesis is in chapter III, which reviews the findings from the research, and discusses limitations and future work. Appendices cover an expanded literature review, methodology, and additional results with discussion.

## II. SCHOLARLY ARTICLE

*Written for consideration of submission to the  
Journal of Env Engineering*

### 2.1 ABSTRACT

Carboneous materials such as carbon nanotube (CNT), granular activated carbon (GAC), and biochar are promising materials for the removal of organic contaminants from aqueous phase solutions. CNTs have astonishing mechanical strength, chemical and thermal stability and high surface area. While biochar, similar to GAC, having an extremely porous structure and high surface area, can be produced in more austere conditions with native materials. In this study, novel CNT-Hybrid structures (CNT-HS), hardwood pellet (HWP) Biochar and standard GAC (F-600 GAC) were used as adsorbents to treat water contaminated by a model nitroaromatic compound, 2,4-dinitrotoluene (DNT). The DNT adsorption capacity of pristine CNT-HS and HWP-Biochar was measured in the laboratory and compared with pulverized GAC over a range of dissolved DNT concentrations (0.15 - 40 mg L<sup>-1</sup>). The kinetics of DNT adsorption on CNT-HS, HWP-Biochar and F-600 GAC, were investigated. Scanning electron microscopy (SEM) was used to characterize size, and surface morphology of adsorbents. Adsorption isotherms and adsorption kinetics of DNT were investigated in batch experiments. Adsorption of DNT was fit to Freundlich and Langmuir isotherm models. The Freundlich constants,  $K_F$ , for GAC was found to be 111.69 (mg g<sup>-1</sup>) (L mg<sup>-1</sup>)<sup>1/n</sup> and 1/n to be 0.24 while  $K_F$  for HWP-Biochar was found to be 37.33 (mg g<sup>-1</sup>) (L mg<sup>-1</sup>)<sup>1/n</sup> and 1/n to be 0.51. Low overall surface area of CNT is believed to be responsible for poorly observed adsorption; however, wettability issues may have also complicated obtaining

values for CNT-HS. This study demonstrates the capacity of pristine HWP-Biochar and begins to investigate the ability of CNT-HS to remove DNT from water and is a first step in using these novel materials in environmental applications.

## **2.2 INTRODUCTION**

The DoD owns and manages federal land that is used for military instruction and training. Many of these locations include firing ranges used for munitions and explosives testing. 2,4-dinitrotoluene (DNT), a nitroaromatic compound, is used in the manufacture of ammunitions and explosives and has been found in military installations' munitions dumps, operational ranges and training sites (Clausen et al., 2011). The EPA has classified DNT as a probable (Class B2) carcinogen and toxic substance (EPA, 1990). When munitions are expended, DNT residue is deposited into the soil that may leach into water sources. This creates a human health concern when firing ranges are located near aquifers that are used as sources of drinking water, or when dermal contact with the contaminated soil is possible (EPA, 2014). For this reason, DNT is a contaminant of DoD concern. Furthermore, multiple Base Closure and Realignment Acts identified numerous military bases and government facilities for closure, relocation or transfer. Prior to transferring to the public, it is prudent to consider possible adverse health effects associated with formerly used defense sites and if necessary, available remedial alternatives prior to being transferred to the public. Ensuring these sites are free of hazards will prevent the local populace from being exposed to probable carcinogens and prevent issues that may arise from adverse medical outcomes and legal action.

Effectively remediating DNT from soil and water sources is a critical step if these sites are to be used for recreational, industrial or residential lots.

DNT is a nitroaromatic compound often found in groundwater and soil in the U.S. and listed as a priority pollutant under the Clean Water Act. DNT is comprised of conjugated double bonds that make it a probable candidate for  $\pi$ - $\pi$  bonding on activated carbon's interlocking aromatic rings known as basal planes (Ridder, 2012).

Nitroaromatics are electron acceptors and can form  $\pi$ - $\pi$  bonds with carbon atoms'  $\pi$  electron orbitals (Pan and Xing, 2008). Pore filling may also contribute to the sorption of DNT, and previous work has shown that pore filling is a principal mechanism of organic sorption onto biochar (Kasozi et al., 2010). The surface area of biochar is believed to be comprised primarily with micropores and mesopores where significant pore filling with organic compounds is known to occur (Pignatello et al., 2006). Additionally, pristine biochars that lack oxygen functional groups are hydrophobic and have shown to sorb neutral organic compounds similar to DNT (Inyang and Dickenson, 2015).

Water treatment applications incorporate a variety of materials and methods, and conventional protocols have used powder activated carbon (PAC) to remediate water and soil contaminated with organic pollutants. Though effective in treatment, a disadvantage to PAC is it is difficult to recover the powder post-treatment. Along with PAC, granular activated carbon has also been used to treat polluted water. Historically, GAC has been utilized in pump and treat methods. Sizes can vary, but 20,000 lb GAC contactors are not uncommon for use in remediation projects. During pump and treat operations, trucks deliver and remove exhausted GAC and replace with new GAC. However, since highly effective for the removal of organics, other (non-target) organic compounds may reduce

the treatment system's capacity for the contaminant of interest and require more frequent replacement of GAC and increased material costs (Suthersan, 1999).

Ho and Daw (1988) conducted DNT adsorption and desorption studies with GAC (Calgon Filtrasorb FS300 and FS400). Their experiment was conducted at the bench scale with 0.25 - 1.25 g L<sup>-1</sup> of GAC in 25-120 mg L<sup>-1</sup> DNT impacted de-ionized water. The findings from the isotherm studies suggest a Freundlich fit to DNT adsorption. Research was also conducted by the US Army and investigated the ability of GAC to remove explosive contaminants from an Army ammunition plant's effluent wastewater (Hinshaw et al., 1987). The study investigated 5 types of GAC including Calgon Filtrasorb 200, 300 and 400. The batch experiments obtained equilibrium concentrations of 0.0007 mg L<sup>-1</sup>, and the adsorption data was fit to Freundlich and Langmuir isotherms. Freundlich values observed by Ho and Daw (1988) are referenced in Table 6.

Current practices have modified carbon nanotubes in various commercial applications to include electrical conductive fillers in plastics, flame-retardants additives, transistors, lithium ion batteries, and biosensors (De Volder et al., 2013). More recently, CNT filters have been manufactured to treat drinking water (De Volder et al., 2013). CNTs are excellent adsorbents due to their distinctive properties that include chemical, mechanical and thermal stability, and high surface area. Because of these properties, CNTs are being used in many applications as sorbents, catalysts, filters, and membranes (Basu-Dutt et al., 2012; Liu et al., 2013; Mubarak et al., 2014; Nepal et al., 2006). The filtration techniques use the powder form of CNT and mix it with contaminants creating a slurry (Yang et al., 2013). Similar to PAC, it is very difficult to recover the CNT powder from the slurry. Loss of nanomaterial to the environment is a cause of concern due to

potential adverse environmental and human health effects resulting from ingestion or inhalation of CNTs. However, CNTs are being produced as solid structures, which claim the same adsorptive characteristics as CNT powder but allow easier recovery post-treatment.

CNTs in water treatment have been investigated and proven effective in purifying water contaminated with bacteria and viruses (Liu et al., 2013; Tiraferri et al., 2011; Vecitis et al., 2011). CNTs possibly could be applied as an adsorbent to clean up hazmat spills, as filters to sorb contaminants in groundwater, or to remediate lakes and rivers contaminated with toxins produced from hazardous algal blooms. More recently, experimental research has studied the ability of CNTs to adsorb nitroaromatic compounds and current research investigated the ability of CNTs to adsorb DNT from aqueous solutions (Kanel et al., 2015; Oh et al., 2013). Kanel et al. (2015) used a different type of CNT that is called CNT yarn. The CNT yarn is a long wire structure that can be easily recovered from aqueous phase solutions. Shen et al. (2009) studied the adsorption of explosive contaminants onto multiwalled CNT (MWCNT). The adsorption data fit well to both the Freundlich and Langmuir isotherm models and kinetics followed pseudo-second-order kinetics (Shen et al., 2009). In addition, the ability of hybrid carbon nanotube structures fixed to graphene substrates to remove contaminants from wastewater has also been pursued (Vijwani et al., 2015). Vijwani et al. (2015) investigated the adsorption of methylene blue (MB) dye from de-ionized water using hybrid carbon nano-structures that were created using a 2-step process by plasma deposition of a silicon dioxide nano layer followed by CNT growth using chemical vapor deposition (CVD). The MB adsorption capacity of the hybrid nano-structures were

comparable to the sorbent materials reported in literature that included isolated CNTs, MWCNTs, GAC, PAC, CNT hybrids, exfoliated graphene oxide, and graphene sponge sorbents. It was determined that the adsorption of the dye followed pseudo-second order kinetics and fit best to the Langmuir isotherm model (Vijwani et al., 2015).

Biochar, similar to GAC, has a high surface area and porous structure, but can be produced at a reduced cost with a variety of materials. Biochar is a carbonaceous material that is manufactured by thermal decomposition of biomass (Oh et al., 2013). Biochar use in water treatment applications is being investigated, and studies have been undertaken involving organic and inorganic contaminants including heavy metal and microbial contaminants (Inyang and Dickenson, 2015). Mohan et al. (2014) performed a comparison study of the biochar adsorption capacities to metal ions and showed that certain biochars favored removal efficiency better than others. Soft wood char obtained a higher  $\text{Zn}^+$  adsorption capacity compared to hardwood char (Mohan et al., 2014). Furthermore, the herbicide (2,4-D) equilibrium adsorptive capacity of biochar was recently pursued (Kearns et al., 2014). 2,4-D is a synthetic organic chemical with an aromatic structure comparable to that of DNT. Additionally, biochar and GAC sorption of explosive contaminants have been researched. Oh and Seo (2014) used 40 mL amber vials with 20 mL of the explosive contaminated solution and  $2.5 - 250 \text{ g L}^{-1}$  of sorbent material in their isotherm experiments. GAC achieved the highest DNT adsorption capacity of  $15.17 \text{ mg g}^{-1}$  followed closely by graphite with  $10.11 \text{ mg g}^{-1}$ . Poultry litter and corn stalk biochar achieved a comparable DNT adsorption capacity to graphite (Oh and Seo, 2014).

Comparative research investigating the DNT adsorptive capacities and kinetics of GAC, CNT-HS, and biochar under similar conditions are lacking in current literature. This study will quantify the DNT adsorption capacities and kinetics of HWP-Biochar, CNT-Foam and CNT-Fabric structures using GC-MS, and compare the data to conventional F-600 GAC and results found in literature. To the best of our knowledge, this is the first study that carbon nanotubes fixed to a substrate using CVD, and HWP-Biochar have been used to remove a nitroaromatic compound from an aqueous solution.

The objective of this study is to characterize three different carboneous materials using a scanning electron microscope (SEM) and to quantify DNT adsorption by these adsorbents using gas chromatography–mass spectrometry, establishing the rate and extent of adsorption and evaluating the findings against literature. The research will focus on adsorption isotherm and kinetic experimental findings presenting the removal of DNT from aqueous solution using GAC, HWP-Biochar, and CNT-HS that include CNT-Foam and CNT-Fabric. We hypothesize that certain carboneous materials will adsorb DNT more effectively than others. An evaluation of novel carbonaceous material will be helpful in future environmental studies and provide a valuable resource for scientists and researchers concerned with a nitroaromatic compounds and advancements in the field of environmental application of biochar and CNTs.



## **2.3 MATERIALS AND METHODS**

### **Materials and chemicals**

Bench scale experiments were conducted at the Air Force Institute of Technology's (AFIT) Bioenvironmental Lab, Wright-Patterson Air Force Base Ohio. Room temperature of the lab was 21°C, and the humidity ranged from 67-86%. Sample analysis was conducted on the GC-MS (Agilent® 7890A and MSD Agilent® 5975C) at the U.S. Air Force School of Aerospace Medicine Occupational and Environmental Health (USAFSAM/OEA) Industrial Hygiene Laboratory, Wright-Patterson Air Force Base, Ohio. The UV-Vis Spectrophotometer (Agilent® Cary 60) at AFIT was used to analyze samples obtained during additional GAC kinetic experiments and is discussed further in Appendix B.

The chemicals consumed during this study were in their pristine state. Reagent grade 2,4-dinitrotoluene (DNT) was obtained from Sigma-Aldrich® (St Louis, MO). The DNT was 97% pure with a vapor pressure of 1 mmHg (102.7° C) and melting point of 60-70 °C (Sigma-Aldrich, 2015). Analytical grade Potassium Chloride (KCl) was obtained from Fisher Chemical (Fair Lawn, NJ). The KCl has a melting point of 773 C°, molecular weight of 74.55 mg mol<sup>-1</sup>, and is 99.0% pure. Additional material used during the study included de-ionized water (DIW) from the reverse osmosis unit (# 67/41-230-BN, U.S. Filter Corp.).

### **Adsorbents**

The adsorbents used during the study included HWP-Biochar, F-600 GAC, and two different forms of CNT-HS. Differences in preparation methods may be responsible

for some of the differences observed between the GAC and HWP-Biochar and the CNT-HS. The procedure used for prepping the GAC before the start of the experiments differed from that of HWP-Biochar and the CNT-HS. Both the HWP-Biochar and CNT-HS were used in their pristine states after receipt. However, GAC was pulverized with a mortar and pestle in order to increase homogeneity of the granules, and reduce variance in DNT adsorption within the triplicate data set. Randtke and Snoeyink (1983) inferred that adsorptive capacities of adsorbents are altered by preparation. The heterogeneity of the HWP-Biochar may have caused an outlier due to variance in DNT adsorption by the pellets.

A sample of 500 g of GAC (FILTRASORB 600-M, F-600) was acquired from Calgon Carbon Corporation. The characteristics and pore size properties of GAC are displayed in Table 2. The GAC was grinded with a mortar and pestle and passed through US Sieve size 80 mesh but was retained on 200 mesh resulting in GAC with a log mean particle diameter of 0.12 mm. Scanning electron microscope (SEM) images of the pulverized GAC taken at the University of Dayton are displayed in Figure 2A and Figure 2B. GAC was rinsed with DI water in a beaker and allowed to settle for ~45 seconds prior to decanting to remove any fines. Washing was repeated eight times until the decanting solution appeared clear and free of fines. After washing, the GAC was transferred to a vacuum oven and dried at 40° C for 24 hours or until mass no longer changed between 2-hour weigh times. Once it was determined the GAC was dry, it was transferred to a vial and placed in a desiccator for future use. Li et al. (2002) performed elemental analysis of pulverized F-600 GAC and showed the chemical makeup of GAC by wt. % to be  $92.50 \pm 1.68$  Carbon,  $0.61 \pm 0.07$  Hydrogen,  $0.41 \pm 0.01$  Nitrogen, and 2.60

Oxygen (Li et al., 2002). The standard deviation for Oxygen was not available. These characteristics make pulverized F-600 GAC hydrophilic and appropriate for adsorption of polar contaminants such as DNT.

A sample of hardwood pellet biochar was obtained from the University of Colorado-Boulder (Boulder, CO). The HWP-Biochar was made in a 55-gallon Top-Lit Up-Draft (TLUD) biomass gasifier at temperatures of 750 to 950 °C that is described by Kearns (2012). The HWP-Biochar has a log-mean diameter of 1.29 mm and passes through an 8 x 30 sieve (2.36 mm x 0.60 mm). Figure 3A through Figure 3C display SEM images of the HWP-Biochar pellets taken at AFIT and scaled from 2-200  $\mu$ m. The figures illustrate the porous structure of the char and high surface area. The HWP-Biochar was unaltered after receipt and used in its pristine form during the study.

CNTs fixed to reticulated vitreous carbon-foam (RVC-foam), and fabric substrates were obtained from Wright State University (WSU). In this study, the CNT structures are referenced as CNT-HS collectively, and separately as CNT-Foam or CNT-Fabric. WSU acquired the RVC-foam from Ultramet© Inc., which is 80 ppi (pores per inch) grade. CNT-Foam characteristics were estimated from SEM analysis and literature (Table 1). Vijwani (2015) describes the growth of the CNTs on RVC-foam by chemical vapor deposition (CVD). The chemical characterization of the CNT-Foam after CVD is shown to contain carbon, no trace of iron, and reduced oxygen composition inferring pristine CNT (Vijwani, 2015). The surface chemistry of the CNT-HS makes them a probable candidate for  $\pi$ - $\pi$  bonding on DNT's conjugated double bonds. Figure 3 shows SEM images of the CNT-Foam and CNT-Fabric substrates before and after CVD, taken and provided by WSU.

The CNT-HS were cut to mass after receipt and used in their pristine state during the study.

### **Preparation of Stock Solutions**

Stock solutions of  $50 \text{ mg L}^{-1}$  DNT were prepared in amber glassware or covered by aluminum foil to avoid photodegradation of the analyte. Approximately 100 mg of DNT was weighed on a digital scale and placed in a 2 L volumetric flask. DI water was added to the flask and brought to volume. A Teflon magnetic stir bar was placed in the solution, and the flask was sealed with parafilm tape and covered with aluminum foil in order to prevent photodegradation. The flask was vigorously shaken for approximately 30 seconds and then placed on a stir plate at medium setting for 7 days. Following 7 days, the DNT solution was removed from the stir plate and visually inspected in order to ensure all flakes had gone into solution. The sealed flask was placed in a fridge for later use.

Stock solution of 1000 mM KCl was prepared by adding 74.55 g of KCl to a 1 L amber volumetric flask. DI water was added to the flask and brought to volume. The solution was shook until the KCl dissolved. Parafilm was used to seal the volumetric flask for storage and later use. The ionic strength of all solutions used in the kinetic and isotherm experiments was set to 10 mM (KCl).

### **Calibration Curve Procedures**

The DNT calibration curve was prepared from a stock solution of  $50 \text{ mg L}^{-1}$  DNT. The stock solution was diluted with DI water to the range of calibration curve

concentrations (0.1- 50 mg L<sup>-1</sup> DNT). The DI water and stock solution were at room temperature prior to mixing. Ten milliliters of each concentration were placed in a test tube and vortexed for 30 seconds. One milliliter of each concentration was pipetted into a 2 mL amber GC vial, capped and stored in the fridge for later analysis by GC-MS. The GC-MS calibration curves are discussed further in Appendix B (Figure B 11 - Figure B 17).

### **Adsorption Kinetics**

The kinetic experiments measured the uptake of a known DNT concentration in DI water over time in the presence of a known mass of adsorbent. It was estimated from previous work that equilibrium occurred before 24 hrs. An equilibrium time of 48 hours was chosen for the kinetic and isotherm studies. The concentration of 15 mg L<sup>-1</sup> DNT used during the kinetics study was prepared from the stock solution of DNT. The kinetic experiments were conducted in bottles containing 250 and 500 mL DNT solutions. The GAC data reported were conducted in volumes of 500 mL solutions while the CNT and biochar data were conducted in 250 mL solutions. The standard volume of 250 mL was chosen for the kinetic CNT and biochar experiments in order to minimize variation found within the triplicates and use a more representative sample of the adsorbent.

KCl was added to the solutions to set the ionic strength of the DNT impacted water at 10 mM. Teflon stirring bars were placed in the reactor bottles after the solutions were brought to volume. Triplicate reactor bottles were used with the 250 mL and 500 mL solutions. Triplicate controls were utilized during the kinetic studies and set at 15 mg L<sup>-1</sup> DNT with an ionic strength of 10 mM KCl.

Samples were pipetted from the DNT aqueous solutions prior to the addition of the adsorbent in order to determine the initial concentrations. Aliquots of 4 milliliters were pipetted into a flask and then transferred with a 10 mL Luer-Lok<sup>®</sup> syringe with a 0.20- $\mu$ m PTFE-membrane disc filter (Cole-Parmer<sup>®</sup>) to test tubes. The filters were washed with 10.0 mL of DI water prior to filtering the DNT impacted solution. Two milliliters of the aliquot was wasted through the filter while the remaining 2 milliliters were retained in test tubes and covered with aluminum foil in order to prevent photodegradation while being stored in the fridge. Upon completion of the kinetic experiments, 1 mL of the retained filtered samples were transferred to 2 mL amber GC vials and analyzed by GC-MS.

The mass concentration of GAC studied during the kinetic experiments was 30 mg L<sup>-1</sup>. The adsorbents were weighed on an 8 digit scale (METTLER TOLEDO XP26). The start time for the kinetics experiment was recorded when the adsorbent made initial contact with the DNT solution. After the addition of the adsorbent, the reactor bottles were sealed and placed on the Magnetic Hotplate Stirrer (RT 15 Power IKAMAG<sup>®</sup> 15-Position Analog), 115 V at ~550 rpm. Clear reactor bottles were covered in aluminum foil in order to prevent photodegradation. At designated times; 4 milliliter samples were collected with a pipette while the solutions remained on the stir plate. The 4 milliliter samples were drawn between 0 and ~48 hours. The samples were filtered as described previously. The pH of each solution was also measured and recorded at designated times during the kinetic experiment using the pH mV/ORP reader (METTLER TOLEDO SevenMulti, Toledo, OH). The bottles were only removed from the stir plate in order to measure the pH. The end time for each sample draw was recorded after the sample

passed through the filter and separated from the adsorbent. Samples were stored as described previously.

The CNT kinetic experiment was normalized to the CNT mass of the CNT-HS, and conducted in 250 mL solutions. The CNT mass comprised 1% of the CNT-Fabric structure and 8.9% of the CNT-Foam structure. In order to compare a similar adsorbent mass to GAC and biochar, the mass concentration was increased to 375 mg L<sup>-1</sup> for both CNT-Foam and CNT-Fabric.

The HWP-Biochar kinetic experiment was conducted in 250 mL solution with 30 mg L<sup>-1</sup> mass concentrations. The same method as described previously was utilized.

### **Adsorption Isotherms**

In the isotherm study experiments, the initial and final concentrations of DNT impacted solution in the presence of a known mass of adsorbent at 0 and 48 hours was measured. The concentration of DNT used during the isotherm study was prepared from the stock solution of DNT. KCl was added to the solutions to set the ionic strength of the DNT impacted water at 10 mM. The initial concentrations of DNT used for the isotherm experiment were 0.15, 1.5 and 15 mg L<sup>-1</sup>. An additional isotherm experiment conducted with GAC investigated initial DNT concentrations of 25 mg L<sup>-1</sup> and 40 mg L<sup>-1</sup>. The volume of DNT solution used during the isotherm experiments was set at 250 mL. The concentrations were measured in triplicate, and single controls for each concentration were utilized.

As described in the kinetics study, initial samples were pipetted and filtered from the solutions prior to the addition of the adsorbent in order to establish the initial

concentration or control ( $C_0$ ). The mass concentration of GAC and HWP-Biochar used during the isotherm study was  $30 \text{ mg L}^{-1}$ , while the mass concentration of the CNT-Foam and CNT-Fabric was  $375 \text{ mg L}^{-1}$ . The mass of the adsorbents were weighed in the same manner as described in the kinetic study. The start time for the isotherm experiment was recorded when the adsorbent made initial contact with the DNT solution. After the addition of the adsorbent, the reactor bottles were sealed and secured on the stirplates as previously described. At the completion of 48 hours, samples were drawn and filtered. The end time for the isotherm experiment was recorded after the sample was filtered into the test tube and separated from the adsorbent. The test tubes were covered with aluminum foil in order to prevent photodegradation and placed in a fridge. One mL of the retained filtered sample was analyzed by the GC-MS.

### **Data Analysis**

The samples were successfully acquired and analyzed by GC-MS using a single ion monitoring (SIM) method. The sequences established for the GC-MS utilized blanks of DI water and methanol between the triplicate samples. By placing the blanks between the triplicate samples, DNT instrument carryover into the blanks could be identified. The area counts in the DNT blanks before and after each triplicate data set were averaged and subtracted from each sample. This method of removing the carryover from each triplicate data set was employed on all GC-MS sequences. The observed DNT carryover concentrations ranged from  $0.085 - 2.85 \text{ mg L}^{-1}$  while analyzing  $0.15 - 15 \text{ mg L}^{-1}$  DNT, respectively. The samples with higher concentrations, particularly the controls, produced more carryover into the blanks.



The solid phase DNT concentration ( $q_e$ ) on adsorbents and the liquid phase concentration ( $C_e$ ) of DNT were determined for kinetic and isotherm studies. A Q-test with a 90% confidence interval was performed on any suspect numbers found within the triplicate data set in order to identify outliers (Table 7 - Table 11). Outliers were removed from the data set and replaced by the average of the remaining 2 points. Further discussion of the Q-test statistical analysis is included in the appendix B. The mean of the initial concentrations was used to establish  $C_0$ . The effluent concentrations were subtracted from  $C_0$  in order to determine the change in concentration and calculate  $q_e$  using equation 2. The  $q_e$  values were averaged at time (hrs), and two standard deviations were calculated and displayed as error bars in figures. The normalized concentrations were displayed in figures as  $C_e/C_0$  at time (hrs).

Zeroth, first, and, second order kinetic rates were explored. Data was fit to each model, and the best-fit was determined by linear regression analysis comparing  $R^2$  values. The reaction rate ( $k$ ) was determined from the slope in the equation of the line in the best-fit model. The statistical package JMP<sup>®</sup> was used to qualify data generated from HWP-Biochar kinetic experiment and data generated from the F-600 GAC Isotherm experiment. JMP<sup>®</sup> is a statistical software program designed for analysis of scientific data.

Data from the isotherm experiments were fit to Langmuir and Freundlich isotherm models, and the best-fit was determined by linear regression analysis comparing  $R^2$  values. Freundlich equilibrium constants were determined, and findings were compared to results found in literature.

## 2.4 RESULTS AND DISCUSSION

### Scanning Electron Microscope (SEM) Analysis

SEM images of the adsorbents taken during this study are illustrated in Figures 2 - 4. The SEM images of the pulverized GAC were taken at the University of Dayton and are represented in Figure 2. Figure 2A is scaled to 300  $\mu\text{m}$  and shows multiple pulverized granules while Figure 2B shows a single granule scaled to 100  $\mu\text{m}$ . SEM images taken at AFIT of the HWP-Biochar pellets are shown in Figure 3. Figure 3A is scaled to 200  $\mu\text{m}$  and represents multiple pellets, and Figure 3B shows a single pellet scaled to 20  $\mu\text{m}$ , and Figure 3C is scaled to 2  $\mu\text{m}$ . SEM images taken at Wright State University of the nano-substrates before and after chemical vapor deposition (CVD) are shown in Figure 3. Figure 3A displays the foam substrate scaled to 100  $\mu\text{m}$  prior to CVD while Figure 3B is the CNT-Foam structure scaled to 100  $\mu\text{m}$  after CVD. A noticeable impressive difference of the substrate is evident after the CVD process. Figure 3C illustrates the fabric substrate scaled to 10  $\mu\text{m}$  prior to CVD while Figure 3D is the CNT-Fabric structure scaled to 10  $\mu\text{m}$  after CVD. Wright State University estimated the values of CNT morphology and the specific surface area of the CNT-Foam structure using SEM analysis and findings from literature. The surface characteristics of the 80 ppi RVC-foam are shown in Table 1. Additionally, Wright State estimated the average length of CNT arrays and growth rate of CNTs through the CNT-Foam structure. The CNT-Foam structures used in this study had a CVD run time of 30 minutes and 17  $\mu\text{m}$  average length of CNT arrays and CNT growth rate through the foam of 0.6  $\mu\text{m}$  per minute.

All images illustrate the macropore range of the adsorbents. Figures 2 and 3 illustrate the heterogeneity of GAC and biochar; however, Figure 4 shows the homogeneity of the CNT-Hybrid structures. The CNTs appear as a homogenous layer over the surface of the Foam and Fabric substrates.

**Table 1. Estimated values of CNT-Foam (RVC 80 ppi) characteristics obtained from Wright State University determined from SEM analysis and literature**

Avg. Outer Diameter, $D_o$	18	nm
Avg. Inner Diameter, $D_i$	8	nm
Avg. Number of walls, $n$	15	#
Density of MWCNT, $\rho_{MW}$	1.86	$\text{g}/\text{cm}^3$
Area Density of CNT on RVC, $N_A$	$1.5 \times 10^{10}$	$\#/\text{cm}^2$
SSA of RVC foam, $A_0$	45	$\text{cm}^2/\text{cm}^3$
Density of RVC foam, $\rho_{RVC}$	0.045	$\text{g}/\text{cm}^3$
BET SA of CNT on RVC foam	2.312	$\text{m}^2 \text{g}^{-1}$

**Table 2. Calgon F-600 GAC Characteristics and Pore Size Distribution obtained from literature (Kempisty, 2014)**

Base Material	U.S. Sieve Size	Iodine # (mg/g)	Apparent bed density ( $\text{g}/\text{cm}^3$ )	Size distribution	Specific Volume (mL/g)	%
Reagglomerated Virgin Bituminous	12 x 40	850	0.62	Adsorption pores (<10 nm)	0.32	19.80%
				Transport Pores (>10 nm)	1.3	80.20%

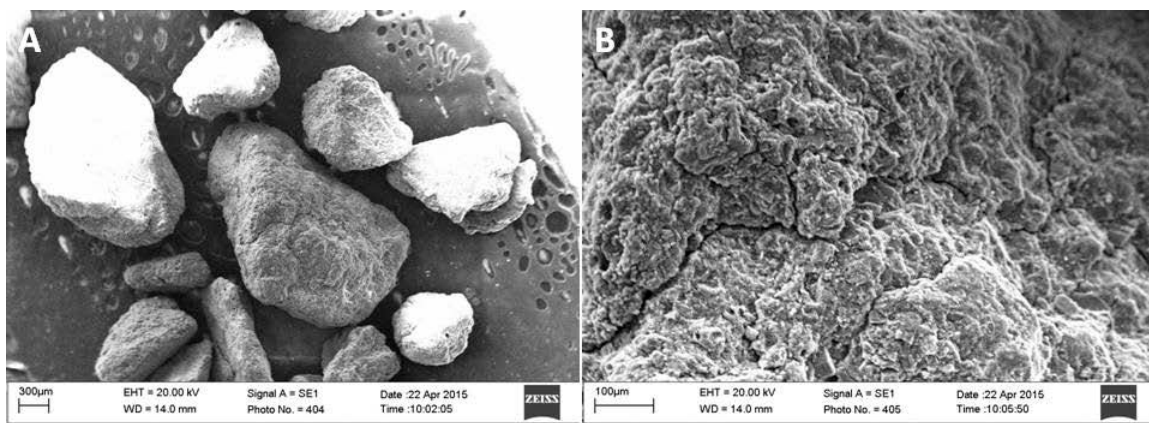


**Figure 2. SEM images of the grinded GAC granules. Multiple GAC granules are visible in Figure 2A and scaled to 300  $\mu\text{m}$  while Figure 2B shows a single GAC granule scaled to 100  $\mu\text{m}$**

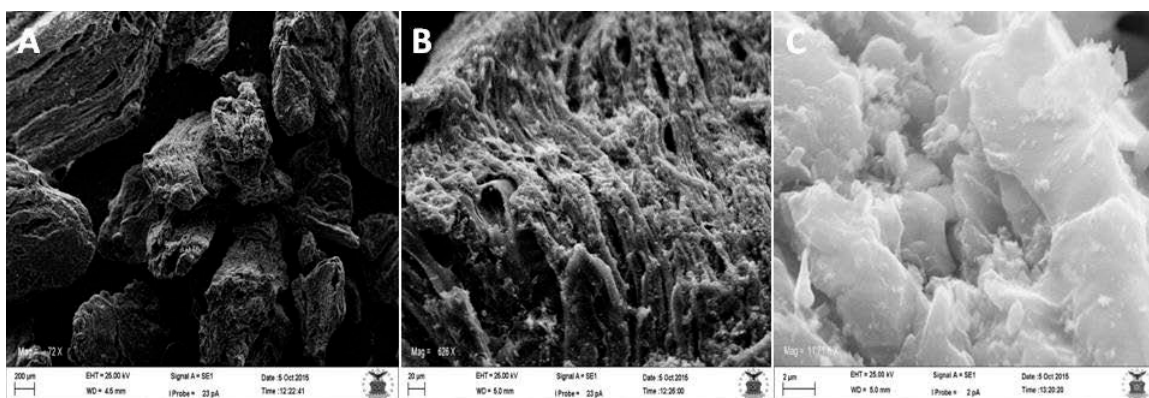


**Figure 3. SEM images of HWP-Biochar pellets. Figure 3A is scaled to 200  $\mu\text{m}$  and contains multiple pellets. Figure 3B shows a single pellet and is scaled to 20  $\mu\text{m}$ , and Figure 3C is scaled to 2  $\mu\text{m}$**

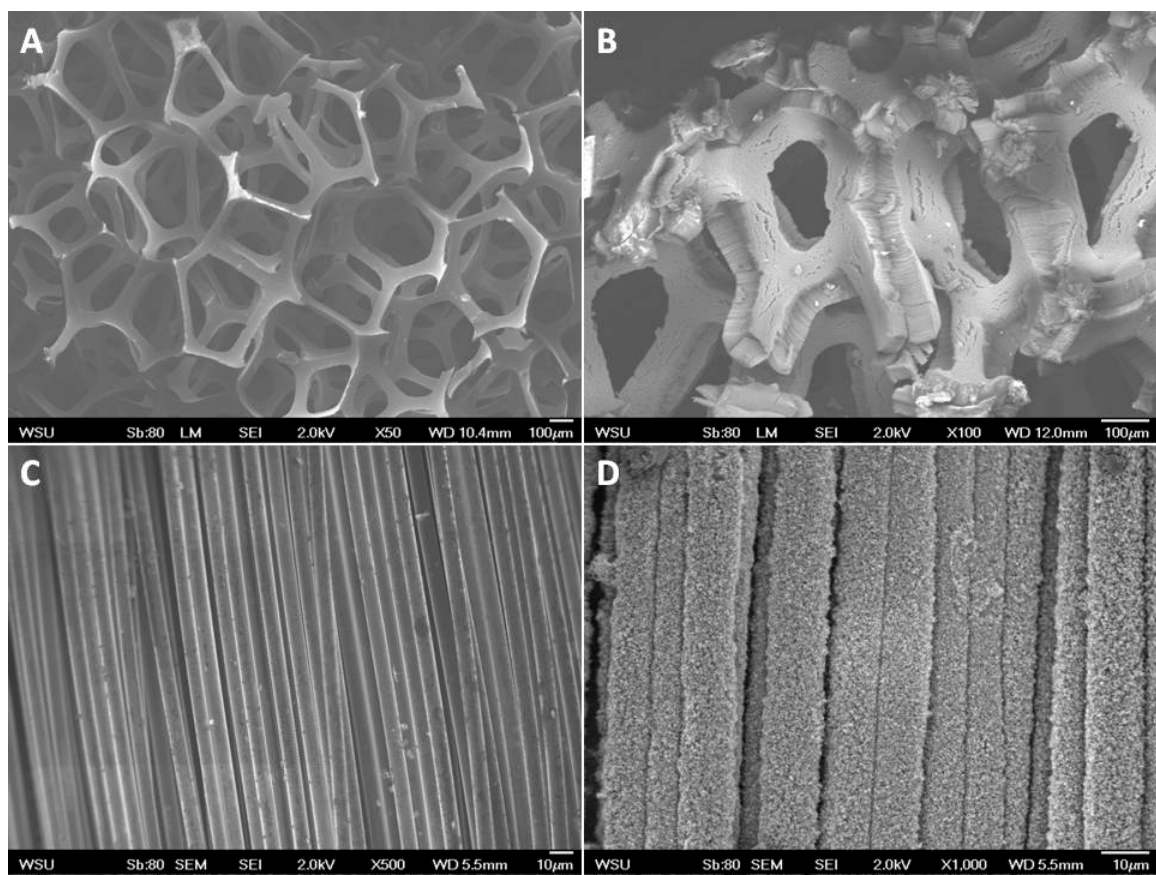


**Figure 4. SEM images of the substrates before and after CVD. Figure 4A shows the foam substrate scaled to 100  $\mu\text{m}$  prior to CVD while Figure 4B is the CNT-Foam scaled to 100  $\mu\text{m}$  after CVD. Figure 4C displays the fabric substrate scaled to 10  $\mu\text{m}$  prior to CVD while Figure 4D is the CNT-Fabric scaled to 10  $\mu\text{m}$  after CVD**

### Adsorption Kinetic Results

The samples were successfully acquired and analyzed by GC-MS using the single ion monitoring (SIM) method. The solid phase concentrations ( $q_e$ ) were calculated at time (hrs) and averaged. Figure 5 displays  $q_e$  (mg DNT  $\text{g}^{-1}$  adsorbent) over  $t$  (hrs) for GAC, HWP-Biochar, and CNT-Foam. The error bars represent two standard deviations. CNT-Fabric was not displayed since the  $q_e$  calculated values were negative at 48 hours and the variation within the triplicates fell above and below the x-axis throughout. At 48 hours, GAC obtained the highest  $q_e$  concentration of  $205.82 \pm 1.71 \text{ mg g}^{-1}$  (2 standard

deviations), followed next by HWP-Biochar with  $90.99 \pm 16.60 \text{ mg g}^{-1}$ , and then CNT-Foam with  $11.37 \pm 9.38 \text{ mg g}^{-1}$ .

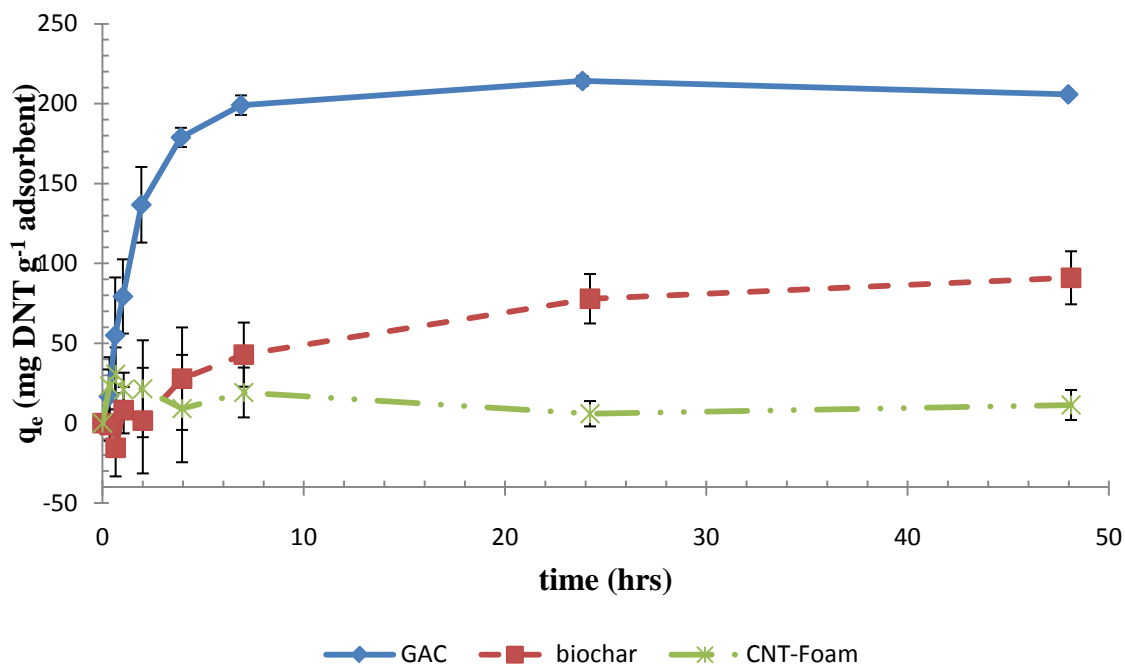


**Figure 5. Kinetic solid phase concentrations at time (hrs). The error bars represent 2 standard deviations. At 48 hours, GAC obtained the highest  $q_e$  concentration of  $205.82 \pm 1.71 \text{ mg g}^{-1}$ , followed next by HWP-Biochar with  $90.99 \pm 16.60 \text{ mg g}^{-1}$ , and then CNT-Foam with  $11.37 \pm 9.38 \text{ mg g}^{-1}$**

The normalized DNT concentrations for each adsorbent were calculated and displayed together in Figure 6. The error bars represent two standard deviations. The CNT kinetic experiment was normalized to the CNT mass of the CNT-HS. The percentage of DNT removal at 48 hours obtained by GAC was  $55.4 \pm 0.02\%$  while HWP-Biochar achieved  $19.08 \pm 0.04 \%$  and CNT-Foam achieved  $0.03 \pm 0.03\%$ . However, it appears that the equilibrium time of DNT adsorption by HWP-Biochar is longer than 24 hours and potentially extends past 48 hours. This is indicated in Figure 5 and shows the

$q_e$  value for HWP-Biochar increasing between 24 to 48 hours. The size of the char used in this study had a log-mean diameter of 1.29 mm and is an order of magnitude larger than the pulverized F-600 granules log-mean diameter of 0.12 mm. The larger char pellets have longer adsorption pathways that extend equilibrium time.

Separate figures for each normalized adsorbent concentrations were created and displayed with their controls (Figure B 1 - Figure B 3) and is included in Appendix B. It was observed that when CNT-Foam is displayed with the control, the normalized control concentration is lower than CNT-Foam (Figure B 3). The lower control concentration infers that the adsorption observed by CNT-Foam may be due to degradation of the sample. Degradation may have occurred by photodegradation when the sample was transferred from the reactor bottles to the test tubes and then from the test tubes to GC-MS vials. A possible explanation why significant DNT adsorption onto CNT-HS was not observed is because DNT adsorption occurs by an alternate mechanism. DNT adsorption on the CNT-HS could be more chemical in nature instead of physical. Furthermore, surface chemistry modification may have occurred during chemical vapor deposition and prevented adsorption. Pure CNTs are hydrophobic in nature and may have prevented water percolation through the CNT matrix. Future research should investigate the effect of various functional groups such as  $-OH$ ,  $-C=O$ ,  $COOH$ , which can be deliberately introduced onto CNT surfaces by acid oxidation (Lou et al., 2014). The functional groups cause CNTs to be more hydrophilic and appropriate for the adsorption of polar contaminants (Yang et al., 2013) such as DNT. Pre-wetting measures have also been used to alter the surface of CNT-HS that were created using CVD. Karumuri et al. (2015) investigated two types of surface modifications on CNT-HS that included an

application of a silica coating. The silica coat is identified as a “wet-sol gel oxide coating” and described by Karumuri et al. (2015). The treatment with the silica gel caused the CNT-HS to become permanently hydrophilic and increased the water flow through the structure (Karumuri et al., 2015). In addition, some rotational speeds can trap air bubbles around samples preventing water or contaminants from making contact with the surface. Future work should investigate pre-wetting measures and different rotational speeds. Furthermore, the feasibility of growing nanotubes onto the surface of GAC or biochar should be explored. This could potentially increase the surface area of the carbon material and increase the DNT adsorptive capacity.

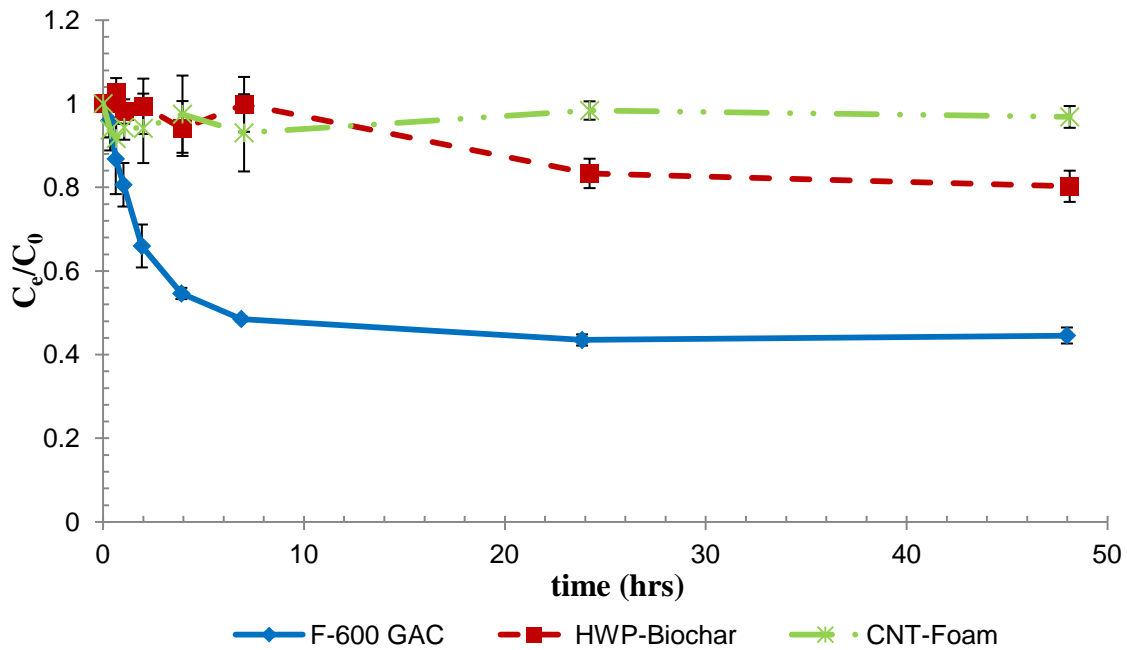


**Figure 6. Normalized liquid phase concentrations at time (hrs). The error bars represent 2 standard deviations. The percentage of DNT removal at 48 hours obtained by GAC was  $55.4 \pm 0.02\%$  while HWP-Biochar achieved  $19.08 \pm 0.04\%$  and CNT-Foam achieved  $0.03 \pm 0.03\%$**



In order to determine the rate constant for the kinetics reaction, zeroth, first, and second order rates were explored and the data was fit to the corresponding models. Since equilibrium was assumed to occur prior to 24 hours, we used the data from 0 to 7 hours to determine the reaction rate. Linear regression analysis was employed, and the best  $R^2$  values were used to identify the best-fit model. However, when fitting the HWP-Biochar data, an outlier was visually identified.  $T^2$  statistical analysis was conducted in JMP<sup>®</sup> software and confirmed that the point fell outside the upper control limit in the second order rate model.  $T^2$  statistical analysis is a method of identifying outliers in a multivariate scatter plot. The method measures the squared distances between the points and determines an upper control limit. Points that fall above the upper control limit may be rejected and considered outliers (Figure B 21). Removing the outlier significantly increased the  $R^2$  value for HWP-Biochar in all models. HWP-Biochar second order rate analysis with and without the outlier is displayed in Appendix B, along with the scatter plot generated using JMP<sup>®</sup>. All adsorbents fit best with the second order kinetics model, however, CNT-Foam did not significantly favor one model over another. Second order kinetics for these adsorbents can be seen in Figure 7. The zeroth and first order rate models are included in Appendix B.

GAC and HWP-Biochar achieved an  $R^2$  value of 0.93 in the second order rate model, and CNT-Foam achieved 0.28. The second order rates,  $k$ , are displayed in Table 3 with the DNT uptake by GAC shown to be  $0.012 \text{ (mg/L)}^{-1} \text{ (hr)}^{-1}$  and HWP-Biochar to be  $0.0015 \text{ (mg/L)}^{-1} \text{ (hr)}^{-1}$  (Table 3). The reaction rate for CNT-Foam was shown to be negative, which was due to negative adsorption at various time intervals between 0 and 7 hours and, therefore, is not included in Table 3.

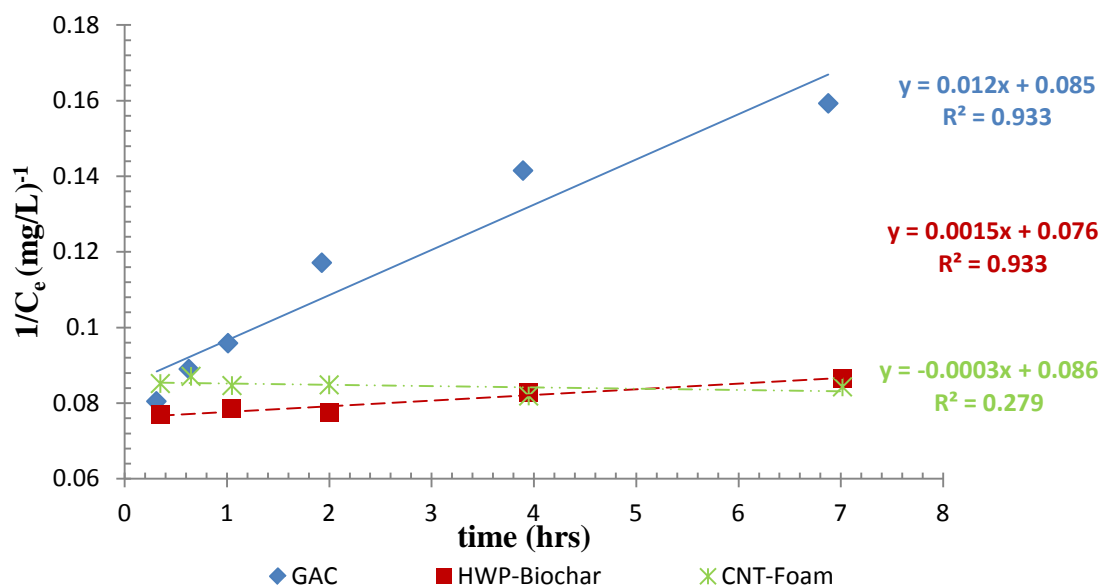


**Figure 7. Second order kinetic rate analysis. Linear regression analysis determined that GAC and HWP-Biochar both achieved an  $R^2$  value of 0.933 while CNT-Foam was 0.279**

**Table 3. Second order reaction rate constants determined from linear regression analysis. The rate for CNT-Foam and CNT-Fabric are not displayed because of negative adsorption between 0 and 7 hours**

Adsorbent	second order reaction rate constant, $k \text{ (mg/L)}^{-1} \text{ (hr)}^{-1}$
F-600 GAC	0.012
HWP-Biochar	0.0015

### Adsorption Isotherm Results

The objective of the adsorption isotherm experiments were to measure the solid phase equilibrium concentrations and fit the results to Langmuir and Freundlich isotherm

models. Samples were successfully obtained and analyzed on the GC-MS using the same method as described in the Data Analysis section. However, when fitting the F-600 GAC data to the Freundlich model, an outlier was visually identified. T<sup>2</sup> statistical analysis was conducted in JMP<sup>®</sup> and confirmed that the point fell outside the upper control limit. The F-600 GAC Freundlich Isotherm analysis included models with and without the outlier. Removing the outlier significantly increased the R<sup>2</sup>. The Freundlich model with and without the outlier is displayed in Appendix B, along with the scatter plot generated using JMP<sup>®</sup>. Linear regression analysis comparing the R<sup>2</sup> values showed that F-600 GAC fits best to the Freundlich Isotherm model while HWP-Biochar favored Langmuir (Figure 8 and Figure 9). CNT-Foam failed to significantly prefer either model and, therefore, is not displayed in the figures. Conversely, CNT-Fabric preferred and fit best to the Langmuir model. Appendix B shows CNT-Foam and CNT-Fabric data fit to Freundlich and Langmuir isotherm models. The Langmuir model infers that adsorption equilibrium is the result of a chemical reaction between the surface of the adsorbent and the solution (Crittenden et al., 2005). Equation 4 shows the linear form of the Langmuir equation. Whereas the Freundlich model infers that adsorption follows an empirical equation and explains the heterogeneity of the adsorbent (Crittenden et al., 2005). The Freundlich constant K<sub>F</sub> describes the equilibrium adsorption capacity of the adsorbent while  $\frac{1}{n}$  signifies the heterogeneity of the site energies on the adsorbent's surface (Kanel et al., 2015; Kearns, et al., 2014). Equation 3 displays the linear form of the Freundlich model. The Freundlich constants were calculated and are displayed in

Table 4. The  $K_F$  value for GAC was found to be  $111.69 (\text{mg g}^{-1})(\text{L mg}^{-1})^{1/n}$  with a  $\frac{1}{n}$  value of 0.24. While the  $K_F$  value for HWP Biochar was found to be  $37.33 (\text{mg g}^{-1})(\text{L mg}^{-1})^{1/n}$  with a  $\frac{1}{n}$  value of 0.51. The Freundlich constants for CNT-Foam and CNT-Fabric were not reported due to poor fit to the model, and large variation above and below the x-axis at  $C_0$   $15 \text{ mg L}^{-1}$  DNT. The  $K_F$  and  $\frac{1}{n}$  values observed for HWP-Biochar falls within the range of values observed by Kearns et al. (2014) in their biochar adsorption of 2,4-D study.

CNT-Foam and CNT-Fabric did achieve a removal of DNT during the isotherm experiment with no degradation observed within the controls at  $C_0$  of  $0.15$  and  $1.5 \text{ mg L}^{-1}$ . The observed adsorption at lower concentrations but not at higher concentrations may be due to saturation of the CNT-HS at higher  $C_0$ . The low adsorption capacity for the CNT samples at higher DNT concentrations may be due to the small mass of adsorbent. The CNT mass fixed to CNT-Foam was 8.9% of the total mass of the structure, while the CNT mass on the CNT-Fabric was only 1% of the structure. Any adsorption that occurred with the small mass was masked by the high  $C_0$  values of DNT and was not significant enough to be observed. Furthermore, literature shows that F-600 GAC has a BET surface area (SA) of  $820 \text{ m}^2 \text{ g}^{-1}$  (Quinlivan et al., 2005), and preliminary work with HWP-Biochar observed a BET SA of  $462 \text{ m}^2 \text{ g}^{-1}$ . Whereas the surface area of the CNT-Foam with a CVD run time of 30 minutes is estimated to be only  $2.3 \text{ m}^2 \text{ g}^{-1}$ . Increasing the length of the CNTs will change the fraction of CNT surface per unit mass of substrate, and potentially significantly influence kinetics and capacity.

The observed Freundlich constant  $K_f$  for F-600 GAC in this study were lower compared to the findings of Ho and Daw (1988). However, the F-600 GAC  $\frac{1}{n}$  value fell within range of observed values reported in literature (Table 6). Additionally, F-600 GAC achieved a higher  $q_e$  value at initial concentrations of  $15 \text{ mg L}^{-1}$  DNT concentration (Table 5), although at the lower initial concentrations of  $0.15$  and  $1.5 \text{ mg L}^{-1}$ , HWP-Biochar achieved a comparable  $q_e$  value to GAC.

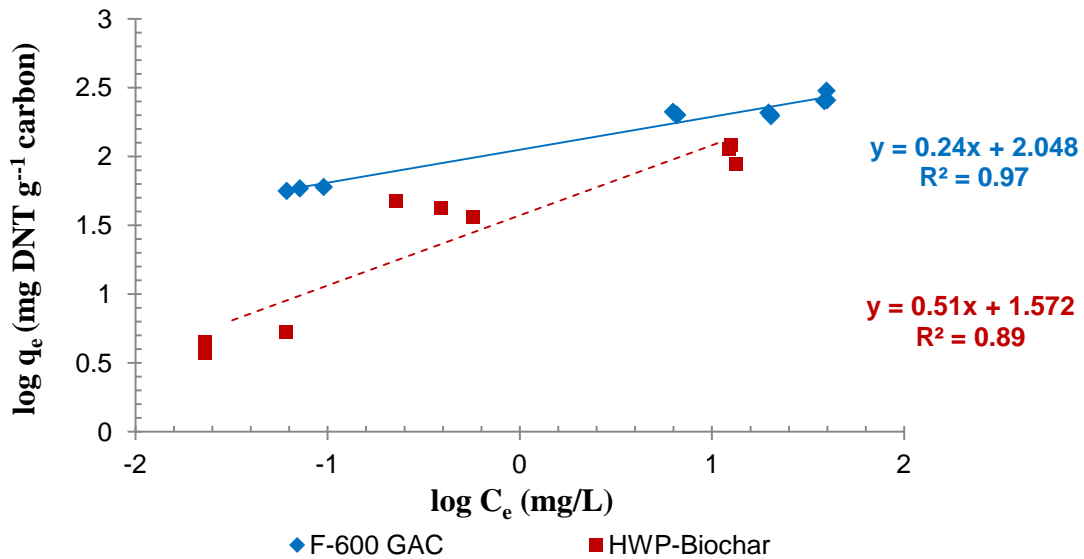


**Figure 8. Freundlich Isotherm models for GAC and HWP-Biochar. Linear regression analysis shows that F-600 GAC fits the Freundlich Isotherm model the best with an  $R^2$  value of 0.97**

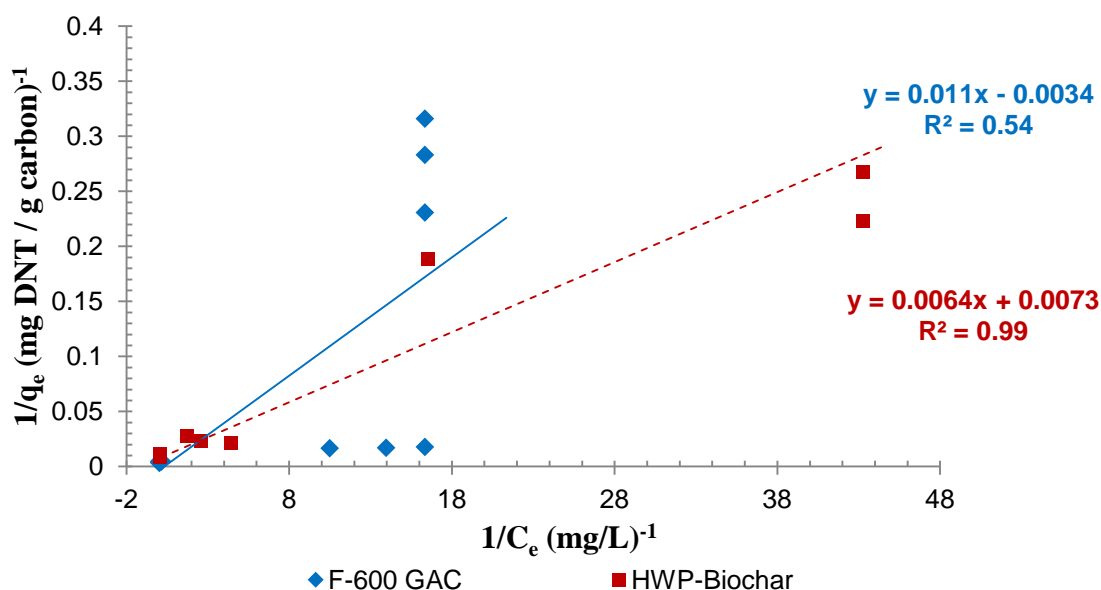


**Figure 9. Langmuir Isotherm models for GAC and HWP-Biochar. Linear regression analysis shows that HWP-Biochar fits the Langmuir Isotherm model the best with an  $R^2$  value of 0.99**

**Table 4. Freundlich constants  $K_F$  and  $1/n$ . The  $R^2$  value was determined from linear regression analysis using Figure 8**

Adsorbent	$K_F(\text{mg g}^{-1})(\text{L mg}^{-1})^{1/n}$	$1/n$	$R^2$
F-600 GAC	111.69	0.24	0.97
HWP-Biochar	37.33	0.51	0.89

**Table 5. Averaged solid phase concentrations ( $q_e$ ) observed from the Isotherm study at the initial known concentrations.  $q_e$  ( $\text{mg g}^{-1}$ ) is displayed with 2 standard deviations**

Adsorbent	$C_0 \sim 0.15$ $\text{mg L}^{-1}$	$C_0 \sim 1.5$ $\text{mg L}^{-1}$	$C_0 \sim 15$ $\text{mg L}^{-1}$	$C_0 \sim 25$ $\text{mg L}^{-1}$	$C_0 \sim 40$ $\text{mg L}^{-1}$
F-600 GAC	$3.7 \pm 1.2$	$58.2 \pm 3.9$	$203.6 \pm 12.1$	$202.0 \pm 11.3$	$269.5 \pm 52.7$
HWP-Biochar	$4.5 \pm 1.6$	$42.1 \pm 10.8$	$106.9 \pm 34.3$	-	-
CNT-Foam	$1.6 \pm 0.9$	$18.1 \pm 1.6$	$2.7 \pm 8.5$	-	-
CNT-Fabric	$19.9 \pm 8.4$	$88.1 \pm 99.4$	$29.0 \pm 38.0$	-	-

**Table 6. Freundlich model constants ( $K_F$  and  $1/n$ ) of DNT adsorption onto various adsorbents obtained from results and literature**

Adsorbent	$C_e$ Range, $\text{mg L}^{-1}$	Sample equilibration time	Freundlich Constants		References
			$K_F \text{ mg/g}*(\text{L/mg})^{1/n}$	$1/n$	
<b>GAC (F400)</b>	0.01-2.01	12 days	284	0.157	Speth and Miltner (1998)
<b>GAC (FS300)</b>	~0.1-100	1 day	210	0.171	Ho and Daw (1988)
<b>GAC (FS400)</b>	0.1-100	5 days	300	0.223	Ho and Daw (1988)
<b>PAC (FS300)</b>	0.1-100	5 days	250	0.333	Ho and Daw (1988)
<b>GAC (F300)</b>	NA	2 hrs	146	0.31	Dobbs and Cohen (1980)
<b>SWCNT</b>	0.001-1.09	30 days	41.2	0.35	Chen et al. (2007)
<b>CNT-Yarn</b>	0.37-13.2	3 days	55	0.737	Kanel et al. (2015)
<b>GAC (F-600)</b>	0.37-5.42	1 day	111.69	0.24	This study
<b>HWP-Biochar</b>	0.11-10.33	~2 days *	37.33	0.51	This study

\* results indicate that equilibration for HWP-Biochar may extend past 48 hours

### Cost Analysis

CNTs are considerably more expensive, but cost is expected to decrease as technology matures. Depending on the quality of CNTs, cost can range on the high end of \$750 per gram, and on the low end of \$100 per pound (AZoNano, 2013). The cost of activated carbon can vary between \$0.70 to \$1.25 per pound while the price of regenerated activated carbon fluctuates from \$0.50 to \$0.78 per pound (EPA, 2000). CNTs are 100 times more expensive than GAC. However, if CNTs can be regenerated, this will reduce the cost substantially. But until then, biochar is a prospective substitute, can be made from native materials, and will have a low cost associated with it. Biochar will have more variability from batch to batch due to fewer controls on the manufacturing

process. Non-activated biochar is estimated to cost approximately \$0.12 per pound (Inyang and Dickenson, 2015).

## **2.5 CONCLUSIONS**

The objective of this study was to characterize various carboneous materials and to quantify DNT adsorption capacity and kinetics. The hypothesis that certain carboneous materials will adsorb DNT more effectively than others was tested by various adsorption experiments and characterization work and the findings were compared to results found in literature.

F-600 GAC outperformed HWP-Biochar and CNT-HS and achieved greater solid phase concentrations during the kinetics experiment, and higher  $q_e$  values in the isotherm experiments at the initial concentrations of 1.5 and 15.0 mg L<sup>-1</sup> DNT. Second order reaction rates were determined from the kinetic experiments and data from isotherm experiments were fit to both Freundlich and Langmuir models. Linear regression analysis showed that GAC fit best to the Freundlich Isotherm model while HWP-Biochar and CNT-HS favored the Langmuir model. CNT-Foam showed adsorption at 48 hours during the kinetic studies, however when displayed with the control in the normalized concentration graph, the control showed a lower concentration. This inferred that the adsorption observed by CNT-Foam in the kinetics experiment might be due to DNT degradation. Conversely, CNT-HS did achieve removal efficiency during the isotherm experiment with no degradation observed within the control at initial concentration of 0.15 and 1.5 mg L<sup>-1</sup>, respectively. The observed adsorption at lower concentrations and



not at higher concentrations may be due to saturation of the CNT-HS. Significant DNT adsorption by the CNT-HS may not have been observed at  $15 \text{ mg L}^{-1}$  in the kinetic and isotherm data for this reason. Additionally, low adsorption may be the result of the small surface area of the CNT-HS.

Our findings suggest that HWP-Biochar may be a suitable substitute for GAC as a nitroaromatic adsorbent. At lower concentrations, HWP- Biochar achieved a comparable DNT removal efficiency to GAC in the isotherm studies. Biochar can be manufactured at a reduced cost compared to GAC, and in more austere conditions with native materials.

Future studies should investigate the equilibrium time of DNT adsorption by HWP-Biochar. Oh and Seo (2014) assumed equilibrium of nitroaromatics to biochar by 24 hours, however, this study indicates that equilibrium was not reached until potentially on or after 48 hours. Furthermore, the biochar used in future work should be grinded, washed, and dried using the same method as GAC given that adsorptive capacities have shown to be altered by preparation of the adsorbent (Randtke and Snoeyink, 1983).

## **2.6 REFERENCES**

The references used in this article are provided in the Reference section of the thesis. The reference section of the thesis was formatted following the Journal of Environmental Engineering publication guidelines.

### **III. CONCLUSIONS**

#### **3.1 CHAPTER OVERVIEW**

Chapter III concludes the thesis and discusses the limitations, significance of the findings and future work in the field. Additional findings from appendices A and B are presented which include an expanded literature review and GAC kinetic experiments.

#### **3.2 REVIEW OF FINDINGS**

This study addressed the following investigative questions:

1. To what extent do various carbonaceous materials remove DNT from aqueous sources?
2. Can Hardwood Pellet Biochar and carbon nanotubes that have been fixed to reticulated vitreous carbon foam and fabric substrates be effective adsorbents to remove DNT?

The DNT adsorptive capacities and kinetics of HWP-Biochar and CNT-HS were successfully quantified by GC-MS and compared to conventional F-600 GAC. Second order reaction rates were determined, and data from the isotherm experiments were fit to both Freundlich and Langmuir models. Linear regression analysis showed that GAC fit best to the Freundlich isotherm model while HWP-Biochar and CNT-HS favored the Langmuir. F-600 GAC outperformed HWP-Biochar and CNT-HS and achieved greater solid phase concentrations ( $q_e$ ) during the kinetics experiment, and higher  $q_e$  values in the isotherm experiments at the initial concentrations of  $1.5 \text{ mg L}^{-1}$  and  $15.0 \text{ mg L}^{-1}$  DNT.

At lower concentrations, HWP-Biochar achieved comparable removal efficiency to GAC in the isotherm studies.

### **3.3 LIMITATIONS**

Limitations of the research included time, available resources, and equipment. DNT peaks from instrument carryover over were observed in the blanks of the GC-MS data. Carryover was due to contamination of the needle and rinse solvents from the high number of samples analyzed in each sequence and high concentrations of DNT in each sample. Future work should be conducted at either lower concentrations, or if, in the same concentration range, samples should be diluted prior to analysis on the GC-MS. This practice may limit and perhaps prevent carryover from occurring at higher concentrations and longer sequences.

A limited number of reactor bottles had to be used during isotherm experiments because of the size of the stir plate. A larger tumbler was designed specifically for the study that would have accommodated additional reactor bottles. However, due to logistical issues and equipment malfunctions, the tumbler was not available for use.

### **3.4 SIGNIFICANCE OF FINDINGS**

HWP-Biochar seems promising as a cost effective suitable substitute for GAC as a nitroaromatic adsorbent. We have potentially determined a lower limit of DNT adsorption by mass of the pristine novel CNT-HS and an upper concentration limit where DNT saturation occurs. CNT-HS did achieve removal efficiency during the isotherm

experiment with no degradation observed within the control at initial concentrations of  $0.15 \text{ mg L}^{-1}$  and  $1.5 \text{ mg L}^{-1}$ . The observed adsorption at lower concentrations and not at higher concentrations may be due to saturation of the CNT-HS. Moreover, low overall surface area of CNT is believed to be responsible for poorly observed adsorption; however, wettability issues may have also complicated obtaining values for CNT-HS. By increasing the chemical vapor deposition run time, it has shown to increase specific surface area and contaminate removal efficiency (Vijwani et al., 2015).

### **3.5 FUTURE RESEARCH**

In order to confirm or reject our findings, additional research into the CNT-HS DNT adsorption capacity should be explored. Kinetic and isotherm studies that involve pristine CNTs without substrates should be tested. Preliminary kinetic research investigated Foam and Fabric substrates that were subjected to the CVD process with no observed CNT growth. The results from the kinetic study without CNTs were indistinguishable from the results of the substrates with CNT growth. Additionally, higher CNT mass concentrations should be employed with the fabric substrates in order to make a similar comparison by mass with GAC, and biochar. Lower DNT concentrations should be used for the kinetics experiment to avoid saturation.

HWP-Biochar shows potential as an alternate option to GAC as a nitroaromatic adsorbent. Future studies should incorporate a diverse range of biomass used to make the char. Different biomass will show differences in DNT adsorption and could be explored further. Lastly, the biochar used during the experiment should be grinded, washed, and

dried using the same method as the GAC since adsorptive capacities have shown to be altered by preparation of the adsorbent (Randtke and Snoeyink, 1983).

Furthermore, research needs to determine the feasibility of large scale applications of CNTs in groundwater remediation and wastewater treatment. More specifically, permeable membranes need to be tested in order to determine if they allow adequate contact time to filter and adsorb contaminants, do not result in significant headloss and prevent loss of the nanomaterial to the environment.

## **APPENDIX A. EXPANDED LITERATURE REVIEW**

This section provides supplementary information regarding the rationale of this document detailing the significant problems associated with DNT, including health effects and exposure risk. Methods and results from previous work in the field are also discussed. The topics in the expanded review incorporate the following: DNT, GAC, and CNTs in isotherm and kinetic studies.

### **A.1 2, 4-DINITROTOLUENE (DNT)**

The Environmental Protection Agency (EPA) has categorized DNT as a probable (Class B2) carcinogen, toxic substance and a priority pollutant (EPA, 2014). Experimental research has examined the toxicity of DNT in laboratory animals. Studies conducted with laboratory rats, and mice revealed malignant tumors after exposure to DNT (EPA, 1990). Limited data is available on the adverse human health effects of DNT exposure. However, studies have shown that the human exposure risks of DNT include inhalation, ingestion and dermal contact, and chronic exposure in occupational workers has lead to adverse health effects in the central nervous system and circulatory system (EPA, 2008; NIH, 2015). The federal government chose not regulate DNT under the Safe Drinking Water Act, nonetheless many states have established regulatory guidelines. Currently, Florida, Maine, Wisconsin and New Hampshire all chose to regulate DNT in drinking water (NIH, 2015).

DNT is commonly used in the manufacture of explosives and is not naturally produced in the environment (ATDSR, 2013). It is created by adding nitric and sulfuric acids with toluene and is a standard isomer in TNT production (ATDSR, 2013; Han et al.,

2011). DNT is frequently deposited into soil and water through live-fire and explosive ranges found on military installations. The EPA has categorized the most severe hazardous waste sites in the country and placed them on a National Priorities List (NPL). DNT has been located on 98 of the 1,699 NPL sites as of 2007 (ATDSR, 2013). Current technology and practices utilized in DNT remediation include the following: bioremediation, anaerobic and aerobic biodegradation, chemical reduction, phytoremediation, electrical oxidation, incineration of contaminated soil, alkaline hydrolysis, and activated carbon adsorption (EPA, 2014).

## **A.2 DNT REMEDIATION TECHNOLOGIES**

Oh and Chiu (2009) investigated the reduction of DNT using graphite and n-hexane soot based Black Carbon (BC). They determined that the BC adsorbs a large quantity of the DNT, and the reduction of DNT continues to occur after adsorption. The experimental design utilized 250 mL reactor bottles with 200 mL of 0.227 mM DNT and 10 g of graphite or 0.05 g of n-hexane soot. The reactor bottles were shook in an orbital shaker at 150 rpm, and 1 milliliter samples were drawn with a glass syringe at designated times. The samples were passed through a 25 nm cellulose filter and analyzed using an HPLC and UV-Vis spectrophotometer. The findings of the experiment determined that the concentration of DNT decreased by 33% over a 21 day period in the presence of the graphite and decreased by 62% in the presence of n-hexane soot (Oh and Chiu, 2009).

Wen et al. (2011) employed biodegradation and UV photo-catalysis using a ceramic carrier with  $\text{TiO}_2$ , and an organic sponge to measure the removal of DNT. The organic sponge was prepared by allowing 100 mL of sludge and 20 mL of glucose to pass

through the sponge for 10 days until a thin biofilm accumulated. The sponge was allowed to dry overnight, and both the sponge and the ceramic carrier were placed into two separate 500 mL reactor bottles with 100 mg L<sup>-1</sup> of DNT. The reactor bottles were exposed to a UV lamp and stirred throughout the experiment. The ceramic carrier with UV photo-catalysis observed 71% DNT removal at 60 hours while the organic sponge carrier achieved DNT removal of up to 90% within the first hour of the study. The final concentration of the DNT with the sponge carrier was measured to be 1 mg L<sup>-1</sup> and followed first order kinetics (Wen et al., 2012).

### **A.3 GRANULAR ACTIVATED CARBON (GAC)**

GAC is an excellent adsorbent due to its porous structure and high surface area. GAC has been used in many applications to remove contaminants from aqueous solutions. Some of the investigated contaminants include N-Nitrosodimethylamine (NDMA), polychlorinated biphenyls, bromate, trinitrotoluene (TNT) and DNT (Azizian and Yahyaei, 2006; Beless et al., 2014; Hanigan et al., 2012; Qiu and Xiong, 2015). Numerous studies researched the remediation of DNT from contaminated soil and water sources (Berchtold et al., 2012; Ho and Daw, 1988; Oh et al., 2013; Rajagopal and Kapoor, 2001).

In 1987, the U.S. Army investigated the capacity of GAC to remove explosive contaminants from an Army ammunition plant's effluent wastewater (Hinshaw et al., 1987). The study investigated 5 types of GAC that included Calgon Filtrasorb 200, 300 and 400. The explosive contaminants included 4 compounds: cyclotrimethylenetrinitramine (RDX), cyclotetramethylenetetranitramine (HMX), TNT,



and DNT. GAC adsorption of the explosive contaminants were studied in batch experiments for isotherm studies. The experimental design of the batch experiment utilized 250 mL of explosive contaminated solution in a 500 mL volumetric flask with a carbon dose ranging from 10 - 5000 mg L<sup>-1</sup>. The flasks were agitated and placed in a water bath to maintain the temperature. The results of the batch experiment were fit to Freundlich and Langmuir isotherms and showed that GAC can obtain equilibrium concentrations of 0.0007 mg L<sup>-1</sup> (Hinshaw et al., 1987).

Ho and Daw (1988) conducted DNT adsorption and desorption studies with Calgon Filtrasorb FS300 and FS400 GAC. Their experiment was conducted at the bench scale in 40 mL glass reactor bottles. The experimental design placed a known amount of 10-20 g of GAC in a 25-120 mg L<sup>-1</sup> DNT impacted solution in 40 mL reactor bottles. The reactor bottles were shook for five days in order to achieve equilibrium concentrations. However, they believed that equilibrium was reached within 24 hours. During the desorption studies, the spent carbon was filtered out of the bottle and rinsed with water, and dried in a fume hood for an additional three days. The amount of DNT adsorbed was measured by HPLC. The adsorption capacities of FS300 and FS400 were fit to Freundlich Isotherm models. They discovered that in addition to DNT, there were up to six different products in the carbon. This led them to assume that DNT continues to react once it adsorbs. It was determined that FS400 was more adsorptive than FS300 and grinding FS300 increased the adsorptive capacity. They also concluded that GAC is able to be recycled, and the best method to wash the GAC was with methanol and acetone (Ho and Daw, 1988).

The removal of DNT from wastewater using GAC has also been investigated. Berchtold et al. (1995) studied the treatment of a wastewater solution containing DNT, ethanol, mineral ether, and a carbonate buffer. They used GAC bioreactors to transform DNT into 2,4-diaminotoluene (DAT). The isotherm adsorption data was fit to the Freundlich isotherm model. They determined that DNT was adsorbed to GAC, and the majority of the remaining byproducts were DAT. However, when ethanol was not present during the process, the conversion of DNT to DAT was deficient. This led to the conclusion that 200 mg L<sup>-1</sup> of ethanol was required to reduce DNT to DAT (Berchtold et al., 2012).

Rajagopal and Kapoor (2001) investigated the adsorption capacity of GAC in the presence of DNT, TNT, and nitrobenzene (NB). They developed a GAC column experiment, varied the bed height, and measured the influent and effluent concentrations in order to determine the breakthrough curves of the explosive contaminants. The study found that DNT achieved a higher effluent concentration at a particular bed height and implies GAC favors adsorption of TNT and NB over DNT.

The reduction of DNT using carbon materials as a catalyst for dithiothreitol (DTL) was investigated by Oh et al. (2013). The study used various black carbon materials that included chemically converted graphene, MWCNT, and GAC. The experimental design that Oh et al. (2013) selected incorporated 250 mL amber bottle reactors on a shaker table. At selected time intervals, 1 mL samples were drawn, filtered and then analyzed with an HPLC. Their findings suggest that when GAC and MWCNT are used as a catalyst with DTL for DNT reduction, GAC had slightly more capacity: GAC reduced DNT by 66.5% while MWCNT reduced DNT by 60.7%. However,

kinetically MWCNT was superior: MWCNT reduce DNT by 60.7% in 72 hours, while it took GAC 240 hours to reduce DNT by the 66.5% (Oh et al., 2013).

#### **A.4 CARBON NANOTUBES (CNT)**

CNT use is a relatively novel technology when applied to the environmental field. Innovative applications of CNT technology are regularly being discovered, and their use in water purification is being pursued. Their application in water treatment has been researched, and studies have investigated the antimicrobial properties of CNTs (Arias and Yang, 2009; Brady-Estévez et al., 2010; Kang et al., 2008). CNTs have also been used to treat water containing heavy metals, perchlorate, and inorganic and organic pollutants (Liu et al., 2013; Lou et al., 2014; Pyrzyńska and Bystrzejewski, 2010). Research into groundwater remediation has been undertaken and more recently, CNTs have been investigated to remove explosive contaminants from aqueous solutions (Kanel et al., 2015; Oh et al., 2013; Shen et al., 2009).

Pyrzyńska and Bystrzejewski (2010) conducted a study that compared the adsorption of heavy metal ions onto GAC, carbon nanotubes, and carbon-encapsulated magnetic nanoparticles (CEMNP). The experimental setup of the study used  $10 \text{ mg L}^{-1}$  of a given carbon material in a 10 mL metal ion solution that was shaken for 4 hours. Characterization of the carbon material by SEM analysis was conducted, and the adsorption capacities of the carbon materials were fit to Freundlich isotherms. The results show that CNTs and CEMNPs have a higher metal ion sorption capacity compared to GAC (Pyrzyńska and Bystrzejewski, 2010).

Lou et al. (2014) investigated the adsorption kinetics of perchlorate onto CNTs in an aqueous solution. The experimental design of the study used 125 mL reactor bottles that contained 20 mg L<sup>-1</sup> of perchlorate and 0.5 g L<sup>-1</sup> of CNTs. Functional groups were deliberately added to the CNTs by acid treatment. The study explored the effect of temperature, time, Ionic Strength and pH on the CNT perchlorate adsorption. The study concluded that the adsorption of perchlorate was fit best to the modified Freundlich isotherm, and lower ionic strengths and pH improve perchlorate adsorption onto CNTs (Lou et al., 2014).

Shen et al. (2009) studied the adsorption of explosive contaminants onto MWCNT. The kinetic experimental design of the study utilized 40 mL reactor bottles that contained 40 mg L<sup>-1</sup> of nitroaromatic compounds and 10 mg of MWCNT. The solutions were shook and samples were drawn at designated times. During the isotherm experiment, the reactor bottles were placed on a rotary shaker for 24 hours and allowed to settle for an additional 24 hours to guarantee partitioning between the MWCNT and the aqueous solution. Samples were analyzed with an HPLC. The adsorption data was fit to Freundlich and Langmuir isotherms and determined to follow pseudo-second-order kinetics (Shen et al., 2009).

Kanel et al. (2015) investigated the remediation of DNT from an aqueous solution using CNT yarn. CNT yarn structures consist of single CNTs bonded together by mechanical interlocking and van der Waal forces (Wei et al., 2014). The study conducted batch kinetic, and isotherm experiments with 50 mL of DNT contaminated aqueous solution in 100 mL reactor bottles, and 1 mg of CNT yarn. Samples were drawn at designated times and analyzed with a UV-Vis spectrophotometer for kinetic studies and

GC-MS for the isotherm studies. Their findings suggest that the DNT adsorption capacity of CNT yarn is similar to that of CNT and, if functionalized, could potentially contend with PAC (Kanel et al., 2015).

## APPENDIX B. EXPANDED METHODOLOGY, RESULTS AND DISCUSSION

This appendix contains an expanded methodology section, including calibration curve data and figures, equations, and additional analytical results and discussion. Images of the experimental process are also included that display the progression of the methodology.

### B.1 NORMALIZED ADSORBENT CONCENTRATIONS

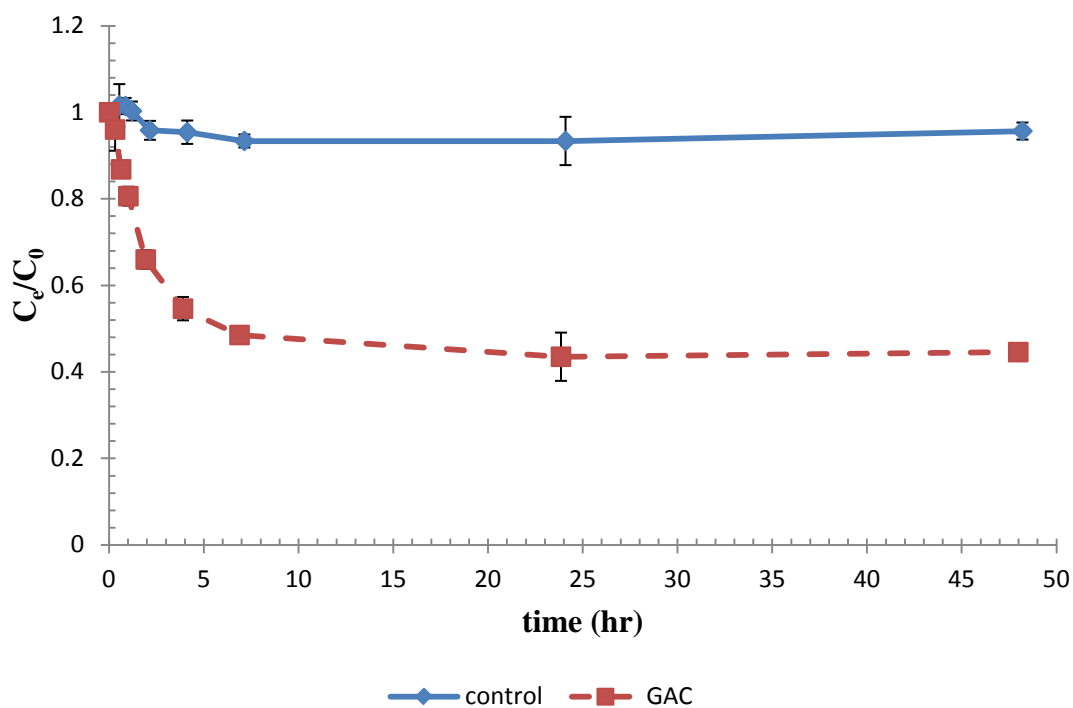


**Figure B 1. Normalized GAC concentrations with control. The DNT percent removal at 48 hours obtained by GAC was  $55.4 \pm 0.02\%$**

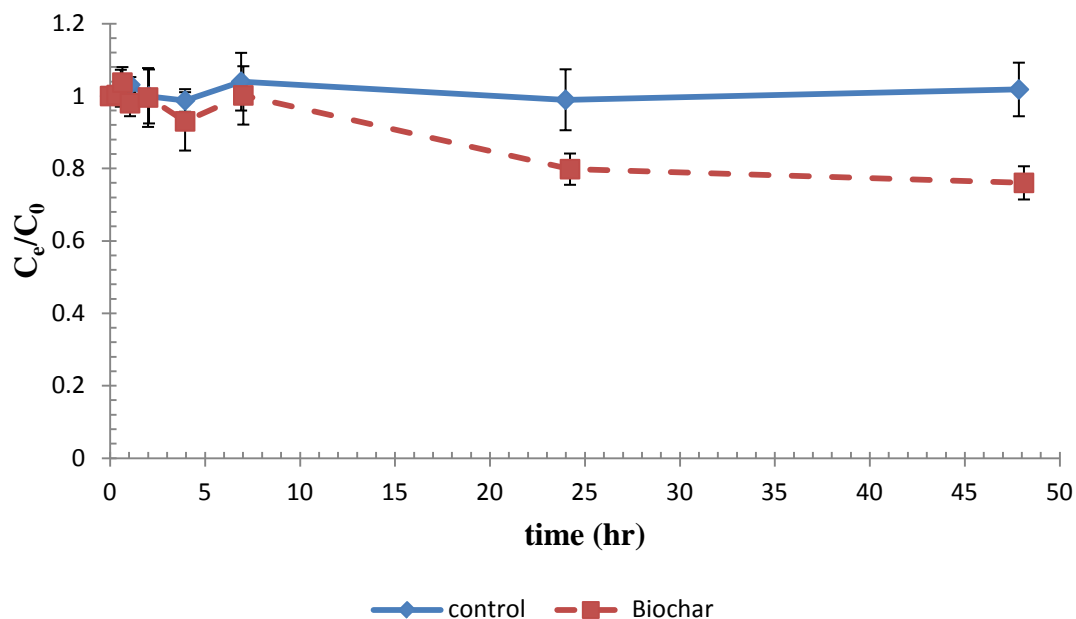


**Figure B 2. Normalized HWP-Biochar concentrations with control. HWP-Biochar achieved  $19.08 \pm 0.04$  % DNT removal at 48 hours**

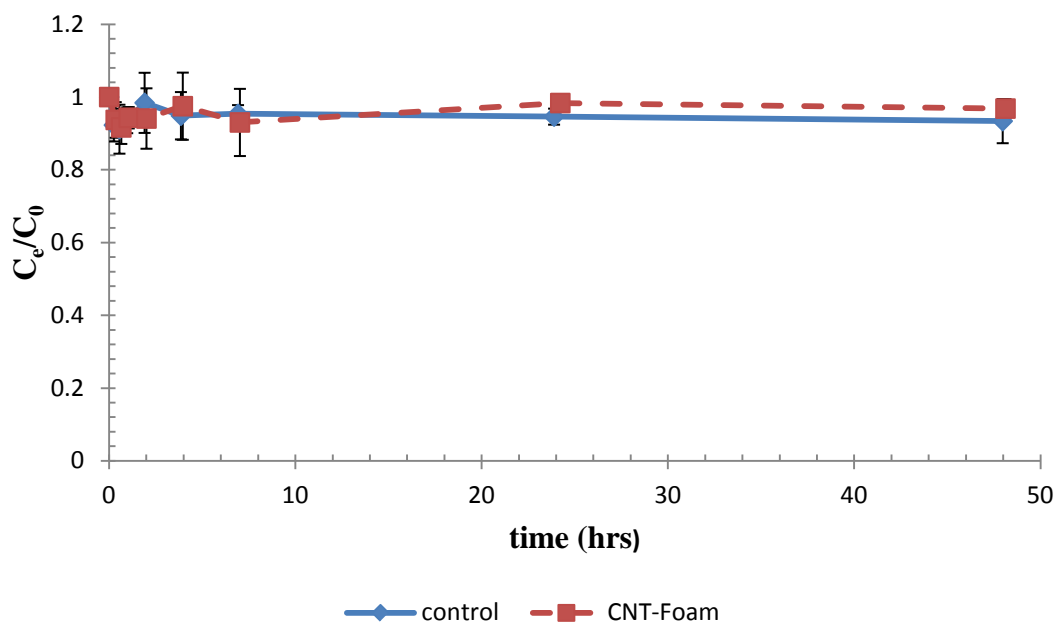


**Figure B 3. Normalized CNT-Foam concentrations with control. CNT-Foam achieved  $0.03 \pm 0.03$  % DNT removal at 48 hours. The normalized control concentration is lower than CNT-Foam and indicates DNT degradation**

## B.2 ADDITIONAL GAC KINETIC EXPERIMENTS

Additional GAC kinetic experiments were investigated. The additional studies used volumes of 40 and 1000 mL solutions and GAC concentrations that included 10, 20, and 50 mg L<sup>-1</sup>. Initially, 50 mg L<sup>-1</sup> of GAC was investigated in a 40 mL volume. In order to simulate more realistic field conditions, the GAC concentration was reduced, however, larger reactor volumes were employed. Eventually, 30 mg L<sup>-1</sup> of GAC was decided as the standard mass concentration for the kinetic studies. The samples from the additional kinetic studies were analyzed using the UV-Vis Spectrophotometer.

The 40 mL solutions were placed on a tumbler with ~2.0 mg of GAC (50 mg L<sup>-1</sup>) at ~240 rpm. The start time for the kinetics experiment was recorded when the GAC made initial contact with the DNT solution. The sampling method utilized with the 40 mL solution GAC kinetic study incorporated a method referred to as the “bottle kill method”. The bottle kill method uses a unique reactor bottle for every aliquot instead of collecting the samples from the same reactor bottle. The bottle is discarded after the aliquot is collected. This method prevents loss of adsorbent mass during the study. Triplicate solutions were used for each time interval. The samples were filtered as described in chapter II. Figure B 4 shows pulverized versus as-received GAC kinetics in 40 mL reactor bottles; these bottles contained 15 mg L<sup>-1</sup> DNT solutions with 2.0 mg of GAC. The error bars represent 2 standard deviations. The pulverized GAC achieved a solid phase concentration value of  $277.47 \pm 16.81$  mg g<sup>-1</sup> while the as-received GAC achieved  $212.41 \pm 67.42$  mg g<sup>-1</sup>. The adsorptive capacities of the pulverized versus the as-received F-600 were not significantly different from each other. However, the pulverized GAC achieved a higher k value than the as-received. The kinetic rate constant



k, for the pulverized was observed at  $0.18 \text{ (mg/L)}^{-1}(\text{hr})^{-1}$  while k for the as-received was  $0.0028 \text{ (mg/L)}^{-1}(\text{hr})^{-1}$ . The pulverized GAC reached equilibrium at ~12 hours while the as-received GAC potentially did not reached equilibrium until 144 hours. The second order rate analysis was conducted from 0-12 hours for the pulverized, and from 0 – 24 hours for the as-received GAC (Figure B 5).

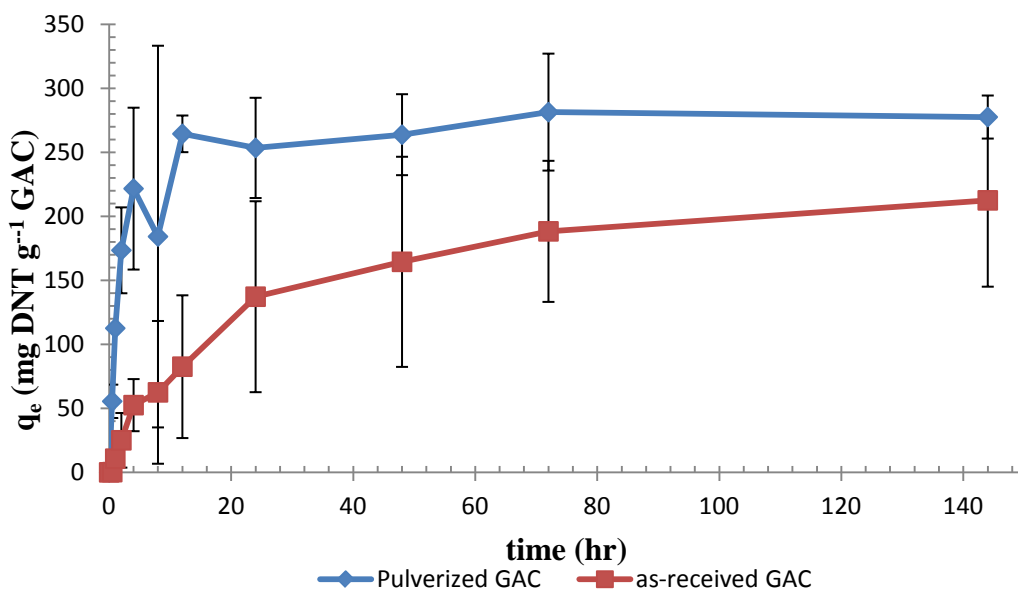


**Figure B 4. Pulverized versus as-received GAC kinetics.** The experiments were conducted with 40 mL,  $15 \text{ mg L}^{-1}$  DNT solutions with 2.0 mg of GAC. Error bars represent 2 standard deviations. Particle size of the pulverized GAC was 0.12 mm log mean diameter while the as-received GAC was 0.92 mm log mean diameter

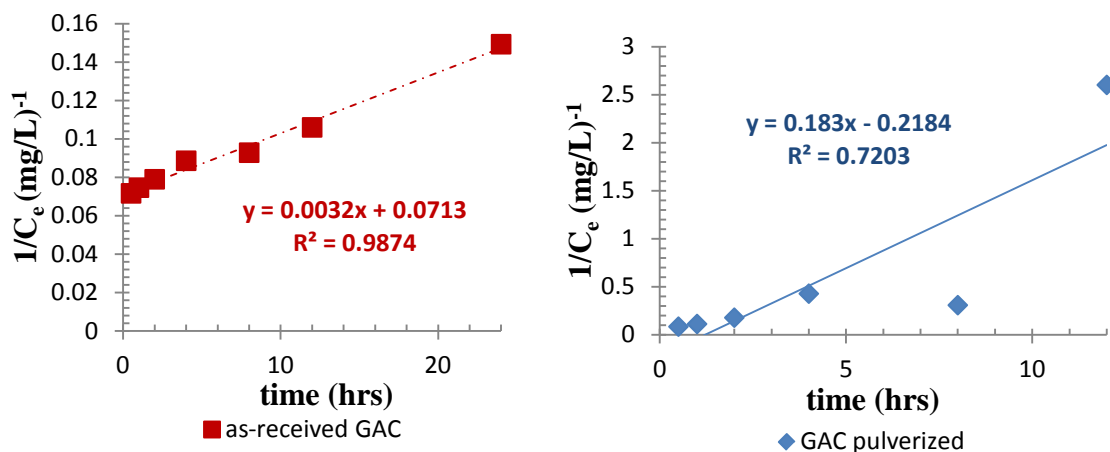


**Figure B 5. GAC pulverized versus as-received second order kinetic rate analysis. The kinetic rate constant,  $k$  for the pulverized is observed at  $0.18 \text{ (mg/L)}^{-1}(\text{hr})^{-1}$  while  $k$  for the as-received GAC was  $0.0032 \text{ (mg/L)}^{-1}(\text{hr})^{-1}$**

The 1000 mL solutions of  $15 \text{ mg L}^{-1}$  DNT were placed on a stir plate as described in chapter II. Duplicate reactors and single controls were used with solutions. The single control concentrations were set at  $15 \text{ mg L}^{-1}$  DNT with an ionic strength of 10 mM KCl. The error bars in Figure B 6 represent 2 standard deviations. The  $10 \text{ mg L}^{-1}$  GAC concentration achieved a solid phase concentration value of  $214.43 \pm 44.16 \text{ mg g}^{-1}$  while  $20 \text{ mg L}^{-1}$  GAC achieved  $265.53 \pm 19.54 \text{ mg g}^{-1}$ . The adsorptive capacities were not statistically different from each other. The kinetic rate constant  $k$  was higher for the  $20 \text{ mg L}^{-1}$  GAC. The kinetic rate  $k$ , for  $20 \text{ mg L}^{-1}$  is shown to be  $0.0065 \text{ (mg/L)}^{-1}(\text{hr})^{-1}$  while  $k$  for the  $10 \text{ mg L}^{-1}$  GAC was  $0.003 \text{ (mg/L)}^{-1}(\text{hr})^{-1}$  (Figure B 7).

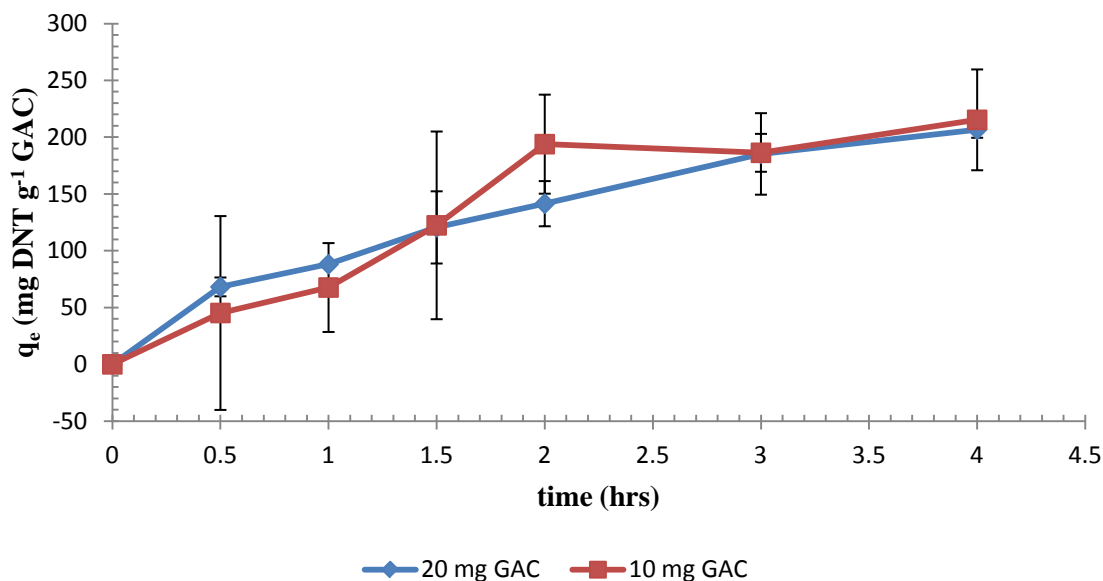


**Figure B 6. Pulverized GAC kinetics mass concentration analysis. 20 mg L<sup>-1</sup> GAC concentration versus 10 mg L<sup>-1</sup> GAC. Experiment was conducted on a stir plate in duplicates with 1 L solutions of 15 mg L<sup>-1</sup> DNT. Error bars represent 2 standard deviations**

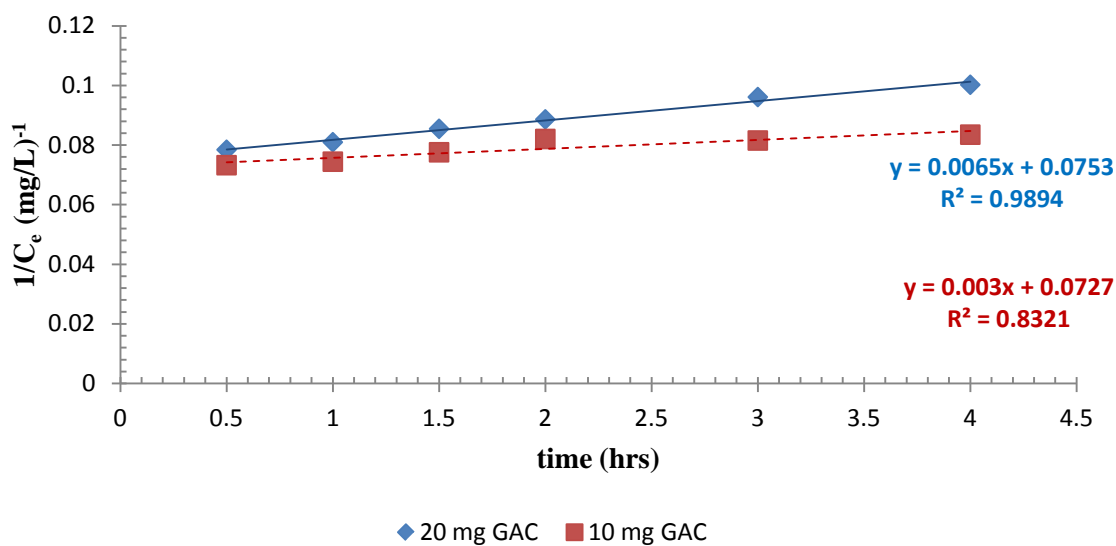


**Figure B 7. Pulverized second order kinetic rate analysis. The kinetic rate constant  $k$ , for the 20 mg L<sup>-1</sup> is shown to be 0.0065 (mg/L)<sup>-1</sup>(hr)<sup>-1</sup>, while  $k$  for the 10 mg L<sup>-1</sup> GAC was 0.003 (mg/L)<sup>-1</sup>(hr)<sup>-1</sup>**

### B.3 EXPERIMENTAL IMAGES



**Figure B 8. Experimental reactor bottle configurations. Figure A displays the tumbler with 50 mL vials in triplicates. Figure B illustrates the 1 L bottles covered with aluminum foil on stir plates. Figure C shows the 500 mL reactor bottles, and Figure D displays the 250 mL amber bottles selected as the final standard configuration**

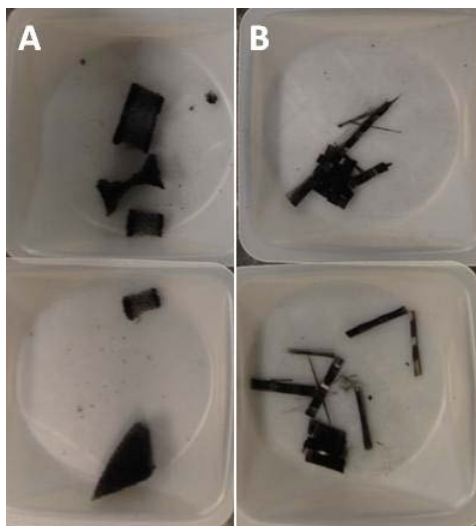


**Figure B 9. CNT-Hybrid structures cut to mass. Figure A is the CNT-Foam, and Figure B is CNT-Fabric**

#### B.4 UV-VIS CALIBRATION CURVE PROCEDURE AND FIGURE

The DNT calibration curve on the Agilent® Cary 60 UV-Vis Spectrophotometer at the Air Force Institute of Technology was prepared from the stock solution of 50 mg L<sup>-1</sup> DNT. The stock solution of 50 mg L<sup>-1</sup> DNT was diluted with DI water to 1, 5, 10, and 15 mg L<sup>-1</sup> DNT. A blank (0 mg L<sup>-1</sup>) was also included in the calibration curve. Ten milliliters of each concentration were placed in a test tube and vortexed for 30 seconds after dilution. One milliliter of sample was used to rinse the 1 cm quartz cuvette, and 1 milliliter was retained in the cuvette to analyze by the UV-Vis Spectrophotometer. Four separate calibration curves were created using the above method, and the average of the curves was used to create the equation of the line to calculate the unknown DNT concentrations in the additional GAC kinetic experiments.

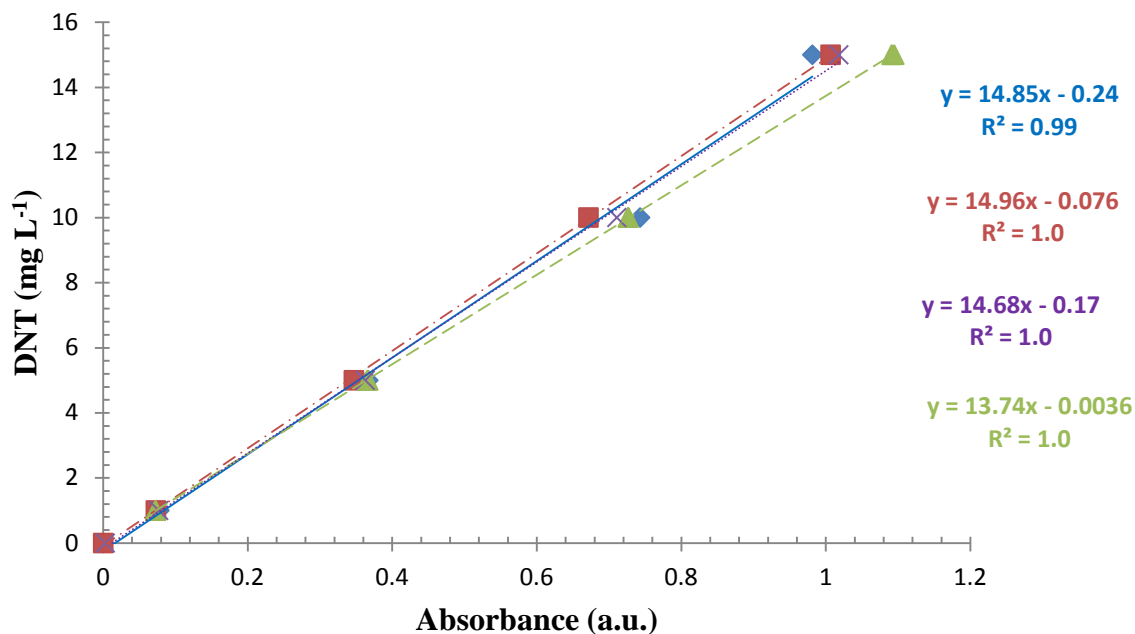


**Figure B 10. UV-Vis spectrophotometer calibration curves. Four separate calibration curves are shown with the concentration represented on the y-axis and absorbance on the x-axis**

## B.5 GC-MS CALIBRATION CURVE METHOD AND FIGURES

The procedure used to prepare the GC-MS calibration curve concentrations is described in the Chapter II methods section. Blanks of methanol were placed between the samples to limit DNT carryover during GC-MS analysis. Nevertheless, DNT instrument carryover was observed in the blanks. The DNT area counts in the blanks before and after each concentration were averaged and subtracted from each sample. Data analysis was conducted, and points in the calibration curve that did not follow predicted increases in magnitude were removed. Calibration curves were created for low ( $0 - 1.5 \text{ mg L}^{-1}$ ) and high concentrations ( $5 - 15 \text{ mg L}^{-1}$ , and  $15 - 40 \text{ mg L}^{-1}$ ) due to an observed non-linear calibration curve created by the GC-MS. The low calibration curve concentrations included a blank of methanol. The GC-MS calibration curves are displayed in Figure B 11 through Figure B 17.

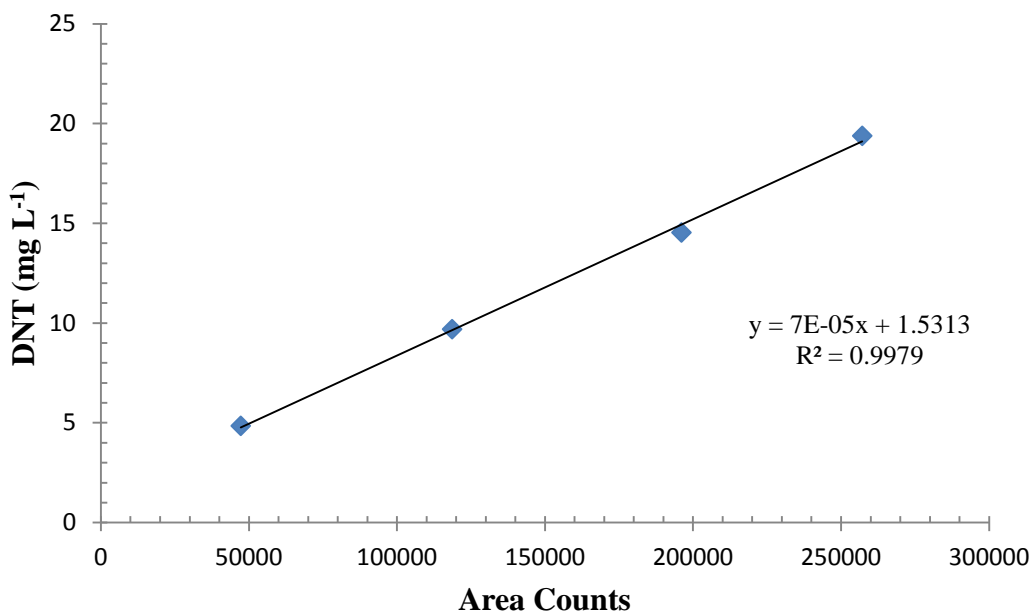


**Figure B 11. GC-MS calibration curve 5 – 20 mg L<sup>-1</sup> DNT for GAC kinetic experiment**

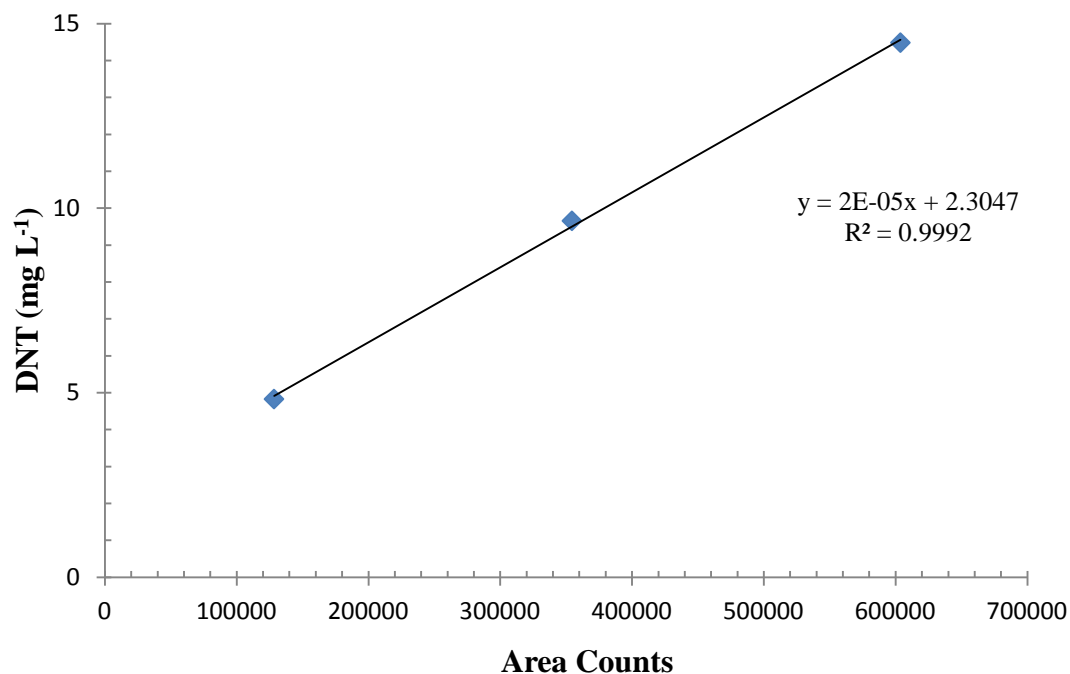


**Figure B 12. GC-MS calibration curve 5 – 15 mg L<sup>-1</sup> DNT for CNT-HS kinetic experiment**

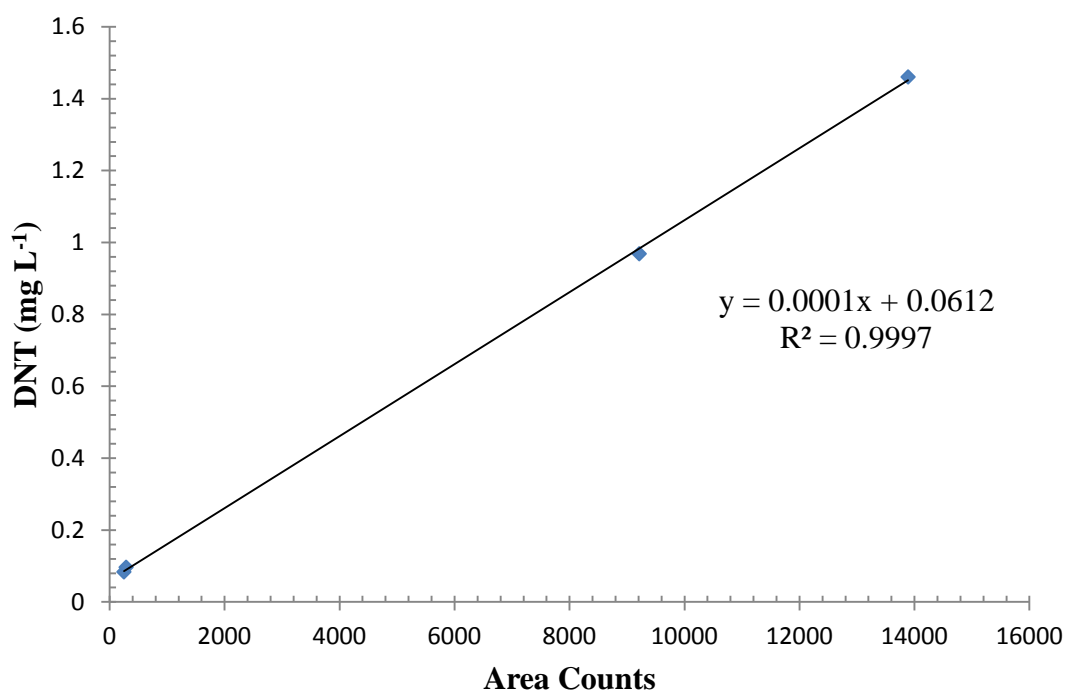


**Figure B 13. GC-MS calibration curve 0 - 1.5 mg L<sup>-1</sup> DNT for GAC and CNT-HS isotherm study**

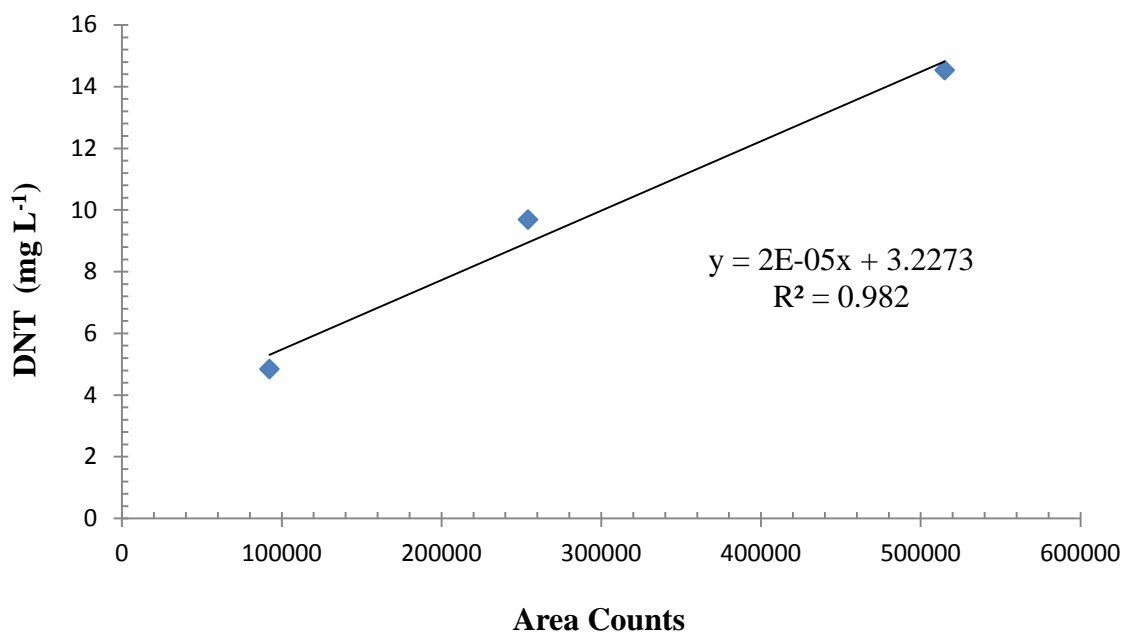


**Figure B 14. GC-MS calibration curve 5 - 15 mg L<sup>-1</sup> DNT for GAC and CNT-HS isotherm study**

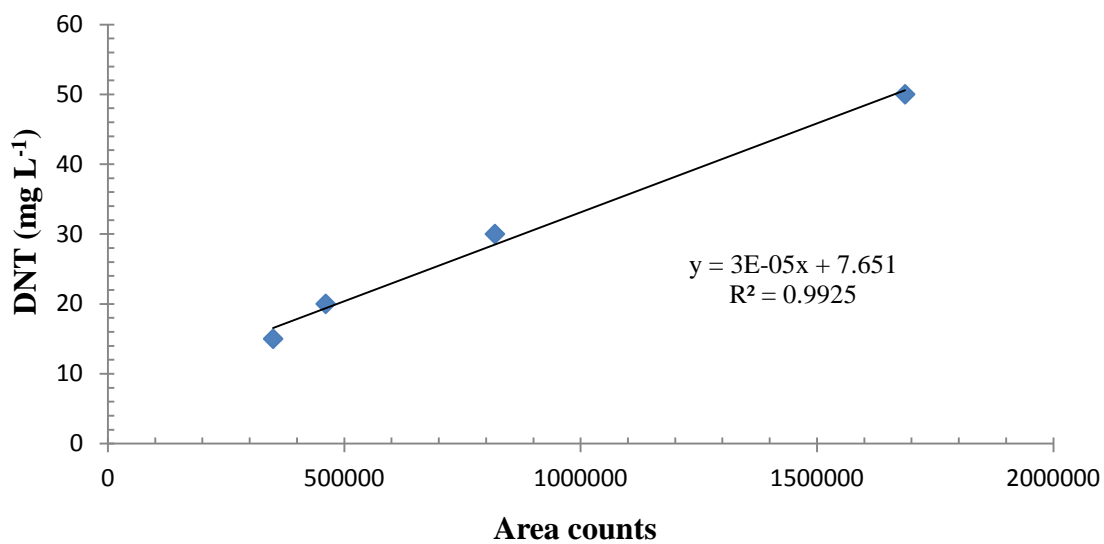


**Figure B 15. GC-MS calibration curve for GAC 25 mg L<sup>-1</sup> and 40 mg L<sup>-1</sup> DNT isotherm study**



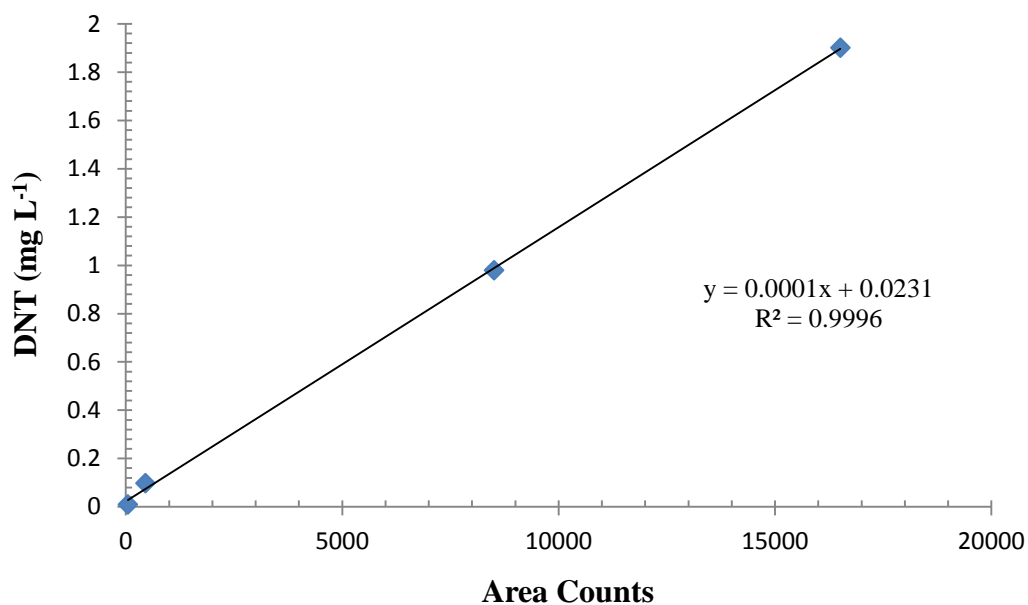


**Figure B 16. GC-MS calibration curve 0 - 1.5 mg L<sup>-1</sup> DNT for Biochar isotherm and kinetic study**

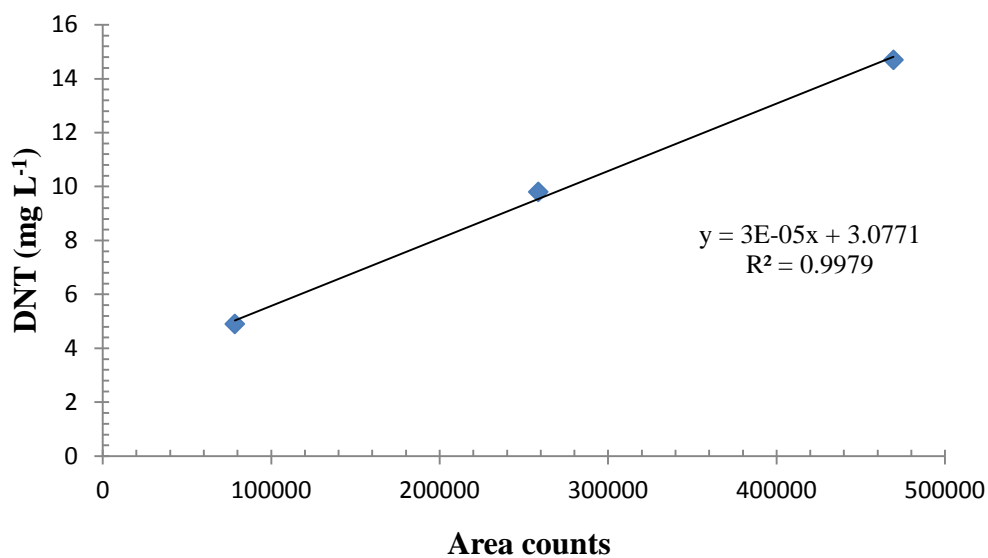


**Figure B 17. GC-MS calibration curve 5 - 15 mg L<sup>-1</sup> DNT for Biochar isotherm and kinetic study**

## B.6 ZEROth AND FIRST ORDER RATE ANALYSIS

In order to determine the rate constant for the kinetics reaction, zeroth, first, and second order rates were explored. Data from 0 to 7 hours obtained from the kinetic experiment was used to determine the reaction rate since equilibrium was assumed to occur prior to 24 hours. Linear regression analysis was employed, and the best  $R^2$  values were used to identify the best-fit model. The zeroth order rate model analysis is displayed in Figure B 18 while the first order rate model is shown by Figure B 19. Second order analysis is discussed in detail in chapter 2.

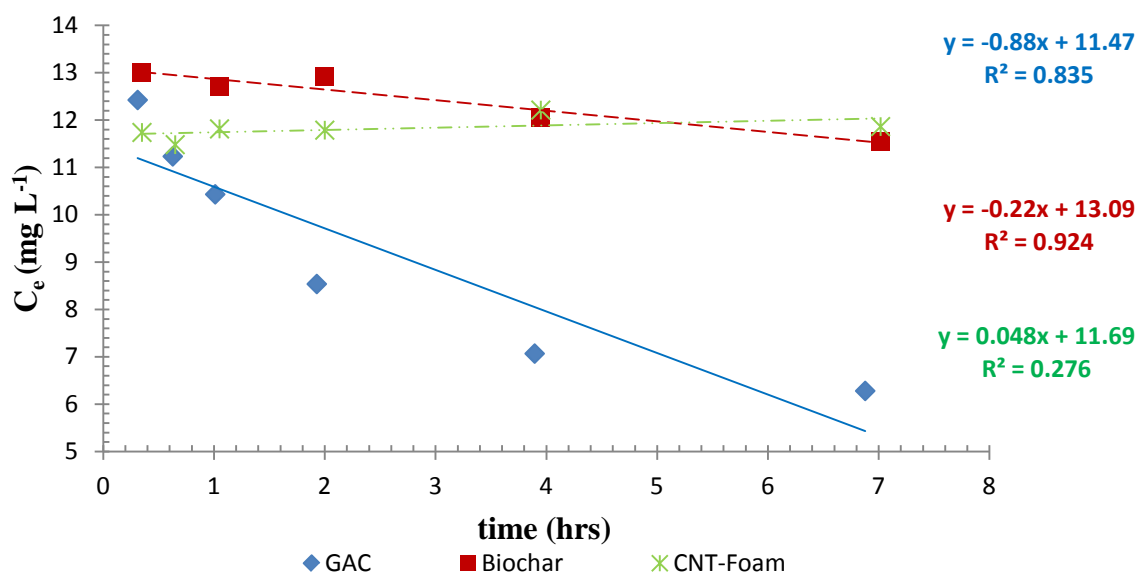


**Figure B 18. Zeroth order kinetic rate analysis. Linear regression analysis determined that GAC achieved an  $R^2$  value of 0.835 while HWP-Biochar was 0.924 and CNT-Foam was 0.276**

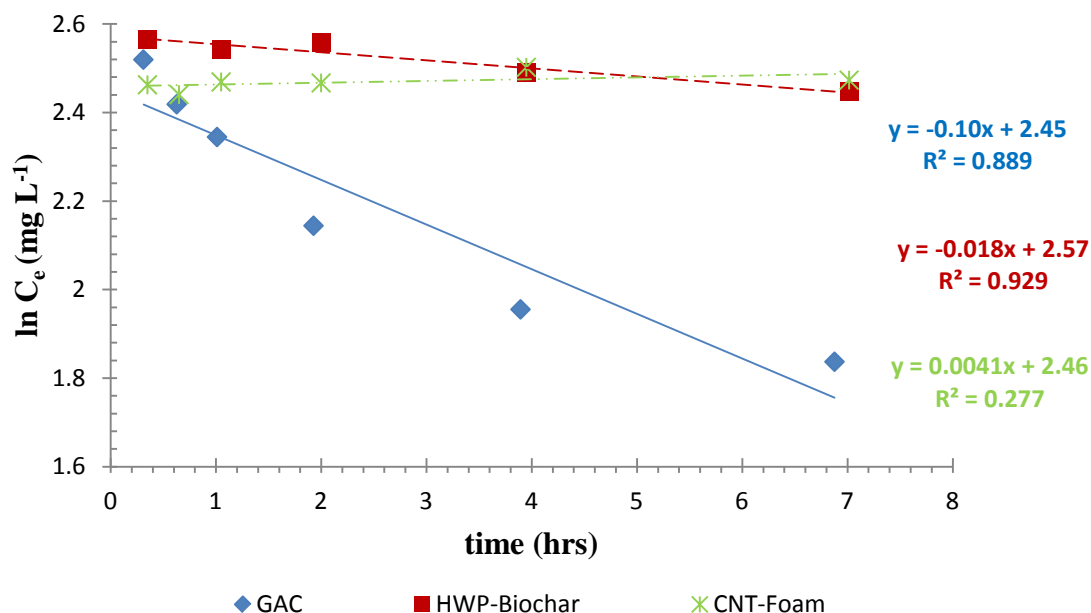


**Figure B 19. First order kinetic rate analysis. Linear regression analysis determined that GAC achieved an  $R^2$  value of 0.889 while HWP-Biochar was 0.929 and CNT-Foam was 0.277**

## B.7 HWP-BIOCHAR SECOND ORDER RATE ANALYSIS

In order to determine the rate constant for the kinetics reaction, second order rates were explored, and the data was fit to the corresponding figures. However when fitting the HWP-Biochar data, an outlier was visually identified. Figure B 20 shows the HWP-Biochar second order rate model with and without the outlier. The  $R^2$  value significantly increased when the outlier was removed.  $T^2$  statistical analysis was conducted in JMP® software and confirmed that the point fell outside the upper control limit in the second order rate model (Figure B 21).

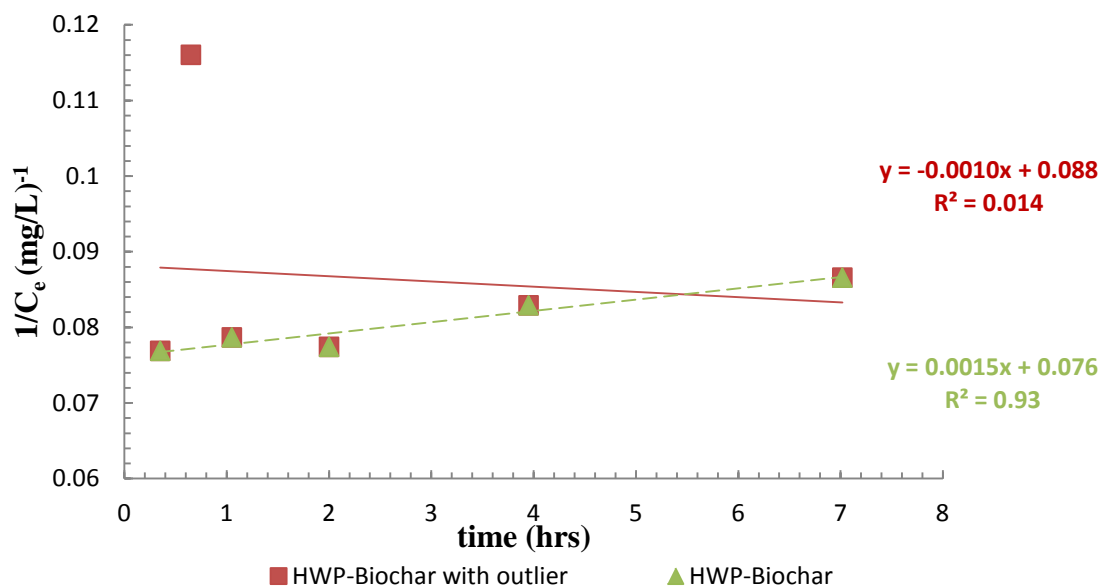


**Figure B 20. HWP-Biochar second order kinetic rate analysis with outlier. Linear regression analysis determined that removing the outlier significantly increased the  $R^2$  value from 0.014 to 0.93**

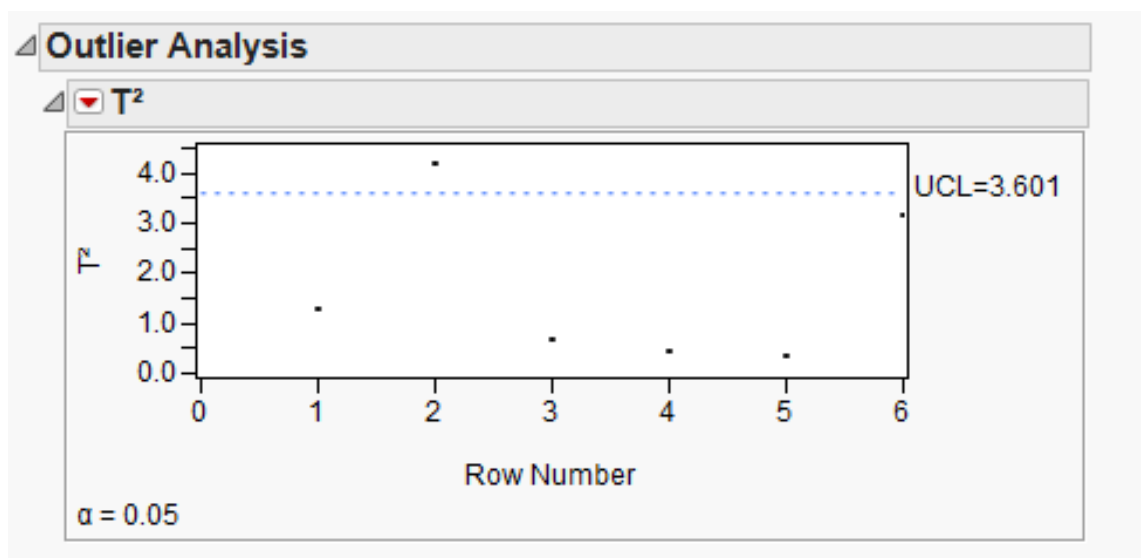


**Figure B 21.  $T^2$  statistic outlier analysis conducted in JMP® software confirming that the second data point fell above the 95% upper confidence level**

## B.8 F-600 GAC FREUNDLICH ISOTHERM OUTLIER ANALYSIS

When fitting the F-600 GAC data to the Freundlich Isotherm, an outlier was visually identified. Figure B 22 shows the F-600 GAC Freundlich Isotherm with and without the outlier. The  $R^2$  value significantly increased when the outlier was removed.  $T^2$  statistical analysis was conducted in JMP® software and confirmed that the point fell outside the upper control limit in the Freundlich Isotherm model (Figure B 23).

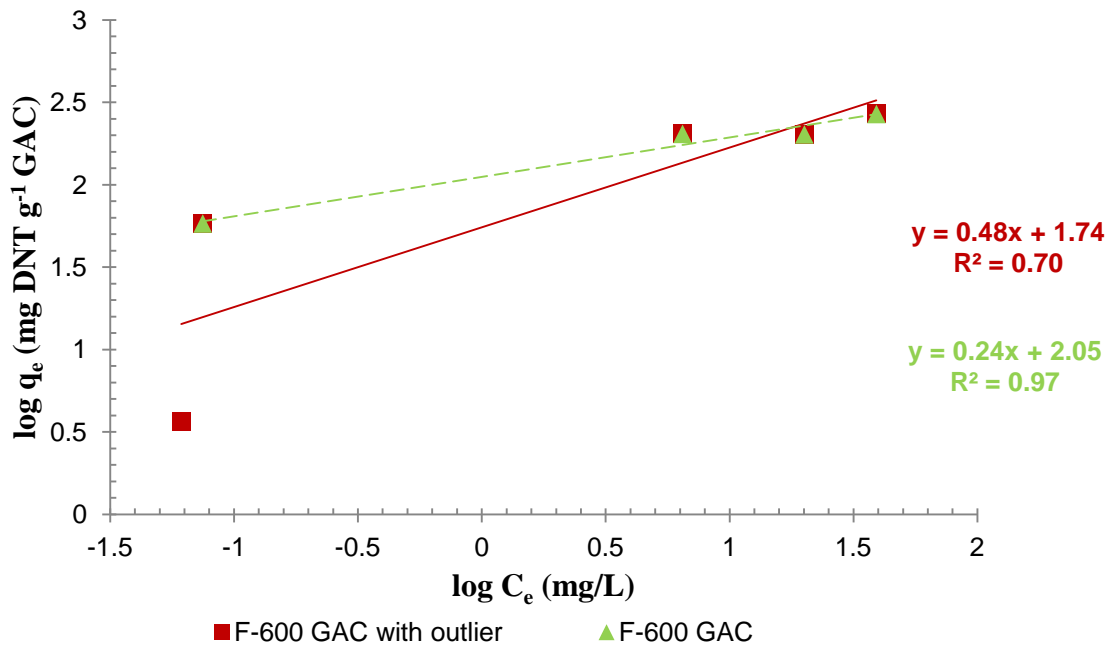


**Figure B 22. F-600 GAC Freundlich Isotherm analysis with outlier. Linear regression analysis determined that removing the outlier significantly increased the  $R^2$  value from 0.70 to 0.97**

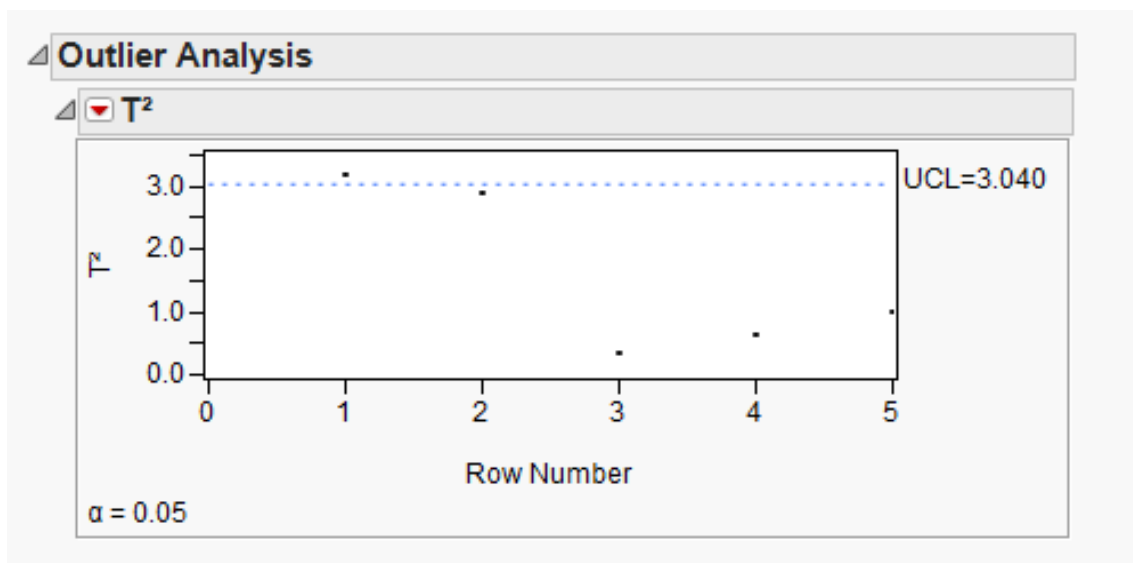


**Figure B 23.  $T^2$  statistic outlier analysis conducted in JMP® software confirming that the first data point fell above the 95% upper confidence level**

## **B.9 ISOTHERM ANALYSIS WITH CNT-HS**

The DNT solid and liquid phase equilibrium concentrations observed for CNT-HS were fit to the Langmuir and Freundlich isotherm models. Linear regression analysis comparing the  $R^2$  values showed that CNT-Foam did not significantly prefer either model while CNT-Fabric preferred and fit best to the Langmuir model. Figure B 24 displays CNT-HS fit to the Freundlich model, and Figure B 25 displays CNT-HS fit to the Langmuir model.

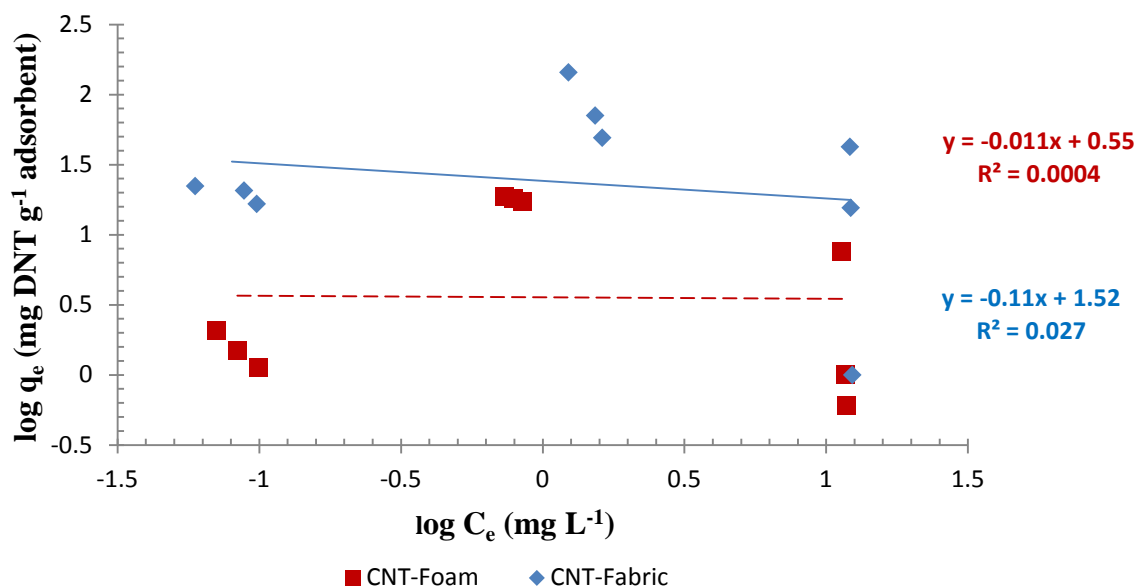


**Figure B 24. Freundlich Isotherm models for CNT-HS adsorbents. Linear regression analysis shows that CNT-Foam and CNT-Fabric both fit poorly to the model**

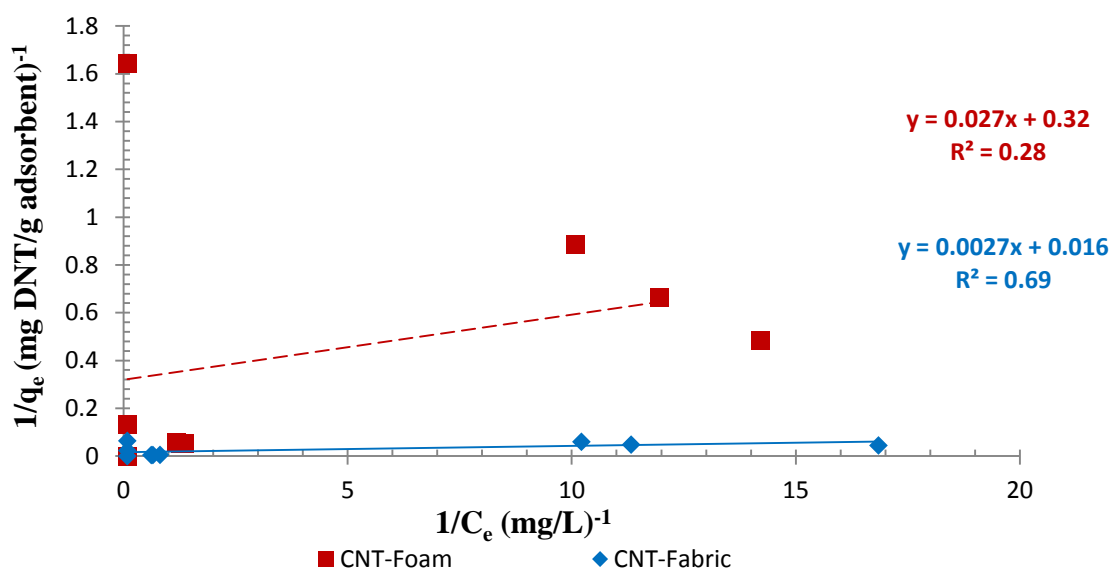


**Figure B 25. Langmuir Isotherm models for CNT-HS adsorbents. Linear regression analysis shows that CNT-Fabric fits the model the best with an  $R^2$  value of 0.69**

## B.10 DNT PEAKS OBSERVED USING THE GC-MS SIM METHOD

The samples were analyzed by GC-MS using a single ion monitoring (SIM). Agilent MassHunter WorkStation Qualitative Analysis version B.06.00 software was used to analyze the data files. Examples of the observed DNT peaks generated using MassHunter are shown in Figure B 26 - Figure B 28.

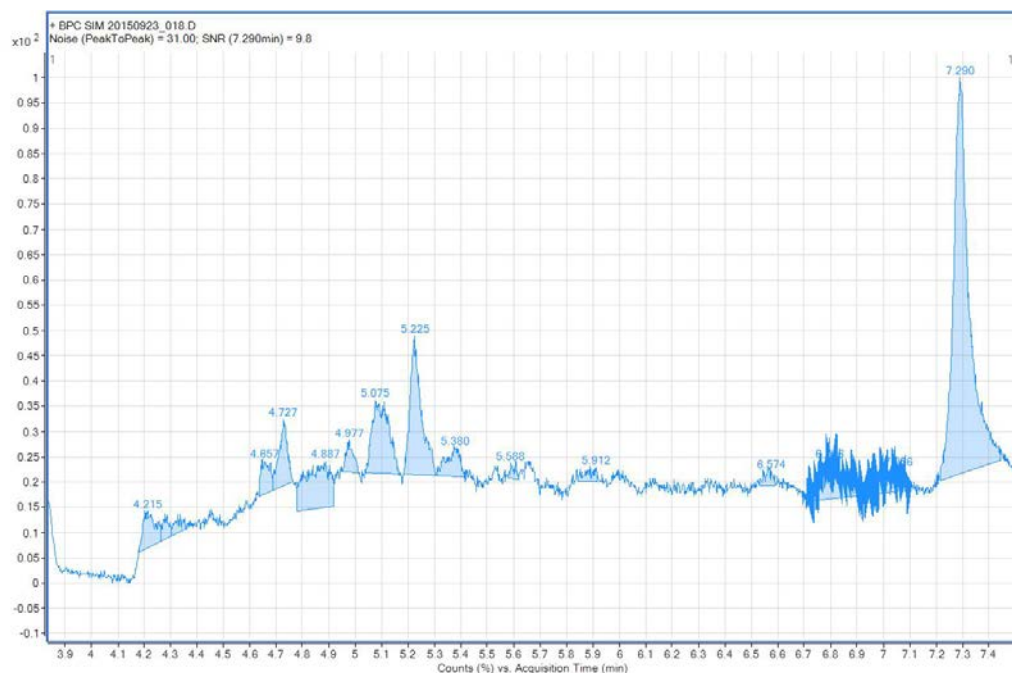


**Figure B 26. DNT peak is on the far right of the figure and occurs at 7.29 minutes with 1260 area counts. Observed for  $C_0$  of  $\sim 0.15 \text{ mg L}^{-1}$  control collected during the CNT-Foam isotherm experiment**



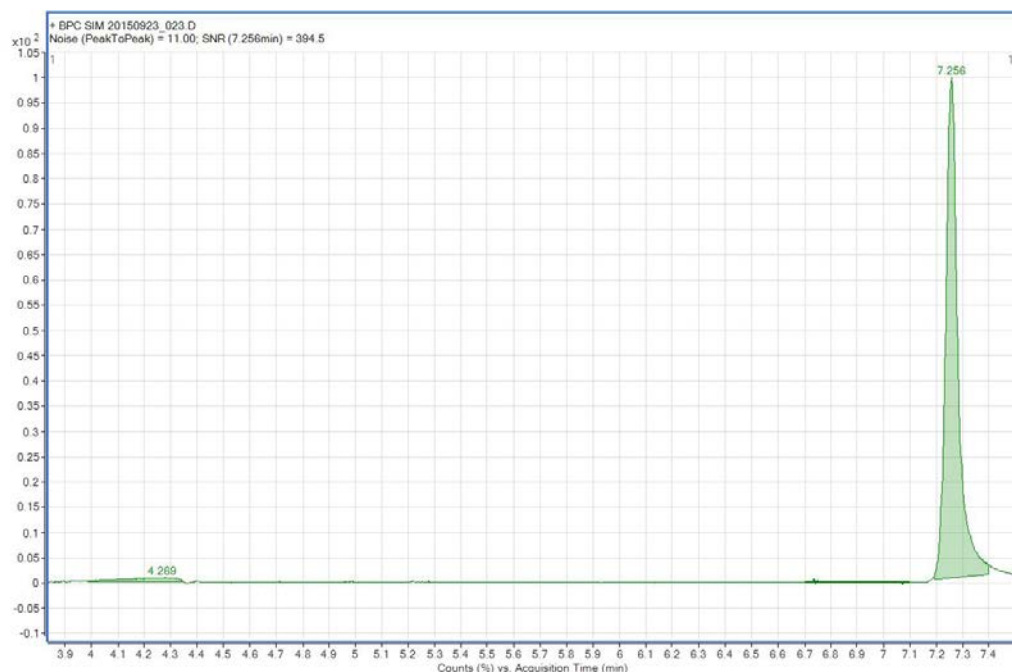


**Figure B 27. DNT peak is on the far right of the figure and occurs at 7.256 minutes with 14172.11 area counts. Observed for  $C_0$  of the  $\sim 1.5 \text{ mg L}^{-1}$  control collected during the CNT-Foam isotherm experiment**

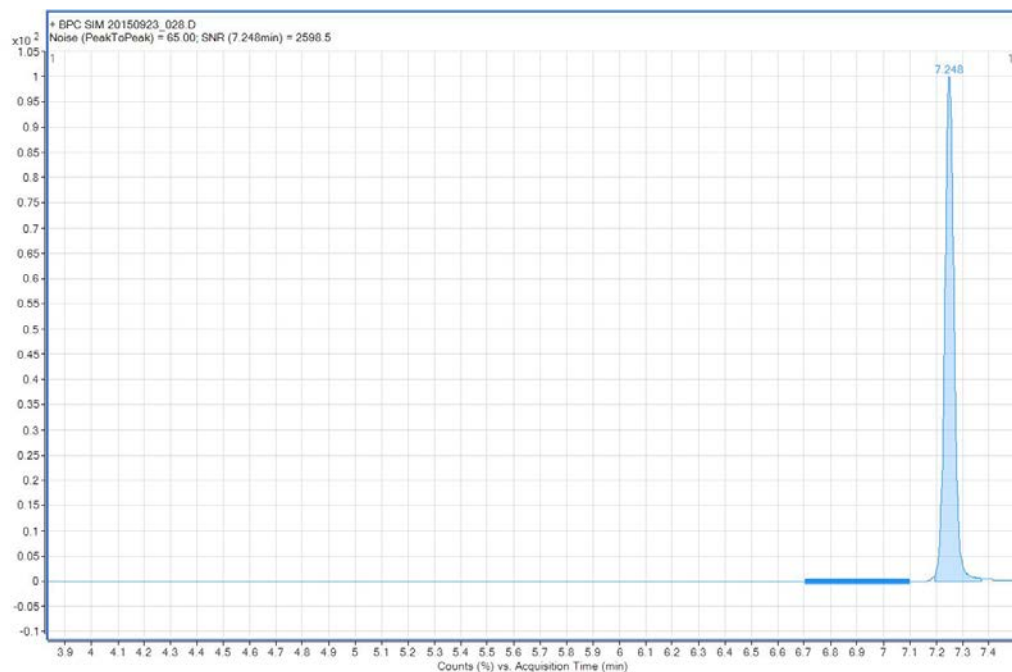


**Figure B 28. DNT peak is on the far right of the figure and occurs at 7.248 minutes with 418644.74 area counts. Observed for  $C_0 \sim 15 \text{ mg L}^{-1}$  control collected during the CNT-Foam isotherm experiment**

## **B.11 pH ANALYSIS**

During the kinetic studies, the pH was measured at various time intervals for all solutions in order to determine the adsorbents effect on pH. The initial pH of the de-ionized water was measured to be 4.40 prior to mixing with DNT and adsorbents. The pH recorded at 48 hours for the controls, GAC and CNT-Foam samples all ranged between 5.33 and 5.57 while the pH recorded for HWP-Biochar was slightly more basic at 5.73 (Figure B 28). The pH properties of various biochars have shown to be more basic than graphite and GAC, which may explain why the HWP-Biochar solution in this study is slightly higher (Oh and Seo, 2014). Previous work has shown that an unbuffered pH inhibits the degradation of a nitroaromatic compound (Nefso et al., 2005). Buffering the DNT solution at a neutral or higher pH in future work may increase DNT degradation. HWP-Biochar may be more appropriate for treatment of acidic contaminated waters if the desire is to achieve a more neutral final pH.

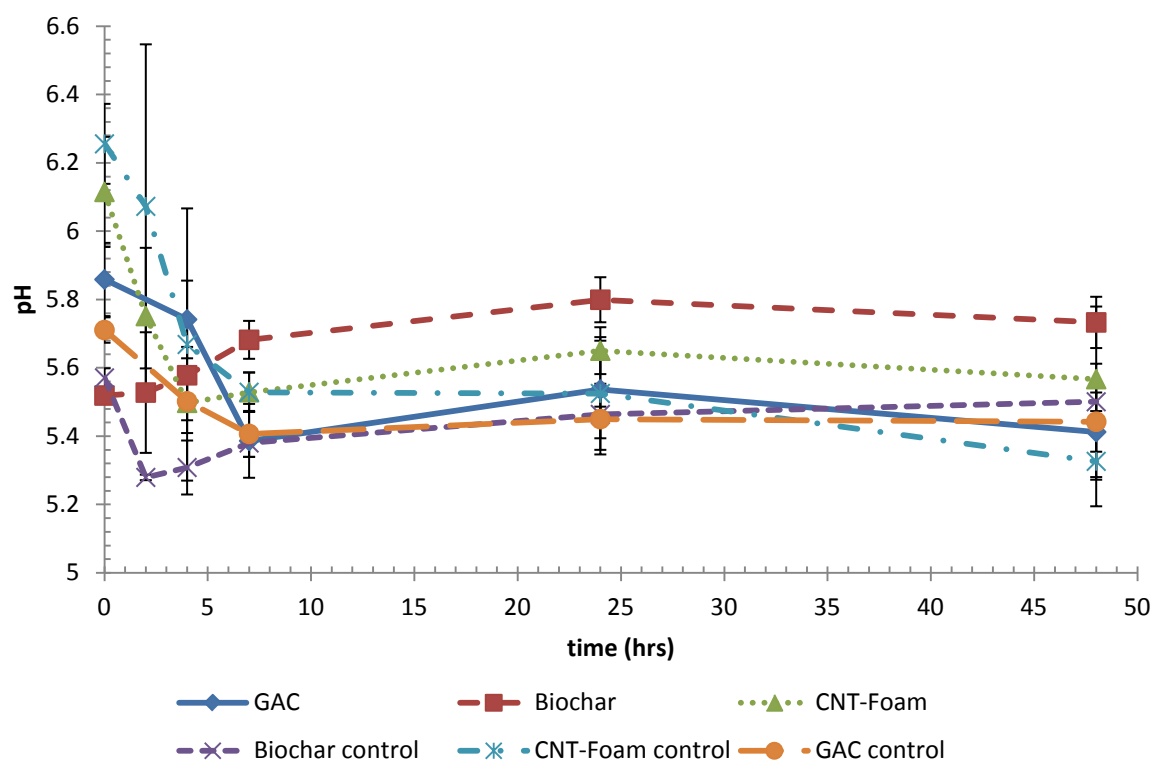


**Figure B 29. pH of solutions observed during the kinetic studies. The error bars represent 2 standard deviations. The pH for the controls, GAC, and CNT-Foam samples all ranged between ~5.33 and ~5.57 pH while the pH recorded for HWP-Biochar was slightly more basic at 5.73**

## B.12 EQUATIONS

### Equation 1. Mass-balance

$$C_1 V_1 + C_2 V_2 = C_T C_T$$

Where C represents the concentration, V, the volume, and the subscripts 1, 2, and T represent sample 1, sample 2, and ‘total’.

### Equation 2. Solid-phase concentration $q_e$ (mg DNT g<sup>-1</sup> adsorbent)

$$q_e = \frac{(C_o - C_e)V}{m}$$

Where,  $q_e$  is the amount of DNT adsorbed onto the adsorbent at time t,  $C_o$  is the initial concentration and  $C_e$  is the effluent concentration of DNT in solution at time t, V is the volume of DNT, and m is the mass of adsorbent.

### Equation 3. Linear Freundlich Isotherm equation

$$\log q_e = \log K_F + \left(\frac{1}{n}\right) \log C_e$$

Where  $K_F$  is the Freundlich adsorption capacity parameter (mg g<sup>-1</sup>)(L mg<sup>-1</sup>)<sup>-1/n</sup> and  $\frac{1}{n}$  is the adsorption intensity parameter.

### Equation 4. Linear Langmuir isotherm equation

$$\frac{C_e}{q_e} = \frac{1}{b_e Q_M} + \frac{C_e}{Q_M}$$

Where,  $b_e$  is the Langmuir adsorption constant. And  $Q_M$  is the maximum solid phase concentration when the surface is saturated with the adsorbate (mg g<sup>-1</sup>) (Crittenden et al., 2005)

### B.13 Q-TEST ANALYSIS

A Q test is a statistical analysis tool that can identify outliers in data sets. It is determined to be accurate and recommended for small observations (Christian, 2003). The Q value (gap/range) is a ratio and calculated by dividing the difference between the suspect number and its nearest neighbor (gap), by the difference between the highest number and the lowest number (range). If the observed Q value is equal or greater than the table value for Q at that specific confidence interval, then the suspect number can be removed and termed an outlier (Christian, 2003).

In this study, a Q-test with a 90% confidence interval was performed on all suspect numbers found within the triplicate data sets in order to identify outliers. A total of 9 outliers from 248 data points were identified and removed from and replaced by the average of the remaining 2 points in the data set (Table 7 - Table 11).

**Table 7. Q-test with a 90% CI conducted on F-600 GAC kinetic and control GC-MS triplicate data samples; highlighted data is suspect**

Sample Name	Area Counts	Range (w)	Gap (a)	Q (a/w)	90% CI (n=3)	reject if Q > 0.941
Initial GAC-1	163272.435	8827.32	4852.02	0.549659466	0.941	no
Initial GAC-2	167247.735					
Initial GAC-3	158420.415					
Initial Control-1	167575.53	2752.32	2202.98	0.800408383	0.941	no
Initial Control-2	169778.51					
Initial Control-3	167026.19					
15 min GAC-1	156118.955	7473.01	4506.91	0.603091659	0.941	no
15 min GAC-2	159085.055					
15 min GAC-3	151612.045					
15 min Control -1	166876.545	8369.48	4520.2	0.540081343	0.941	no
15 min Control -2	171396.745					
15 min Control -3	175246.025					

<b>0.5 hr GAC-1</b>	129734.135	14696.16	11860.91	0.807075454	0.941	no
<b>0.5 hr GAC-2</b>	144430.295					
<b>0.5 hr GAC-3</b>	141595.045					
<b>0.5 hr Control-1</b>	168026.125	5686.26	5272.47	0.927229849	0.941	no
<b>0.5 hr Control-2</b>	173712.385					
<b>0.5 hr Control-3</b>	168439.915					
<b>1 hr GAC-1</b>	121682.57	9120.43	7244.07	0.794268472	0.941	no
<b>1 hr GAC-2</b>	128926.64					
<b>1 hr GAC-3</b>	130803					
<b>1 hr Control-1</b>	170475.895	3616.79	1865.08	0.515672737	0.941	no
<b>1 hr Control-1</b>	168724.185					
<b>1 hr Control-1</b>	166859.105					
<b>2 hr GAC-1</b>	98059.09	8824.04	7434.34	0.84250978	0.941	no
<b>2 hr GAC-2</b>	96669.39					
<b>2 hr GAC-3</b>	105493.43					
<b>2 hr Control-1</b>	166858.03	6697.4	6630	0.989936393	0.941	yes
<b>2 hr Control-1</b>	160160.63					
<b>2 hr Control-1</b>	160228.03					
<b>4 hr GAC-1</b>	80272.555	2486.86	1377.95	0.554092309	0.941	no
<b>4 hr GAC-2</b>	77785.695					
<b>4 hr GAC-3</b>	79163.645					
<b>4 hr Control-1</b>	161769.65	5279.52	3366.5	0.637652665	0.941	no
<b>4 hr Control-1</b>	159856.63					
<b>4 hr Control-1</b>	156490.13					
<b>7 hr GAC-1</b>	68227.91	1110.92	961.36	0.865372844	0.941	no
<b>7 hr GAC-2</b>	67116.99					
<b>7 hr GAC-3</b>	68078.35					
<b>7 hr Control-1</b>	156613.375	2604.02	1926.21	0.7397063	0.941	no
<b>7 hr Control-1</b>	155935.565					
<b>7 hr Control-1</b>	154009.355					
<b>24 hr GAC-1</b>	58439.975	2276.67	1968.14	0.864481897	0.941	no
<b>24 hr GAC-2</b>	56471.835					
<b>24 hr GAC-3</b>	56163.305					
<b>24 hr Control-1</b>	152520.88	11979.67	9290.82	0.775548909	0.941	no
<b>24 hr Control-1</b>	155209.73					
<b>24 hr Control-1</b>	143230.06					
<b>48 hr GAC-1</b>	60788.115	3539.15	1629.27	0.4603563	0.941	no
<b>48 hr GAC-2</b>	58878.235					
<b>48 hr GAC-3</b>	57248.965					
<b>48 hr Control-1</b>	160464.65	54858.53	53690.12	0.978701398	0.941	yes

48 hr Control-2      159296.24  
48 hr Control-3      214154.77

**Table 8. Q-test with a 90% CI conducted on CNT-Foam kinetics and control GC-MS data; highlighted data is suspect**

Sample Name	Area Counts	Range (w)	Gap (a)	Q (a/w)	90% CI (n=3)	reject if Q > 0.941
Initial Control-1	548757.41	20328.32	18356.37	0.9029949	0.941	no
Initial Control-2	530401.04					
Initial Control-3	528429.09					
Initial Foam-1	385723.61	128194.91	122388.8	0.9547087	0.941	yes
Initial Foam-2	513918.52					
Initial Foam-3	508112.4					
15 min Control-1	480863.72	11493.73	8885.53	0.7730763	0.941	no
15 min Control-2	492357.45					
15 min Control-3	483471.92					
15 min Foam-1	475414.4	29968.69	20618.76	0.6880101	0.941	no
15 min Foam-2	484764.33					
15 min Foam-3	454795.64					
0.5 hr Control-1	471646.2	32065.64	25865.47	0.8066413	0.941	no
0.5 hr Control-2	497511.67					
0.5 hr Control-3	465446.03					
0.5 hr Foam-1	448532.175	26461.14	22194.6	0.838762	0.941	no
0.5 hr Foam-2	474993.315					
0.5 hr Foam-3	452798.715					
1hr Control-1	493194.625	7280	5191.86	0.7131676	0.941	no
1hr Control-2	498386.485					
1hr Control-3	491106.485					
1hr Foam-1	465540.07	18143.96	11487.02	0.6331043	0.941	no
1hr Foam-2	483684.03					
1hr Foam-3	477027.09					
2hr Control-1	519236.225	40693.25	29469.95	0.7241975	0.941	no
2hr Control-2	508012.925					
2hr Control-3	548706.175					
2hr Foam-1	460662.125	46511.4	43393.22	0.9329588	0.941	no
2hr Foam-2	504055.345					
2hr Foam-3	457543.945					
4hr Control-1	497778.93	32747.4	23154.73	0.7070708	0.941	no
4hr Control-2	520933.66					
4hr Control-3	488186.26					

4hr Foam-1	462179.305	53262.93	46109.6	0.8656978	0.941	no
4hr Foam-2	515442.235					
4hr Foam-3	508288.905					
7hr Control-1	515011.3	20288.66	12786.19	0.6302136	0.941	no
7hr Control-2	494722.64					
7hr Control-3	507508.83					
7hr Foam-1	477560.4	26952.21	13907.64	0.5160111	0.941	no
7hr Foam-2	491468.04					
7hr Foam-3	464515.83					
24hr Control-1	514235.915	31839.59	25498.14	0.8008313	0.941	no
24hr Control-2	539734.055					
24hr Control-3	546075.505					
24hr Foam-1	506150.94	13138.15	10119.68	0.7702515	0.941	no
24hr Foam-2	503132.47					
24hr Foam-3	493012.79					
48hr Control-1	481598.98	17783.76	15219.52	0.85581	0.941	no
48hr Control-2	499382.74					
48hr Control-3	496818.5					
48hr Foam-1	485497.5	15066.15	13017.94	0.8640522	0.941	no
48hr Foam-2	500563.65					
48hr Foam-3	487545.71					

**Table 9. Q-test with a 90% CI conducted on HWP-Biochar kinetic, isotherm and control GC-MS data; highlighted data is suspect**

Sample Name	Area Counts	Range (w)	Gap (a)	Q (a/w)	90% CI (n=3)	reject if Q > 0.941
Initial Biochar-1	400441.75	28662.76	27469.87	0.958381886	0.941	yes
Initial Biochar-2	427911.62					
Initial Biochar-3	429104.51					
Initial Control-1	408587.21	30061.4	16688.58	0.555149793	0.941	no
Initial Control-2	425275.79					
Initial Control-3	438648.61					
15 min Biochar-1	427835.58	9761.11	6951.17	0.712129051	0.941	no
15 min Biochar-2	425025.64					
15 min Biochar-3	434786.75					
15 min Control-1	415368.375	24661.25	13329.1	0.540487607	0.941	no
15 min Control-2	426700.525					
15 min Control-3	440029.625					
0.5 hr Biochar-1	433067.73	18542.5	9676.84	0.521873534	0.941	no
0.5 hr Biochar-2	442744.57					



<b>0.5 hr Biochar-3</b>	451610.23					
<b>0.5 hr Control-1</b>	418441.5	20715.5	13499.75	0.651673867	0.941	no
<b>0.5 hr Control-2</b>	439157					
<b>0.5 hr Control-3</b>	431941.25					
<b>1hr Biochar-1</b>	421579.95	14584.92	11824.05	0.810703795	0.941	no
<b>1hr Biochar-2</b>	409755.9					
<b>1hr Biochar-3</b>	424340.82					
<b>1hr Control-1</b>	414908.36	39811.32	23279.04	0.584734191	0.941	no
<b>1hr Control-2</b>	438187.4					
<b>1hr Control-3</b>	454719.68					
<b>2hr Biochar-1</b>	443602.535	34996.39	20149.75	0.575766529	0.941	no
<b>2hr Biochar-2</b>	423452.785					
<b>2hr Biochar-3</b>	408606.145					
<b>2hr Control-1</b>	421690.76	29434.82	14742.72	0.500859866	0.941	no
<b>2hr Control-2</b>	406948.04					
<b>2hr Control-3</b>	436382.86					
<b>4hr Biochar-1</b>	414891.73	34794.69	15871.96	0.456160408	0.941	no
<b>4hr Biochar-2</b>	395969					
<b>4hr Biochar-3</b>	380097.04					
<b>4hr Control-1</b>	407540.59	26514.73	22775.66	0.141018596	0.941	no
<b>4hr Control-2</b>	411279.66					
<b>4hr Control-3</b>	434055.32					
<b>7hr Biochar-1</b>	385132.72	19883.99	17878.33	0.899131915	0.941	no
<b>7hr Biochar-2</b>	387138.38					
<b>7hr Biochar-3</b>	367254.39					
<b>7hr Control-1</b>	430473.13	6313.98	3432.26	0.543596907	0.941	no
<b>7hr Control-2</b>	433354.85					
<b>7hr Control-3</b>	427040.87					
<b>24hr Biochar-1</b>	350626.415	17310.77	14713.24	0.849947172	0.941	no
<b>24hr Biochar-2</b>	333315.645					
<b>24hr Biochar-3</b>	335913.175					
<b>24hr Control-1</b>	385824.365	51984.76	46654.91	0.897472836	0.941	no
<b>24hr Control-2</b>	437809.125					
<b>24hr Control-3</b>	432479.275					
<b>48hr Biochar-1</b>	334538.545	19323.91	13465.62	0.696837234	0.941	no
<b>48hr Biochar-2</b>	321072.925					
<b>48hr Biochar-3</b>	315214.635					
<b>48hr Control-1</b>	430862.62	18371.68	17454.93	0.950099828	0.941	yes
<b>48hr Control-2</b>	412490.94					
<b>48hr Control-3</b>	429945.87					

<b>Initial 0.15 S1</b>	1986	851.55	613.76	0.720756268	0.941	no
<b>Initial 0.15 S2</b>	1372.24					
<b>Initial 0.15 S3</b>	1134.45					
<b>Initial 1.5 S1</b>	16510.55	205.22	173.99	0.84782185	0.941	no
<b>Initial 1.5 S2</b>	16715.77					
<b>Initial 1.5 S3</b>	16541.78					
<b>Initial 15 S1</b>	430180.095	16526.04	8688.51	0.52574664	0.941	no
<b>Initial 15 S2</b>	421491.585					
<b>Initial 15 S3</b>	438017.625					
<b>Final 0.15 S1</b>	374.36	678.76	504.64	0.743473393	0.941	no
<b>Final 0.15 S2</b>	-130.28					
<b>Final 0.15 S3</b>	-304.4					
<b>Final 1.5 S1</b>	2025.185	3466.86	1820.43	0.525094754	0.941	no
<b>Final 1.5 S2</b>	5492.045					
<b>Final 1.5 S3</b>	3671.615					
<b>Final 15 S1</b>	340591.415	34342.12	24775.42	0.721429545	0.941	no
<b>Final 15 S2</b>	306249.295					
<b>Final 15 S3</b>	315815.995					

**Table 10. Q-test with a 90% CI conducted on CNT-HS and F-600 GAC isotherm GC-MS data; highlighted data is suspect**

Sample Name	Area Counts	Range (w)	Gap (a)	Q (a/w)	90% CI (n=3)	reject if Q > 0.941
<b>Foam Initial 0.15 S1</b>	734.97	13085.43	13027.22	0.995551541	0.941	yes
<b>Foam Initial 0.15 S2</b>	793.18					
<b>Foam Initial 0.15 S3</b>	13820.4					
<b>Foam Initial 1.5 S1</b>	882.905	12849.27	12193.11	0.948934064	0.941	yes
<b>Foam Initial 1.5 S2</b>	13076.015					
<b>Foam Initial 1.5 S3</b>	13732.175					
<b>Foam Initial 15 S1</b>	418528.11	9139.04	6864.13	0.751077794	0.941	no
<b>Foam Initial 15 S2</b>	420803.02					
<b>Foam Initial 15 S3</b>	427667.15					
<b>Foam Final 0.15 S1</b>	224.435	288.5	132.52	0.459341421	0.941	no
<b>Foam Final 0.15 S2</b>	91.915					
<b>Foam Final 0.15 S3</b>	380.415					
<b>Foam Final 1.5 S1</b>	7296.735	1197	598.6	0.500083542	0.941	no
<b>Foam Final 1.5 S2</b>	6698.335					
<b>Foam Final 1.5 S3</b>	7895.335					
<b>Foam Final 15 S1</b>	405613.345	21020.43	15629.43	0.743535218	0.941	no
<b>Foam Final 15 S2</b>	421242.775					

<b>Foam Final 15 S3</b>	426633.775					
<b>GAC Initial 0.15 S1</b>	1315.705	349.76	233.23	0.666828683	0.941	no
<b>GAC Initial 0.15 S2</b>	965.945					
<b>GAC Initial 0.15 S3</b>	1082.475					
<b>GAC Initial 1.5 S1</b>	18667.99	1521.01	773.83	0.508760626	0.941	no
<b>GAC Initial 1.5 S2</b>	17894.16					
<b>GAC Initial 1.5 S3</b>	17146.98					
<b>GAC Initial 15 S1</b>	471518.94	24946.33	24452.82	0.98021713	0.941	yes
<b>GAC Initial 15 S2</b>	472012.45					
<b>GAC Initial 15 S3</b>	496465.27					
<b>GAC Final 0.15 S1</b>	-647.83	-453.39	-363.31	0.801318953	0.941	no
<b>GAC Final 0.15 S2</b>	-1011.14					
<b>GAC Final 0.15 S3</b>	-1101.22					
<b>GAC Final 1.5 S1</b>	341.26	528.13	236.72	0.448222975	0.941	no
<b>GAC Final 1.5 S2</b>	104.54					
<b>GAC Final 1.5 S3</b>	-186.87					
<b>GAC Final 15 S1</b>	167235.805	15319.96	13887.02	0.906465813	0.941	no
<b>GAC Final 15 S2</b>	151915.845					
<b>GAC Final 15 S3</b>	165802.865					
<b>Fabric Initial 0.15 S1</b>	1121.14	224.32	152.63	0.680411912	0.941	no
<b>Fabric Initial 0.15 S2</b>	1049.45					
<b>Fabric Initial 0.15 S3</b>	896.82					
<b>Fabric Initial 1.5 S1</b>	17627.285	780.34	755.45	0.968103647	0.941	yes
<b>Fabric Initial 1.5 S2</b>	17602.395					
<b>Fabric Initial 1.5 S3</b>	16846.945					
<b>Fabric Initial 15 S1</b>	453309.125	13942.81	12537.92	0.899239106	0.941	no
<b>Fabric Initial 15 S2</b>	451904.235					
<b>Fabric Initial 15 S3</b>	439366.315					
<b>Fabric Final 0.15 S1</b>	271.01	385.22	289.35	0.751129225	0.941	no
<b>Fabric Final 0.15 S2</b>	366.88					
<b>Fabric Final 0.15 S3</b>	-18.34					
<b>Fabric Final 1.5 S1</b>	11705.575	3886.73	2983.74	0.767673597	0.941	no
<b>Fabric Final 1.5 S2</b>	14689.315					
<b>Fabric Final 1.5 S3</b>	15592.305					
<b>Fabric Final 15 S1</b>	444586.5	11825.48	7707.88	0.651802718	0.941	no
<b>Fabric Final 15 S2</b>	448704.1					
<b>Fabric Final 15 S3</b>	456411.98					

**Table 11. Q-test with a 90% CI conducted on F-600 GAC isotherm 25 – 40 mg/L GC-MS data; highlighted data is suspect**

Sample Name	AREA Counts	Range (w)	Gap (a)	Q (a/w)	90% CI (n=3)	reject (yes or no)
GAC Initial 25ppm S1	609318.025	15061.66	11174.77	0.74193482	0.941	no
GAC Initial 25ppm S2	624379.685					
GAC Initial 25ppm S3	620492.795					
GAC Initial 40ppm S1	1283369.73	83986.31	43772.85	0.521190299	0.941	no
GAC Initial 40ppm S2	1323583.19					
GAC Initial 40ppm S3	1367356.04					
GAC Fianl 25ppm S1	401050.125	19896.12	15232.88	0.765620634	0.941	no
GAC Final 25ppm S2	416283.005					
GAC Final 25ppm S3	420946.245					
GAC Final 40ppm S1	1023155.82	43720.91	35409.68	0.80990263	0.941	no
GAC Final 40ppm S2	1066876.73					
GAC Final 40ppm S3	1058565.5					

## REFERENCES

- Arias, L. R., and Yang, L. (2009). "Inactivation of bacterial pathogens by carbon nanotubes in suspensions." *Langmuir*, 25(5), 3003–3012.  
<http://doi.org/10.1021/la802769m>
- ATDSR. (2013). *Draft Toxicological Profile for Dinitrotoluenes*. US Agency for Toxic Substances and Disease Registry.  
 <<http://scholar.google.com/scholar?hl=en&btnG=Search&q=intitle:DRAFT+TOXICOLOGICAL+PROFILE+FOR+ARSENIC#0>>.
- Azizian, S., and Yahyaei, B. (2006). "Adsorption of 18-crown-6 from aqueous solution on granular activated carbon: A kinetic modeling study." *Journal of Colloid and Interface Science*, 299(1), 112–115.  
<http://doi.org/http://dx.doi.org/10.1016/j.jcis.2006.01.058>
- AZoNano. (2013). "Comparative Study of Carbon Nanotubes and Carbon Nanofibers." <<http://www.azonano.com/article.aspx?ArticleID=2885>> (Oct. 28, 2015).
- Basu-Dutt, S., Minus, M. L., Jain, R., Nepal, D., and Kumar, S. (2012). "Chemistry of carbon nanotubes for everyone." *Journal of Chemical Education*, 89(2), 221–229.  
<http://doi.org/10.1021/ed1005163>
- Beless, B., Rifai, H. S., and Rodrigues, D. F. (2014). "Efficacy of Carbonaceous Materials for Sorbing Polychlorinated Biphenyls from Aqueous Solution." *Environmental Science & Technology*. 48, 10372-10379.  
<http://doi.org/10.1021/es502647n>
- Berchtold, S. R., Vanderloop, S. L., Suidan, M. T., and Maloney, S. W. (2012). "Fluidized-bed system : activated activated of a using anaerobic reactors reactors granular and aerobic carbon sludge." *Water Environment Research* 67(7), 1081–1091.
- Brady-Estévez, A. S., Schnoor, M. H., Kang, S., and Elimelech, M. (2010). "SWNT-MWNT hybrid filter attains high viral removal and bacterial inactivation." *Langmuir*, 26(24), 19153–19158. <http://doi.org/10.1021/la103776y>
- Chen, W., Duan, L., and Zhu, D. (2007). "Adsorption of Polar and Nonpolar Organic Chemicals to Carbon Nanotubes." *Environmental Science & Technology*, 41(24), 8295–8300. <http://doi.org/10.1021/es071230h>
- Christian, G. D. (2003). *Analytical Chemistry*, 6<sup>th</sup> Ed., John Wiley & Sons, Inc., 3, 98-99.

- Clausen, J. L., Scott, C., and Osgerby, I. (2011). "Fate of Nitroglycerin and Dinitrotoluene in Soil at Small Arms Training Ranges." *Soil and Sediment Contamination: An International Journal*, 20(6), 649–671.  
<http://doi.org/10.1080/15320383.2011.594108>
- Crittenden, J. C., et al. (2005). *Water Treatment Principles and Design*, 2<sup>nd</sup> Ed., J. Wiley, Hoboken, New Jersey.
- De Ridder, D. J. (2012). *Adsorption of organic micropollutants onto activated carbon and zeolites*. Water Management Academic Press. Netherlands.
- De Volder, M. F. L., Tawfick, S. H., Baughman, R. H., and Hart, A. J. (2013). "Carbon nanotubes: present and future commercial applications." *Science*, 339(6119), 535–539. <http://doi.org/10.1126/science.1222453>
- Dobbs, R. A. and Cohen, J. M. (1980). *Carbon Adsorption Isotherms for Toxic Organics*. EPA-600/8-80-023, Cincinnati.
- EPA. (1990). "Integrated Risk Information System (IRIS). 2,4-/2,6-Dinitrotoluene mixture; no CASRN." <<http://www.epa.gov/iris/subst/0397.htm>> (Sep. 5, 2015).
- EPA. (2000). *Wastewater Technology Fact Sheet: Granular Activated Carbon Adsorption and Regeneration*. EPA 832-F-00-017, Washington, D.C.
- EPA. (2008). *Drinking Water Health Advisory for 2,4-Dinitrotoluene and 2,6-Dinitrotoluene*. EPA 822-R-08-010, Washington, D.C.
- EPA. (2014). *Technical Fact Sheet – Dinitrotoluene (DNT)*. EPA 505F-14-010
- EPA. (2015). "The Environmental Challenge of Military Munitions and Federal Facilities." <<http://www2.epa.gov/enforcement/environmental-challenge-military-munitions-and-federal-facilities>> (Oct. 21, 2015).
- Han, S., Mukherji, S. T., Rice, A., and Hughes, J. B. (2011). "Determination of 2,4- and 2,6-dinitrotoluene biodegradation limits." *Chemosphere*, 85(5), 848–853.  
<http://doi.org/10.1016/j.chemosphere.2011.06.100>
- Hanigan, D., Zhang, J., Herckes, P., Krasner, S. W., Chen, C., and Westerhoff, P. (2012). "Adsorption of N-Nitrosodimethylamine precursors by powdered and granular activated carbon." *Environmental Science and Technology*, 46(22), 12630–12639.  
<http://doi.org/10.1021/es302922w>
- Hinshaw, G. D., Fanska, C. B., Fiscus, D. E., and Sorensen, S. A.. (1987). *Granular Activated Carbon (GAC) System Performance Capabilities And Optimization*. U.S. Army Toxic And Hazardous Materials Agency. Kansas City, MO.

- Ho, P. C., and Daw, C. S. (1988). "Adsorption and Desorption of Dinitrotoluene on Activated Carbon." *Environ. Sci. Technol.*, 22(8), 919–924.
- Inyang, M., and Dickenson, E. (2015). "The potential role of biochar in the removal of organic and microbial contaminants from potable and reuse water: A review." *Chemosphere*, 134, 232–240. <http://doi.org/10.1016/j.chemosphere.2015.03.072>
- Kanel, S. R., Misak, H., Mall, S., Nepa, D., Brittle, S. W., Pavel-Sizemore, I., Kempisty, D. M., and Goltz, M. N. (2015). "Application of Carbon Nanotube Yarns as a Filter Media to Treat Nitroaromatic-contaminated Water." *New Carbon Materials*, in press.
- Kang, S., Herzberg, M., Rodrigues, D. F., and Elimelech, M. (2008). "Antibacterial effects of carbon nanotubes: size does matter!" *Langmuir : The ACS Journal of Surfaces and Colloids*, 24(13), 6409–6413. <http://doi.org/10.1021/la800951v>
- Karumuri, A. K., He, L., and Mukhopadhyay, S. M. (2015). "Tuning the surface wettability of carbon nanotube carpets in multiscale hierarchical solids." *Applied Surface Science*, 327(0), 122–130. <http://doi.org/http://dx.doi.org/10.1016/j.apsusc.2014.10.154>
- Kasozi, G. N., Zimmerman, A. R., Nkedi-Kizza, P., and Gao, B. (2010). "Catechol and Humic Acid Sorption onto a Range of Laboratory-Produced Black Carbons (Biochars)." *Environmental Science & Technology*, 44(16), 6189–6195. <http://doi.org/10.1021/es1014423>
- Kearns, J. (2012). *Sustainable Decentralized Water Treatment for Rural Developing Communities Using Gasifier Biochar*, Aqueous Solutions, University of Colorado-Boulder.
- Kearns, J. P., Wellborn, L. S., Summers, R. S., and Knappe, D. R. U. (2014). "2,4-D adsorption to biochars: Effect of preparation conditions on equilibrium adsorption capacity and comparison with commercial activated carbon literature data." *Water Research*, 62, 29–28. <http://doi.org/10.1016/j.watres.2014.05.023>
- Kempisty, D. M., unpublished manuscript. (2014). *Adsorption of Volatile and Perfluorinated Compounds from Groundwater using Granular Activated Carbon*. University of Colorado.
- Li, L., Quinlivan, P. A., and Knappe, D. R. U. (2002). "Effects of activated carbon surface chemistry and pore structure on the adsorption of organic contaminants from aqueous solution." *Carbon*, 40(12), 2085–2100. [http://doi.org/Pii S0008-6223\(02\)00069-6](http://doi.org/Pii S0008-6223(02)00069-6)

- Liu, X., Wang, M., Zhang, S., and Pan, B. (2013). "Application potential of carbon nanotubes in water treatment: A review." *Journal of Environmental Sciences*, 25(7), 1263–1280. [http://doi.org/http://dx.doi.org/10.1016/S1001-0742\(12\)60161-2](http://doi.org/http://dx.doi.org/10.1016/S1001-0742(12)60161-2)
- Lou, J. C., Lee, R. H., Chen, W. H., Chang, C. J., Hsu, K. L., and Han, J. Y. (2014). "Adsorption Kinetics and Thermodynamics of Perchlorate on Carbon Nanotubes in Water." *J. Environ. Eng.*, 140, 1–6. [http://doi.org/10.1061/\(ASCE\)EE.1943-7870.0000859](http://doi.org/10.1061/(ASCE)EE.1943-7870.0000859).
- Mohan, D., Sarswat, A., Ok, Y. S., and Pittman, C. U. (2014). "Organic and inorganic contaminants removal from water with biochar, a renewable, low cost and sustainable adsorbent - A critical review." *Bioresource Technology*, 160, 191–202. <http://doi.org/10.1016/j.biortech.2014.01.120>
- Mubarak, N. M., Sahu, J. N., Abdullah, E. C., and Jayakumar, N. S. (2014). "Removal of Heavy Metals from Wastewater Using Carbon Nanotubes." *Separation & Purification Reviews*, 43(4), 311–338. <http://doi.org/10.1080/15422119.2013.821996>
- Nefso, E. K., Burns, S. E., and McGrath, C. J. (2005). "Degradation kinetics of TNT in the presence of six mineral surfaces and ferrous iron." *Journal of Hazardous Materials*, 123(1-3), 79–88. <http://doi.org/10.1016/j.jhazmat.2004.07.023>
- Nepal, D., and Geckler, K. E. (2006). *Functional Nanomaterial. Functionalization of Carbon Nanotubes*. American Scientific Publishers, Valencia, California.
- NIH. (2015). "Hazardous Substances Data Bank (HSDB): 2,4-Dinitrotoluene." <<http://toxnet.nlm.nih.gov/cgi-bin/sis/search2/f?./temp/~FTZ56V:2>> (Sept. 5, 2015).
- Oh, S.-Y., and Chiu, P. C. (2009). "Graphite- and Soot-Mediated Reduction of 2,4-Dinitrotoluene and Hexahydro-1,3,5-trinitro-1,3,5-triazine." *Environ. Sci. Technol.*, 43(18), 6983–6988.
- Oh, S.-Y., and Seo, Y.-D. (2014). "Sorptive Removal of Nitro Explosives and Metals Using Biochar." *Journal of Environment Quality*, 43(5), 1663. <http://doi.org/10.2134/jeq2014.02.0097>
- Oh, S.-Y., Son, J.-G., and Chiu, P. C. (2013). "Biochar-mediated reductive transformation of nitro herbicides and explosives." *Environmental Toxicology and Chemistry*, 32(3), 501–508. <http://doi.org/10.1002/etc.2087>
- Oh, S.-Y., Son, J.-G., Hur, S. H., Chung, J. S., and Chiu, P. C. (2013). "Black Carbon-Mediated Reduction of 2,4-Dinitrotoluene by Dithiothreitol." *Journal of Environment Quality*, 42(3), 815. <http://doi.org/10.2134/jeq2012.0411>



- Pan, B., and Xing, B. (2008). "Adsorption Mechanisms of Organic Chemicals on Carbon Nanotubes." *Environmental Science & Technology*, 42(24), 9005–9013. <http://doi.org/10.1021/es801777n>
- Pignatello, J. J., Kwon, S., and Lu, Y. (2006). "Effect of Natural Organic Substances on the Surface and Adsorptive Properties of Environmental Black Carbon (Char): Attenuation of Surface Activity by Humic and Fulvic Acids." *Environmental Science & Technology*, 40(24), 7757–7763. <http://doi.org/10.1021/es061307m>
- Pyrzyńska, K., and Bystrzejewski, M. (2010). "Comparative study of heavy metal ions sorption onto activated carbon, carbon nanotubes, and carbon-encapsulated magnetic nanoparticles." *Colloids and Surfaces A: Physicochemical and Engineering Aspects*, 362(1-3), 102–109. <http://doi.org/10.1016/j.colsurfa.2010.03.047>
- Qiu, M., and Xiong, S. (2015). "Kinetic and Equilibrium Studies for the Removal of Bromate by the Modified Activated Carbon." *Advanced Journal of Food Science and Technology*, 7(7), 548–552.
- Quinlivan, P. A., Li, L., and Knappe, D. R. U. (2005). "Effects of activated carbon characteristics on the simultaneous adsorption of aqueous organic micropollutants and natural organic matter." *Water Research*, 39(8), 1663–1673. <http://doi.org/10.1016/j.watres.2005.01.029>
- Rajagopal, C., and Kapoor, J. C. (2001). "Development of adsorptive removal process for treatment of explosives contaminated wastewater using activated carbon." *Journal of Hazardous Materials*, 87(1-3), 73–98.
- Randtke, S. J., and Snoeyink, V. L. (1983). "Evaluating GAC Adsorptive Capacity." *Journal American Water Works Association*, 75(8), 406–413.
- Shen, X.-E., Shan, X.-Q., Dong, D.-M., Hua, X.-Y., and Owens, G. (2009). "Kinetics and thermodynamics of sorption of nitroaromatic compounds to as-grown and oxidized multiwalled carbon nanotubes." *Journal of Colloid and Interface Science*, 330(1), 1–8. <http://doi.org/10.1016/j.jcis.2008.10.023>
- Sigma-Aldrich. (2015). Safety Data Sheet. 2,4-Dinitrotoluene 97%. <http://www.sigmaaldrich.com/catalog/product/aldrich/101397?lang=en&region=US> (Sep. 7, 2015).
- Speth, T. F., and Miltner, R. J. (1998). "Technical note : adsorption capacity of GAC for Synthetic Organics." *Research and Technology*, 72–75.
- Suthersan, S. S. (1999). *Pump And Treat Systems*. CRC Press LLC, Boca Raton.

- Tiraferrri, A., Vecitis, C. D., and Elimelech, M. (2011). "Covalent Binding of Single-Walled Carbon Nanotubes to Polyamide Membranes for Antimicrobial Surface Properties." *ACS Applied Materials & Interfaces*, 3(8), 2869–2877. <http://doi.org/10.1021/am200536p>
- U.S. Department of Defense. (2014). *Defense Environmental Programs Annual Report to Congress for FY 2013*.
- Vecitis, C. D., Schnoor, M. H., Rahaman, M. S., Schiffman, J. D., and Elimelech, M. (2011). "Electrochemical Multiwalled Carbon Nanotube Filter for Viral and Bacterial Removal and Inactivation." *Environmental Science & Technology*, 45(8), 3672–3679. <http://doi.org/10.1021/es2000062>
- Vijwani, H., unpublished manuscript. (2015). *Hierarchical Porous Structures with Aligned Carbon Nanotubes as Efficient Adsorbents and Metal-Catalyst Supports*. Wright State University.
- Vijwani, H., Nadagouda, M. N., Namboodiri, V., and Mukhopadhyay, S. M. (2015). "Hierarchical hybrid carbon nano-structures as robust and reusable adsorbents: Kinetic studies with model dye compound." *Chemical Engineering Journal*, 268, 197–207. <http://doi.org/10.1016/j.cej.2015.01.027>
- Wei, G., Yu, H., Quan, X., Chen, S., Zhao, H., and Fan, X. (2014). "Constructing All Carbon Nanotube Hollow Fiber Membranes with Improved Performance in Separation and Antifouling for Water Treatment." *Environmental Science and Technology*, 48(14), 8062-8068.
- Wen, D., Li, G., Xing, R., Park, S., and Rittmann, B. E. (2012). "2,4-DNT removal in intimately coupled photobiocatalysis: The roles of adsorption, photolysis, photocatalysis, and biotransformation." *Applied Microbiology and Biotechnology*, 95(1), 263–272. <http://doi.org/10.1007/s00253-011-3692-6>
- Yang, H. Y., Han, Z. J., Yu, S. F., Pey, K. L., Ostrikov, K., and Karnik, R. (2013). "Carbon nanotube membranes with ultrahigh specific adsorption capacity for water desalination and purification." *Nature Communications*, 4,2220. <http://dx.doi.org/10.1038/ncomms3220>

<b>REPORT DOCUMENTATION PAGE</b>					<i>Form Approved OMB No. 0704-0188</i>	
<small>The public reporting burden for this collection of information is estimated to average 1 hour per response, including the time for reviewing instructions, searching existing data sources, gathering and maintaining the data needed, and completing and reviewing the collection of information. Send comments regarding this burden estimate or any other aspect of this collection of information, including suggestions for reducing the burden, to Department of Defense, Washington Headquarters Services, Directorate for Information Operations and Reports (0704-0188), 1215 Jefferson Davis Highway, Suite 1204, Arlington, VA 22202-4302. Respondents should be aware that notwithstanding any other provision of law, no person shall be subject to any penalty for failing to comply with a collection of information if it does not display a currently valid OMB control number.</small>						
<b>PLEASE DO NOT RETURN YOUR FORM TO THE ABOVE ADDRESS.</b>						
<b>1. REPORT DATE (DD-MM-YYYY)</b>		<b>2. REPORT TYPE</b>			<b>3. DATES COVERED (From - To)</b>	
<b>4. TITLE AND SUBTITLE</b>				<b>5a. CONTRACT NUMBER</b>		
				<b>5b. GRANT NUMBER</b>		
				<b>5c. PROGRAM ELEMENT NUMBER</b>		
<b>6. AUTHOR(S)</b>				<b>5d. PROJECT NUMBER</b>		
				<b>5e. TASK NUMBER</b>		
				<b>5f. WORK UNIT NUMBER</b>		
<b>7. PERFORMING ORGANIZATION NAME(S) AND ADDRESS(ES)</b>					<b>8. PERFORMING ORGANIZATION REPORT NUMBER</b>	
<b>9. SPONSORING/MONITORING AGENCY NAME(S) AND ADDRESS(ES)</b>					<b>10. SPONSOR/MONITOR'S ACRONYM(S)</b>	
					<b>11. SPONSOR/MONITOR'S REPORT NUMBER(S)</b>	
<b>12. DISTRIBUTION/AVAILABILITY STATEMENT</b>						
<b>13. SUPPLEMENTARY NOTES</b>						
<b>14. ABSTRACT</b>						
<b>15. SUBJECT TERMS</b>						
<b>16. SECURITY CLASSIFICATION OF:</b>			<b>17. LIMITATION OF ABSTRACT</b>	<b>18. NUMBER OF PAGES</b>	<b>19a. NAME OF RESPONSIBLE PERSON</b>	
a. REPORT	b. ABSTRACT	c. THIS PAGE			<b>19b. TELEPHONE NUMBER (Include area code)</b>	